T.C.
REPUBLIC OF TURKEY
HACETTEPE UNIVERSITY
GRADUATE SCHOOL OF HEALTH SCIENCES

IMPROVEMENT OF GERM STEM CELL POOL BY LEPTIN SUPPLEMENTATION AND GENE EDITING FOR MALE INFERTILITY

Nilgün YERSAL

Program of Histology-Embryology
DOCTOR OF PHILOSOPHY THESIS

ANKARA
2020

ACKNOWLEDGEMENTS

This thesis is the culmination of a challenging and fruitful journey. The completion of this journey has been made possible by the support of professors, mentors, my family, and friends. I wish to thank all the people whose assistance enabled the completion of this project. First and foremost, I wish to express my sincere appreciation to my advisor and mentor, Professor Petek Korkusuz, who convincingly guided and encouraged me to do rigorous and intellectually stimulating work, even when the road got tough. Truly, the goals and objectives of my research were achieved thanks to her persistent help. I would like to express my gratitude to members of thesis assessment committee for their contributions and insightful comments and suggestions to improve my thesis.

I give my gratitude to the financial support of the TUBITAK (BIDEB-2214/A) scholarship, which provided me with the opportunity to live and study in the United States at the University of Pittsburgh Magee-Womens Research Institute for the last year of my thesis, which was a great experience for me. I wish to express my deepest gratitude to Professor Kyle E. Orwig for giving me the opportunity to perform research in his Orwig lab and providing invaluable guidance throughout my residence in the lab. It was a great privilege and honor to work and study under his guidance.

I also thank my fellow lab mates and lab managers Kien Tran, Amanda Zielen, Chatchanan Doungkamchan, Sherin David, Sarah Munyoki, Meena Sukhwani, and Yi Sheng in Magee-Womens Research Institute for the warm welcome at the beginning and continuous help and accompany.

I would like to say thanks to my friends and research colleagues Sevil Köse, Utku Horzum, Merve Gizer, Selin Önen, Özge Boyacıoğlu, Eda Çiftçi Dede, and Emrah Tosun for their constant encouragement.

I am extremely grateful to my parents for their love, prayers, caring and sacrifices for educating and preparing me for my future. I am very much thankful to my sister for her support and interest shown to complete this thesis successfully.

Finally, my thanks go to all the people who have supported me to complete the research work directly or indirectly.

ABSTRACT

Yersal N., Improvement of Germ Stem Cell Pool by Leptin Supplementation and Gene Editing for Male Infertility, Hacettepe University Graduate School Health Sciences Doctor of Philosophy Thesis in Program of Histology-Embryology, Ankara, 2020. Infertility affects up to 12-15% of sexually active couples, and male factors contribute about 30-55% of these cases. Infertility can be caused by injuries, genetic factors, exposure to toxicants, immune-suppressive and anti-cancer treatments, but a large number are unexplained (idiopathic). Impairment of fertility is a major concern for the pediatric cancer survivors (PCSs). Freezing of testicular tissue containing spermatogonial stem cell (SSCs) is the only option to preserve the fertility. Sperm collection or culture of SSCs are not available in azoospermic patients with *MCM8* gene disorders. For these infertile men, somatic cells can be reprogrammed into induced pluripotent stem cells (iPSCs) and differentiated into germ cells after correction of mutation via gene editing. Culture is critical to expand the number SSCs from small biopsies obtained from the testes of prepubertal patients prior to transplantation and to enable gene editing if SSCs or iPSCs for patients with genetic infertility. We tested the hypothesis that leptin supplementation may induce proliferation of neonatal mouse SSCs *in vitro* via ERK and/or STAT3 pathways. We also hypothesized that *Mcm8* mutation may be corrected by CRISPR/Cas9 to produce gene edited primordial germ cells like cells (PGCLCs) that could be transplanted to restore fertility in $Mcm8^{-/-}$ infertile mouse. C57BL/6 neonatal SSCs were cultured and treated with leptin (0-200 ng/ml). 100 ng/ml leptin supplementation enhances proliferation SSC cultures via ERK and STAT3 pathways. Two novel $Mcm8^{-/-}$ mouse iPSC lines (591 and 574) were generated from $Mcm8^{-/-}$ mice fibroblasts. A validated $Mcm8^{-/-}$ iPSC (591-14) clone was gene-edited via CRISPR/Cas9 and identified with one *Mcm8* allele corrected back to the wild type by DNA sequencing. Gene-corrected ($Mcm8^{gc/-}$) clone 14 was differentiated to PGCLCs that exhibited a SSEA1+/CD61+ phenotype. These studies may allow the expansion of SSC pool, *in vitro,* prior to auto-transplantation to regenerate spermatogenesis in cancer survivors and correction of single gene mutation causing infertility by CRISPR/Cas9 tool in infertile male.

Key Words: male infertility, spermatogonial stem cell, induced pluripotent stem cell, leptin, *Mcm8*-gene editing

The thesis was supported by HUBAP (THD-2017-13430) and TUBİTAK 2214-A International Research Fellowship Programme (for PhD Students) 2017/2

ÖZET

Yersal N., Erkek İnfertilitesi için Germ Kök Hücre Havuzunun Leptin İlavesi ve Gen Düzenleme ile İyileştirilmesi, Hacettepe Üniversitesi Sağlık Bilimleri Enstitüsü Histoloji-Embriyoloji Programı Doktora Tezi, Ankara, 2020. İnfertilite çiftlerin %12-15'ini etkiler ve erkek faktörler bu vakaların %30-55 nedenidir. Travmalar, genetik bozukluklar, immusupresif ve kanser tedavileri, infertiliteye neden olsa da birçok infertil vaka idiyopatiktir. Kanser tedavi sırasında gonadotoksik tedavilere maruz kalan çocukluk çağı kanser hastaları için en önemli sorunlardan birisi fertilitenin devamının sağlanmasıdır. Bu hastalar için tedavi öncesi spermatogonyal kök hücreler (SKH) içeren testiküler dokuların dondurulması fertilitenin korunmasında tek etkili yoldur. Küçük testis biyopsi dokularından elde edilen SKH'lerin transplantasyon öncesi *in vitro* koşullarda kültüre edilmesi ve çoğaltılması gerekmektedir, Sperm elde edilmesi veya SKH kültürü *MCM8* gen bozukluğu olan infertil olan hastalarda mümkün değildir. Bu infertil olan hastalar için, somatik hücrelerinden elde edilen indüklenmiş pluripotent kök hücreler (İPKH) mutasyon düzeltildikten sonra germ kök hücrelerine farklılaştırılabilir. Bu tez çalışmasının hipotezi, leptin ilavesi SKH havuzunu zenginleştirebilir ve azoospermik *Mcm8*$^{-/-}$ fare modelinde mutasyon CRISPR/Cas9 ile düzeltildikten sonra primordiyal germ hücre benzeri hücrelere farklılaştırılabilir. C67BL/6 neonatal SKH izole edilip, kültüre edildive kültüre SKH' ler leptin (0-200 ng/ml) ile muamale edilerek proliferasyon testleri ile etki ve western blotlama ile ERK ve STAT3 yolakları üzerinden etkinin mekanizması araştırıldı. 100 ng/ml leptin SKH çoğalmasını ERK and STAT3 sinyal yolakları üzerinden arttırdı. *Mcm8*$^{-/-}$ fibroblastlardan iki yeni İPKH hattı (591ve 574) üretildi. CRISPR/Cas9 gen düzenleme ile bir alleli mutasyon olmayan *Mcm8* gen dizisi içeren koloni (*Mcm8*$^{gc-/-}$) (591-14) elde edildi. Mutasyonu düzeltilmiş olan heterozigot koloniden SSEA1+/CD61+ primordiyal germ hücre benzeri hücreler farklılaştırıldı. Bu çalışma, çocukluk çağı kanser hastalarında, SKH havuzunun *in vitro* olarak transplantasyon öncesi çoğaltılması ve spermatogenez restorasyonuna ve tek gen mutasyonu nedeniyle infertil olan hastalarda mutasyonun CRISPR/Cas9 gen düzenleme teknolojisi ile düzeltilmesine olanak sağlar.

Anahtar Kelimeler: erkek infertilitesi, spermatogonyal kök hücre, indüklenmiş pluripotent kök hücre, leptin, *Mcm8*-gen düzenleme

Bu tez çalışması HUBAP (THD-2017-13430) ve TUBİTAK 2214-A doktora sırasında araştırma bursu (2017/2) ile desteklenmiştir.

TABLE OF CONTENT

LIST OF ABBREVATIONS

ABP	Androgen Binding Protein
AgRP	Agouti-Related protein
ARC	Arcuate Nucleus
AZF	Azoospermia Factor
bFGF	Basic Fibroblast Growth Factor
BMP	Bone Morphogenetic Protein
BTB	Blood Testis Barrier
CART	Cocaine and Amphetamine Related Transcript
CFTR	Cystic fibrosis transmembrane conductance regulator
CNS	Central Nervous System
CRISPR/Cas9	Clustered Regularly Interspaced Short Palindromic Repeats/CRISPR-associated protein-9 nuclease
CSF1	Colony Stimulating factor 1
CSFR1	CSF1 Receptor
CtIP	C-terminal Binding protein (CtBP)-Interacting Protein
CXCL12	Chemokine (C-X-C motif) Ligand 12
CXCR4	Chemokine receptor type 4
DBY Y.	Dead Box Polypeptide 3
DSBR	Double Strand Break Repair
EC	Endothelial Cell
ECM	Extracellular Matrix
ERK	Extracellular Signal Regulated Kinase
EWAT	Epididymal White Adipose Tissue
FACS	Fluorescent-Activated Cell Sorting
FGF	Fibroblast Growth Factor
FGFR2	FGF Receptor 2
FSH	Follicle-Stimulating Hormone
GDNF	Glial Cell-Line Derived Neutrophic Factor
GFRA1	GDNF-Family Receptor α1
HJ	Holliday Junction
HPG	Hypothalamic-Pituitary-Gonadal

IM	Interstitial Macrophage
IRS	Insulin Receptor Substrate
IVF	In Vitro Fertilization
JAK2	Janus Kinase 2
KDR	Kinase Insert Domain Receptor
LC	Leydig Cell
LH	Luteinizing Hormone
MACS	Magnetic-Activated Cell Sorting
MAPK	Mitogen-Activated Protein Kinase
MC3R	Melanocortin 3 Reseptor
MC4R	Melanocortin 4 Receptor
MCM8	Minichromosome Maintenance 8
MEF	Mouse Embryonic Fibroblast
MMP	Matrix Metalloproteinase
NHEJ	Non-Homologous End Joining
NOD/SCID	Non Obese Diabetic/Severe Combined Immunodeficiency Disease
PAM	Protospacer Adjacent Motif
PCS	Pediatric Cancer Survivor
PGC	Primordial Germ Cell
PGCLC	Primordial Germ Cell Like Cell
PI3K	Phosphatidyl Inositol 3 Kinase
PM	Peritubular Macrophage
PMC	Peritubular Myoid Cell
PN	Postnatal
POMC	Propiomelanocortin
RA	Retinoic acid
RET	Receptor Tyrosine Kinase
SC	Sertoli Cell
SCF	Stem Cell Factor (KIT ligand)
SDSA	Synthesis-Dependent Strand Annealing
SHP2	SH2-Containing Protein Tyrosine Phosphatase 2
SOCS3	Suppressor of cytokine signaling 3

SOHLH1	Spermatogenesis and oogenesis specific basic helix-loop-helix 1
SOHLH2	Spermatogenesis and oogenesis specific basic helix-loop-helix 2
SSC	Spermatogonial Stem Cell
STAT3	Signal Transducer and Activator of Transcription 3
STO	SIM Mouse Embryo-Derived Thioquanine and Quabian Resistant Cells
SYCE1	Synaptonemal Complex Central Element 1
SYCP3	Synaptonemal Complex Central Protein 3
TALEN	Transcription Activator Like Effector Nuclease
TEX11	X- linked meiosis-specific gene
TEX14	Testis-expressed gene 14
TEX15	Testis expressed 15, meiosis and synapsis associated
TJ	Tight Junction
USP9Y	Ubiquitin Spesific Protease 9
UTY Y	Ubiquitously Transcribed Tetraciopeptide Repeat Gene
VEGF	Vascular Endothelial Growth Factor
VEGFR2	Vascular Endothelial Growth Factor Receptor-2
VSMC	Vascular Smooth Muscle Cells
ZFN	Zing Finger Nuclease

LIST OF FIGURES

LIST OF TABLES

1. INTRODUCTION

Infertility affects up to 12- 15% of sexually active couples, and male factors contribute about 30-55% of these cases (1). Infertility can be caused by injuries, **genetic factors,** exposure to toxicants, immune-suppressive and **anti-cancer treatments,** but a large number are of unknown cause (idiophathic) (2, 3). Majority of unknown causes are postulated to be genetic abnormalities since at least 2000 genes have been implicated in human spermatogenesis (4). **Cancer treatments** such as chemotherapy and/or radiation can cause infertility due to permanent testicular damage and degeneration. As the diagnosis and treatment options in pediatric cancer have evolved in the last decades, the survival rate in pediatric cancer patients (PCPs) overall has exceeded 80%. However, 46% of pediatric cancer survivors (PCSs) have lifelong subfertility or infertility. Impairment of fertility is a major concern for the survivors who received gonadotoxic treatments (5, 6). Several technologies have emerged to preserve reproductive potential of sterile PCSs. Since the spermatogenesis has not yet been started; testicular tissue (TT) biopsy could be collected before cancer therapy. Spermatogonial stem cells (SSCs) can be obtained from TT and propagated in an *in vitro* culture system and then they can be used for auto-transplantation to generate sperm in cancer survivors (7-17) . With this approach, PCSs could regain their fertility and have their own biological children (18). This method is however challenged in clinic because of the inadequate number of SSCs in pre-pubertal TT biopsies.

The testicular microenvironment (niche) modulates the compartment of SSCs. The accessory niche cells and their secretions play a crucial role in the self-renewing and differentiating capability of SSCs (13, 19-22). In order to increase the limited stem cell pool before transplantation, SSCs may need to be propagated with appropriate conditions by addition of niche factors *in vitro*. Epididymal white adipose tissue (EWAT) located adjacent to testicular niche produces several factors containing androgens and leptin to regulate spermatogenesis (23-25) thus removal of EWAT causes spermatogenic failure (26). Leptin has the ability to cross the blood-testis barrier (BTB), its specific functional receptor OB-Rb is located on type A spermatogonia (27-29). Proliferative effect of leptin on somatic stem (30-34) and mature (35-38) cells is reported; **however, leptin's effects on SSCs in prepubertal testis have not yet been investigated.**

Genetic factors explain 21-29% of azoospermia, whereas the majority of azoospermic cases are idiopathic and the unknown causes are most likely to be genetic factors. Structural and numerical chromosomal abnormalities, single gene disorders, multifactorial genetic disorders and epigenetic changes are among genetic reasons of reproductive failure (1). Deletions of long arm of chromosome Y (Yq) and numerical chromosomal abnormalities (primarily 47, XXY (Klinefelters Syndrome (KFS)) are common and known genetic causes of spermatogenic failure (18). Recently, several monogenic defects such as SOHLH1, TEX11, TEX15, SCYP3, SYCE1, **MCM8** have been related to infertility in men (39). Mini-Chromosome Maintenance (MCM)-8 is the recently found components of MCM proteins and has essential functions for maturation and maintenance of gonads of in both sexes (40). In gametogenesis, several hundreds of double strand breaks (DSBs) are generated to exchange maternal and paternal genetic information during meiotic prophase I. While only 10% of DSBs results with chromosomal crossover, the rest of the DNA breaks should be fixed through non-homologous end joining (NHEJ) or homologous repair (HR) to regulate genomic integrity of germ cells (41). *Mcm8*$^{-/-}$ mice have impairment in DNA repair process through HR mechanism and *Mcm8*$^{-/-}$ females and males are infertile and females develop ovarian tumors (42). In some adult infertile cases, sperm can be collected from testes or other parts of the reproductive tract by several types of minimal invasive procedures such as testicular sperm extraction (TESE). Due to the relatively small numbers of sperm recovered, intracytoplasmic sperm injection (ICSI), *in vitro* fertilization (IVF), and intrauterine insemination (IUI) can be used to achieve pregnancy. However, those infertility treatment approaches are inconvenient for *MCM8*$^{-/-}$ males due to spermatogenic failure characterized by arrested development during meiosis.

Induced pluripotent stem cells (iPSC) enable novel personalized therapeutic approaches for *MCM8*$^{-/-}$ azoospermic males. Somatic cells from patient skin or blood could be reprogrammed into iPSCs and then mutation causing infertility can be corrected in iPSCs by recently discovered genome editing tool **CRISPR/Cas9**. These gene corrected iPSCs could be induced to differentiate to primordial germ cell like cells (PGCLCs) and injected into testes to regenerate spermatogenesis and to have functional sperm. The other possible way is that haploid germ cells could be produced

by iPSCs reprogrammed from patient somatic cells after gene editing to correct mutation. **The correction of mutation of *Mcm8*$^{-/-}$ on iPSCs and regeneration of spermatogenesis with gene edited germ stem cells (GSCs) has not yet been investigated.**

In this thesis study we hypothesized 1) that leptin may stimulate proliferation of pre-pubertal mouse testis SSCs in culture prior to transplantation in experimental pediatric cancer treatment model and 2) that *Mcm8*$^{-/-}$ mouse fibroblast-derived iPSCs may be differentiated to PGCLCs after correction of mutation via CRISPRCas9 for regeneration of spermatogenesis in *Mcm8*$^{-/-}$ azoospermia models (Figure 1.1.)

To address these hypotheses, we propose the following aims:

1. To isolate, characterize the neonatal male C57BL/6 SSCs, to assess the time and dose dependent proliferative effect and the mechanism of action of leptin supplementation on cultured SSCs.

2. To generate *Mcm8*$^{-/-}$ mouse fibroblast-derived iPSCs, to correct the genetic defect *ex vivo* using CRISPR/Cas9 gene editing in iPSCs, and to produce PGCLCs from gene-corrected heterozygous iPSCs.

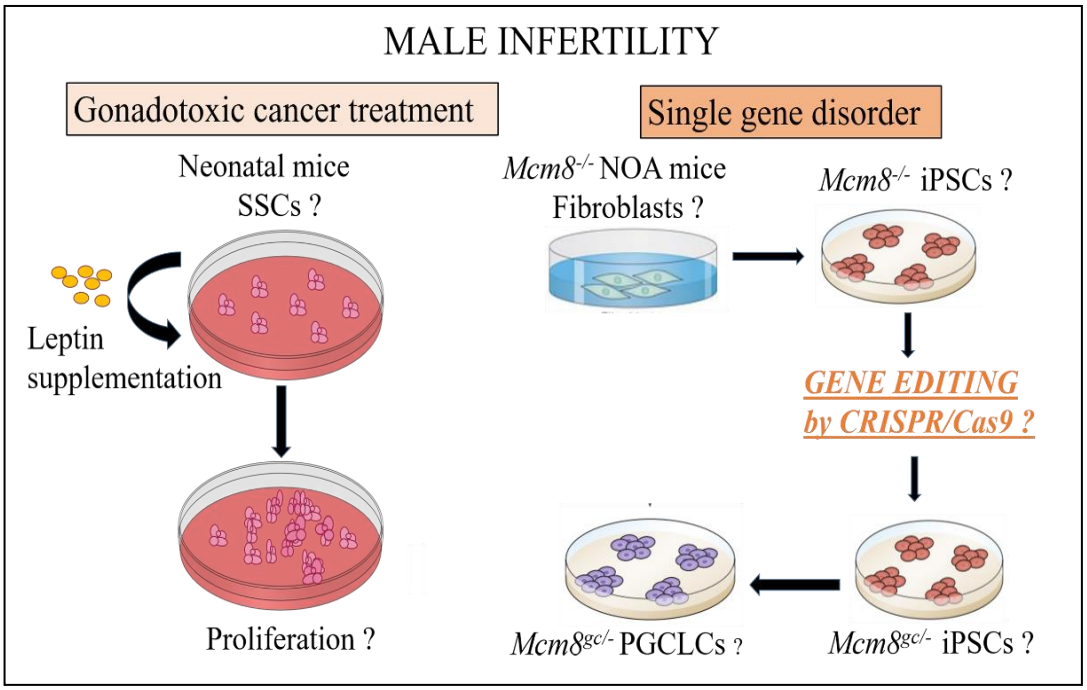

Figure 1.1. Schematic presentation of the hypothesis. In this thesis study, we aimed to investigate two major problems for male infertility. First; we asked if leptin exerts dose and time dependent proliferative effect on SSCs from pre-pubertal mouse testis. Secondly; if the *Mcm8*$^{-/-}$ mouse fibroblast-derived iPSCs differentiate to PGCLCs after correction of mutation via CRISPR/Cas9 for regeneration of spermatogenesis in experimental *Mcm8*$^{-/-}$ azoospermia mouse model.

If we are able to isolate, maintain and enrich the number of SSCs without losing stemness features *in vitro* by leptin supplementation and correct genetic defect by CRISPR/Cas9 on *Mcm8*$^{-/-}$ iPSCs to produce gene corrected PGCLCs, these applications would provide important insights into the clinical treatment approaches to PCSs and azoospermic infertile male due to single gene mutations.

2. GENERAL INFORMATION

2.1. Causes of Male Infertility

Infertility affects up to 12-15% of sexually active partners and male factor is the sole or a contributing cause in about 30-55% of all infertile couples (43, 44). Azoospermia is the most severe phenotype of infertility and affects 1% of all men worldwide. It can be subdivided into two major forms: Obstructive (OA) and non-obstructive azoospermia (NOA). Sperm are generated normally, but there is a physical blockage or obstruction in the male ductal tract in patients with OA. On the other hand, NOA is a consequence of spermatogenic failure during spermatogenesis (45). Infertility can be caused by exposure to toxic chemotherapy agents and/or irradiation, genetic defects, and immune suppressive treatments; however, in most cases, cause of male infertility is unknown (46). It is supposed that genetic abnormalities are the major cause of infertility since probably at least 2000 genes play pivotal role to modulate human spermatogenesis (47).

2.1.1. Cancer Treatments

In 2016, 10.380 recent cancer cases and 1.250 deaths from cancer under the age of 15 years were reported (48). Pediatric cancer patients may face temporary or permanent gonadal damage as a consequence of exposure to chemotherapeutic agents and/or irradiation (6, 49). Despite the fact that 80% of pediatric cancers are cured successfully with highly effective cancer treatments in recent decades, chemoradiotherapeutics have adverse effect on survivor's ability to have his/her own biological child in the future (5). Cryopreservation of testicular tissues (containing SSCs) is the only option to preserve fertility in PCPs who are not producing sperm. Therefore, it is important to determine possible negative effects of cancer treatment on SSCs. An adequate number of SSC is essential to restore spermatogenesis after transplantation. Negative effect of cancer treatments on testis depends on multiple factors including the dosage, delivery method, and sensitivity of patients to chemotherapeutic agents and/or irradiation (50). Germ stem cell pool is more vulnerable to cytotoxic treatment when compared to somatic cells in the testis (51, 52). The three frequently used chemotherapy drugs such as doxorubicin,

cyclophosphamide, and cisplatin led to a decrease in the SSC pool, but they had no adverse effect on somatic cells including Sertoli cells (SCs) and Leydig cells (LCs) of testis (53). On the other hand, exposure to chemotherapeutic agents *in vivo* caused dysfunction of SCs with a reduced production of transferrin and androgen binding protein (ABP) (54). Doxorubicin treatment did not have any effect on the proliferation of peritubular myoid cells (PMCs), function and morphology of LCs from rat TT *in vitro*. Even though there was not any effect on morphology of LCs *in vitro*, increased level in Luteinizing hormone (LH) suggests a functional alteration of LCs in PCSs exposed to chemoterapeutic agents (55). Cyclophosphamide, cisplatin doxorubicin and Irinotecan's metabolite SN38 led to abnormal morphology with decreased diameter of seminiferous tubules and reduced SSCs pool in pre-pubertal 5-day-old mouse testes (53, 56). Imatinib mesylate, a tyrosine kinase inhibitor, impaired the development of the SSCs pool, reduced the number of undifferentiated spermatogonia in prepubertal rodent (57). Similarly, chemotherapeutic agents (doxorubicin, bleomycin, cyclophosphamide etoposide, and cisplatin) caused DNA damages in SSC line *in vitro* (58). Moreover, adverse effect on SSC pool was observed in PCPs received chemotherapeutic agents (59). Furthermore, direct or scattered irradiation could cause gonadal impairment (60). A dose from 0.1 to 1.2 Gy impairs spermatogenesis and 4 Gy radiation dose induces irreversible damage on gonads (61). The interstitial LCs are more resistant to the negative radiation effects. Damage to LCs occurs at 20 Gy and 30 Gy in prepubertal boys and adult males, respectively (52).

Because of gonadotoxic effect of chemotherapeutic agents and/or irradiation PCPs may face infertility problems. To preserve fertility, testis biopsies containing SSCs before cancer treatment need to be obtained in PCSs

2.1.2. Genetic Causes

Genetic abnormalities have been believed account for about 30% of male infertility (62, 63). Majority of infertile male cases are idiopathic (46). Since at least 2000 genes are involved in human spermatogenesis, unknown causes are probably due to genetic defects (47). Genetic causes of spermatogenic failure include numerical and structural chromosome aberrations and single gene disorders. Deletions of long arm of chromosome Y and chromosomal aneuploidy (mainly 47, XXY Klinefelter syndrome

(KFS)) are frequent known genetic reasons of infertility (18). Another important cause of infertility problem is defect in CFTR gene that leads to single or bilateral lack of vas deferens (39). Recently, several single gene disorders have been related to infertility such as *SOHLH1* (64), *SOHLH2* (65) T*EX11* (66), *TEX15* (67), *SYPC3* (68), *SYCE1* (69), and *MCM8* (40) in men.

Chromosome Y Microdeletion

The human Chromosome Y contains several genes that are essential for testis determination and also for spermatogenesis. Yq chromosome microdeletions are the most predominant genetic causes of impaired sperm generation and spermatogenic failure (70). Microdeletions of Yq have been demonstrated in about 5% of men with severe oligozoospermia and in 13% of men with NOA (1). Azoospermia factor (AZF) region of Yq chromosome is clustered in interval 5 and 6th of Yq which plays a vital role to modulate spermatogenesis. The region is subdivided into four regions that are called as AZFa, AZFb, AZFc, and AZFd; and gene deletions in these four regions have been implicated to be pathogenically involved in spermatogenic failure associated with NOA or severe oligozoospermia.

The AZFa region is found in the proximal area of interval 5 and includes three candidate genes: *USP9Y, DBY (DDX3Y)* and *UTY.* Full deletions of both *USP9Y* and *DBY* genes lead to Sertoli cell- only syndrome (SCOS) characterized by absence of male germ cells (MGCs) in seminiferous tubules (71, 72). The AZFa subregion deletions cause 9-55% of infertile males diagnosed with SCOS (73). The AZFb subregion is located in the distal area of interval 5 and the proximal area of interval 6. Deletion of AZFb leads to meiotic arrest at the primary spermatocyte stage. The AZFb subregion includes 32 genes and partially overlaps with AZFc subregion (74). *RBMY* and *PRY* are main protein-encoding genes in AZFb subregion. When both genes are deleted, spermatogenesis is completely arrested due to meiotic maturation arrest (75). The AZFc subregion includes 7 distinct gene families involved in the maturation process of postmeiotic germ cells: *PRY, TTY, BPY, DAZ, GOLGA2LY, CSPYG4LY, CDY* (73*)*. Deletions in AZFc subregion only or combined with other AZF regions account for 87% of Yq microdeletions (76). AZFc subregion deletions can explain about 12% and 6% of NOA and severe oligozoospermia cases, respectively (75).

Klinefelter Syndrome

Klinefelter syndrome is the most prevalent sex chromosal error causing spermatogenic failure in men as a result of one or more excess X chromosomes (77). Approximately 3% of all infertile men and, 14% of NOA individuals have KFS (78). The extra X chromosome prevents normal testicular growth and leads to reduced testosterone level, premature degeneration of PGCs before puberty and the early or late maturation arrest at the primary spermatocyte stage of spermatogenesis and impairment of sperm development in later stage (1).

Single Gene Disorders

Several mutated genes related with infertility (*SOHLH1* (64), *SOHLH2* (65), *TEX11* (66), *TEX15* (67), *SYCE1* (69), *SYCP3* (68), and *MCM8* (40)) have been discovered in human so far.

TEX11, TEX14, and TEX15

TEX11 promotes meiotic recombination, chromosomal synapsis, and crossovers formation (79). *Tex11* null mice exhibited synaptic failure, reduced formation of crossovers and apoptotic spermatocytes at the pachytene stage (80). Recurring deletion of three exons of *TEX11* and 5 novel *TEX11* mutations occurred in 2.4% of infertile participants with NOA. Phenotype of these patients with meiotic arrest was similar to the *Tex11*-deficient male mice (66). TEX14 serves as one of the important component to form intercellular bridges between germ cells (81). Even though spermatogonia proliferated and differentiated, they did not have the capability to complete spermatogenesis which stopped before first division of meiosis in *Tex14* mutant mice (81). TEX15 is crucial for chromosomal synapsis and meiotic recombination, similar to TEX11. It modulates transfer of mediators to site of DSBs (82). Loss of function in *Tex15* resulted in meiotic arrest and spermatocytes show impaired chromosomal synapsis in mice (82). A nonsense mutation (c.2130T>G, pY710*) in *TEX15* has been shown in a consanguineous Turkish family. Nonsense mutation was identified in three brothers of eight siblings (67).

SOHLH1 and SOHLH2

SOHLH1 and SOHLH2 play critical role in gametogenesis (83, 84). Both *Sohlh1* and *Sohlh2* null male mice are sterile (83, 85). *Sohlh1* was first detected in A_{al} spermatogonia in stage IV and its expression was most important in from A1 to B spermatogonia and deficiency of *Sohlh1* disrupted spermatogenesis (83). Postpartum *Sohlh2*-null mice had functional undifferentiated spermatogonia (A_{undiff}) with normal morphological appearance and degenerated differentiating spermatogonia. The *Sohlh2*-null A_{undiff} spermatogonia proliferated normally, but did not express KIT receptor *in vitro* (85). New nonsynonymous exonic (c.346-1G>A) and intronic (c.91T>C, c.529C>A) variants were discovered in the *SOHLH1* gene in 96 Korean sterile men with NOA. Partial deletion at a cryptic splicing site in exon 4 due to the c.346-1G>A intronic variant resulted in truncated bHLH domain and this splice-acceptor site mutation impaired the function of SOHLH1 protein (64). In Chinese population, *SOHLH2* gene SNPs (rs1328626 and rs6563386) were demonstrated as the probable genetic risk factors of spermotogenic failure (65).

SYCP3 and SYCE1

These proteins are the main elements of synaptonemal complex that is critical for chromosomal synapsis and meiotic recombination (86, 87). Although *Sycp3* and *Syce1* null male mice exhibited normal development, they have no reproductive potential and their small testes showed meiotic arrest, lack round and mature sperm (88, 89). Two affected men with spermatogenic failure in an Iranian Jewish consanguineous family has been recently reported. The c.197-2 A>G mutation impaired the acceptor site of intron three in *SYCE1* gene that resulted in premature stop codon. Those cases exhibited absent testicular immunostaining for SYCE1 and maturation arrest by histology (69). 643delA in *SYCP3* resulting in nonsense mutation was found in two NOA patients with maturation arrest. The examination of TT showed defective spermatogenic process (68).

MCM8

The *MCM8* gene is found on chromosome 2 and chromosome 20 in mice and humans (90), respectively. It has essential function for maturation and maintenance of gonads in both sexes (40). During gametogenesis, hundreds of programmed DSBs are generated endogenously to attain accurate segregation of chromosomes. In general, only 10% of DSBs results in chromosomal crossover, the rest of DNA breaks should be repaired via HR in order to maintain chromosomal integrity of germ cells (41). In meiotic recombination, programmed DSBs are induced by Spo11 which leads to phosphorylation of histone H2AX (γH2AX) (91). Spo11 is removed and 5′ DNA strands are degraded to give 3′ ending ssDNA tails by MRN (MRE11-RAD50-NBS1), CtlP, and EXO11 (92). RAD51 and DMC1 bind these tails and form nucleoprotein filaments formation which catalyzes search for a homology target and strand invasion (93). It has been shown that ATPase motifs of MCM8-9 are required for recruitment of MRE11 (94) and RAD51 (95). Following invasion, the DNA strand is extended by a polymerase to create a D-loop. After D-loop formation, there are two pathways proposed for HR in mammalian cells: DSBR (Double Strand Break Repair) and SDSA (Synthesis-Dependent Strand Annealing). The first pathway involves the formation of a Holliday junction (dHJ) and resolution of the dHJ forms non-crossover or crossover products. In SDSA pathway, the invading 3′ strand is displaced and anneals to the other 3′ end of the DSB resulting in a non-crossover product (96) (Figure 2.1.). *Mcm8*$^{-/-}$ mice exhibited normal development, but they were sterile because of small testes without post meiotic germ cells. Even though Spo11 induced DSBs, over recruitment of DMC1 and γ-H2AX to chromatin was observed in *Mcm8*$^{-/-}$ testes. Homologous chromosomes failed to synapse, and *Mcm8*$^{-/-}$ testes became apoptotic due to defective DSB repair via HR (42). Two novel mutations; a frameshift mutation (c.1469-1470insTA) and a splice mutation (c.1954-1G>A) and in *MCM8* gene cause primary gonadal failure in men (40).

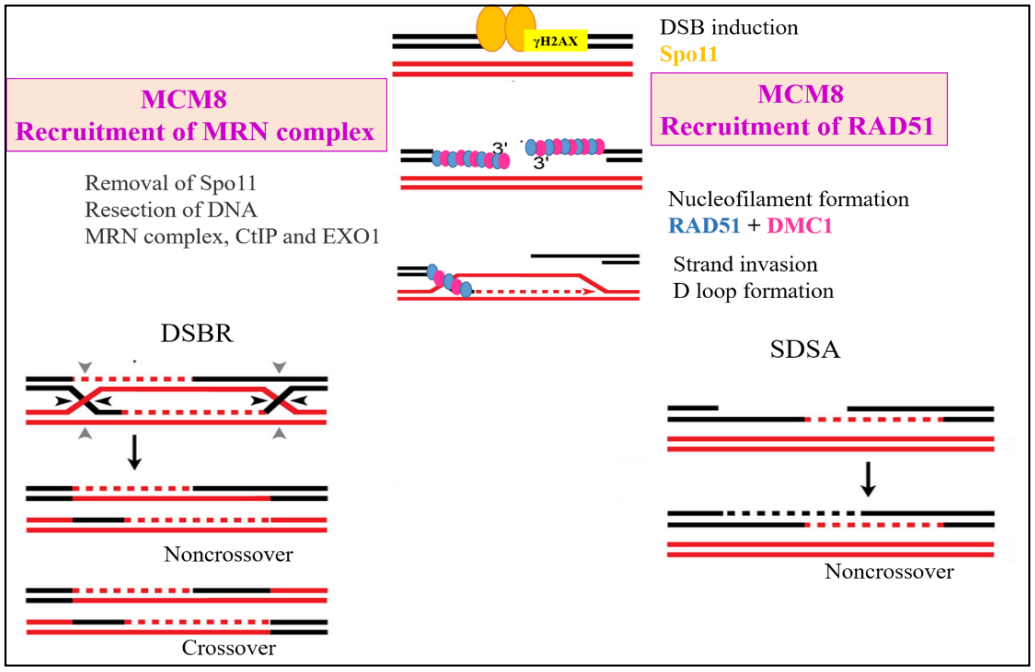

Figure 2.1. The function of MCM8 in meiotic recombination. Figure was modified from reference (97).

2.2. Treatment Approaches in Male Infertility

Recent technologies have emerged to increase reproduction option for PCSs and infertile men. For some adult infertile cases sperm can be collected from testes or other parts of the reproductive tract by using minimal invasive procedures (98-100). Due to the relatively small numbers of sperm recovered by these methods, ICSI is usually needed for fertilization (101, 102). Moreover, for adult cancer patient's semen can be cryopreserved before treatment and thawed in the future for IVF/ICSI for fertilization (101-103). Frozen sperm for 21 years was used for ICSI and healthy boy was born in 2001 (104). The cryopreserved sperm for 21 and 28 years was used for IUI and the couple had a healthy daughter and a healthy boy in 1994 and 2001, respectively (105). Healthy dizygotic twins were born and showed normal development from ICSI with frozen semen stored for 40 years (106).

The SSCs can be obtained by TT biopsy from newborn to adult in order to restore spermatogenesis when sperm cannot be obtained (107). Testicular cell suspension (TCS) including SSCs and somatic cells can be transplanted to testes (108-114) or grafted under skin to reorganize seminiferous tubules of testes (115-118).

Transplantation of TCS from infertile Sl/Sld mutant male mice (lacking SCF on SCs) to infertile male mice with c-kit receptor deficiency restored fertility in the recipient (108). Testicular single cell suspension including SSCs from sexually mature goat completed spermatogenesis after transplantation into recipient seminiferous tubules of pre-pubertal goat after puberty. In this study, the pre-pubertal recipient testis provided efficient microenvironment for SSCs for spermatogenesis and mating of recipient goat resulted in live offspring (109). Autologous transplantation of TCS from 5 months old bovine (110) and pre-pubertal monkey (113) restored spermatogenesis in their irradiated testes. Pre-pubertal boar TCS was injected into recipient boars with immotile short-tail sperm defect provided the detection of motile spermatozoa in seminiferous tubules after 3 months of transplantation (111). While TCS from 3-6 month old dog induced complete spermatogenesis in pre-pubertal recipient dogs with irradiated testes, cultured SSCs caused allergic response after transplantation (112). Functional sperm were capable to fertilize rhesus oocytes produced from TCS resulting in preimplantation embryo development in busulfan-treated rhesus macaques after allogenic transplantation of TCS (114). When TCS from 3–5 months old rabbits and 1–5 years old dogs were transplanted into the testes of recipient mice, colonies of donor SSCs were located at the basal area of tubules; however there was no post-meiotic cells in the recipient tubules (119).

When neonatal rat testicular cells enclosed by extracellular matrix gel was grafted under the skin of SCID mice, vascularized grafts formed seminiferous tubules and grafts had spermatogonia at the basement of tubules (115). Reorganization of germ cells and somatic cells to form TT and complete spermatogenesis had been reported with neonatal porcine (116) and sheep (117) testicular cells, when the mix cell population was grafted under the skin of SCID mice. The embryonic or neonatal pig, mouse, and rat testicular cells showed capability to reconstitute seminiferous tubules after grafting. Moreover, mouse cultured SSCs were mixed with embryonic or neonatal rat and mouse testicular cells. Cultured SSCs or original SSCs completed spermatogenesis and post-meiotic cells were observed in the lumen of reconstituted seminiferous tubules. The reconstituted tubules supported integration of SSCs. Spermatogenesis was completed by integrated SSCs and healthy offspring were

generated by haploid spermatids (118). No one has reported testicular reconstitution with mix of human SSCs and testicular cells so far (107).

Another experimental option to treat infertility is to isolate SSCs from TCS and propagate them in *in vitro* culture system to use for auto-transplantation in order to generate functional sperm. Since the size of testicular biopsy obtained from the testes of PCPs before cancer treatment is relatively small and includes insufficient amount of SSCs; enhancement of SSCs *in vitro* prior to transplantation provides increasing chances to PCSs to have their biological children. Methods for isolating and maintaining SSCs for long term were established in 2003 and 2005 in mouse (7) and rat (8) SSCs, respectively. Long term cultured rodent SSCs maintain their biological potential to regenerate spermatogenesis after transplantation (7-12). Moreover, Kanatsu et al. (7) and Kubota et al. (9) reported live offspring via sperm generated from cultured SSCs after transplantation. Healthy progeny were generated via microinsemination of spermatozoa that are recovered from W/W^v recipient pup testis transplanted with cultured SSCs from 2 weeks old W^v/W^v mice into oocytes (120). Several research groups have attempted to culture human SSCs (hSSCs) by using different protocols (13-17); however, to date no protocol to culture hSSCs has been replicated successfully.

Testicular tissue could be grafted into the scrotum or under the skin to generate functional sperm. Complete spermatogenesis, fertilization competent sperm and live offspring from mice (121, 122), pigs (121), goats (121), and primate (123) TT grafting under the skin of SCID mice or scrotum (124) were reported (121-124). Fragments of TT from neonatal mice, pigs or goats were grafted under the back skin of SCID mice and sperm recovered from TT was used for ICSI(121). Ectopic grafting under the skin of SCID mouse from neonatal mice TT produced functional sperm and healthy pups were generated by ICSI (122). Grafting of TT from immature rhesus monkeys into recipient mice resulted in production of fertilization-competent sperm in testis xenografts (123). The autologous fresh TT from pre-pubertal monkey grafted into the scrotum exhibited full spermatogenesis (124). In 2019, Dr. Kyle Orwig's team produced the first monkey baby from sperm recovered from frozen/thawed, autologous grafted pre-pubertal TT pieces (125). However, xenografted human TT has not

completed spermatogenesis in mice despite survival of spermatogonia for long period to date (126-131).

Sperm could also be produced in TT organ culture systems. The neonatal mice testes organ cultures positioned at air-liquid phase generated functional haploid male germ cells. In this study, researchers obtained healthy offspring by sperm recovered from the testes organ culture (132). Same research group also reported complete spermatogenesis in adult mice and vitamin A-deficient mice including only spermatogonia by organ culture approaches (133). Neonatal rat organ culture system supplemented by RA, glutamax, EWAT produced Acrosin(+) germ cells and seminiferous tubules showed spontaneous contractility by supplementation of EWAT (134). Until now, generation of haploid germ cells from human testis by organ culture approach has not been achieved.

Autologous somatic iPSCs may have major advantage to provide personalized strategies for infertile couples (135). In mice, miPSCs reprogrammed from somatic cells were differentiated into PGCLCs (136, 137) and meiotic germ cells (138-142). Hayashi et al. (143) achieved to generate PGCLCs from epiblast like cells (EpiLCs) derived from iPSCs by mimicking *in vivo* known factors in male germ cells development. The PGCLCs completed spermatogenesis and produced haploid germ cells after transplantation into sterile mice testes and these haploid germ cells were used to have healthy offspring. Some groups were reprogrammed hiPSCs from somatic tissues (PMBCs and skin) and differentiated these hiPSC into PGCLCs (144-149) and acrosin(+) germ cells (2, 150-153), but the findings were not confirmed by transplantation or fertilization with haploid germ cells. Mutations causing infertility can be corrected in SSCs or iPSCs that were reprogrammed from somatic cells of NOA patients with single gene disorder using new gene editing tool CRISPR/Cas9. Spermatogenesis can be restarted after transplantation of gene corrected germ cells to the testes of infertile men (154, 155). Recently, a mutation causing infertility was corrected by CRISPR/Cas9 in SSCs from 14-day-old Kit^{w}/Kit^{wv} mouse. Then, the gene edited SSCs were propagated, transplanted into testis, and completed spermatogenesis (154). Figure 2.2. summarizes above mentioned standard and experimental approaches to treat male infertility.

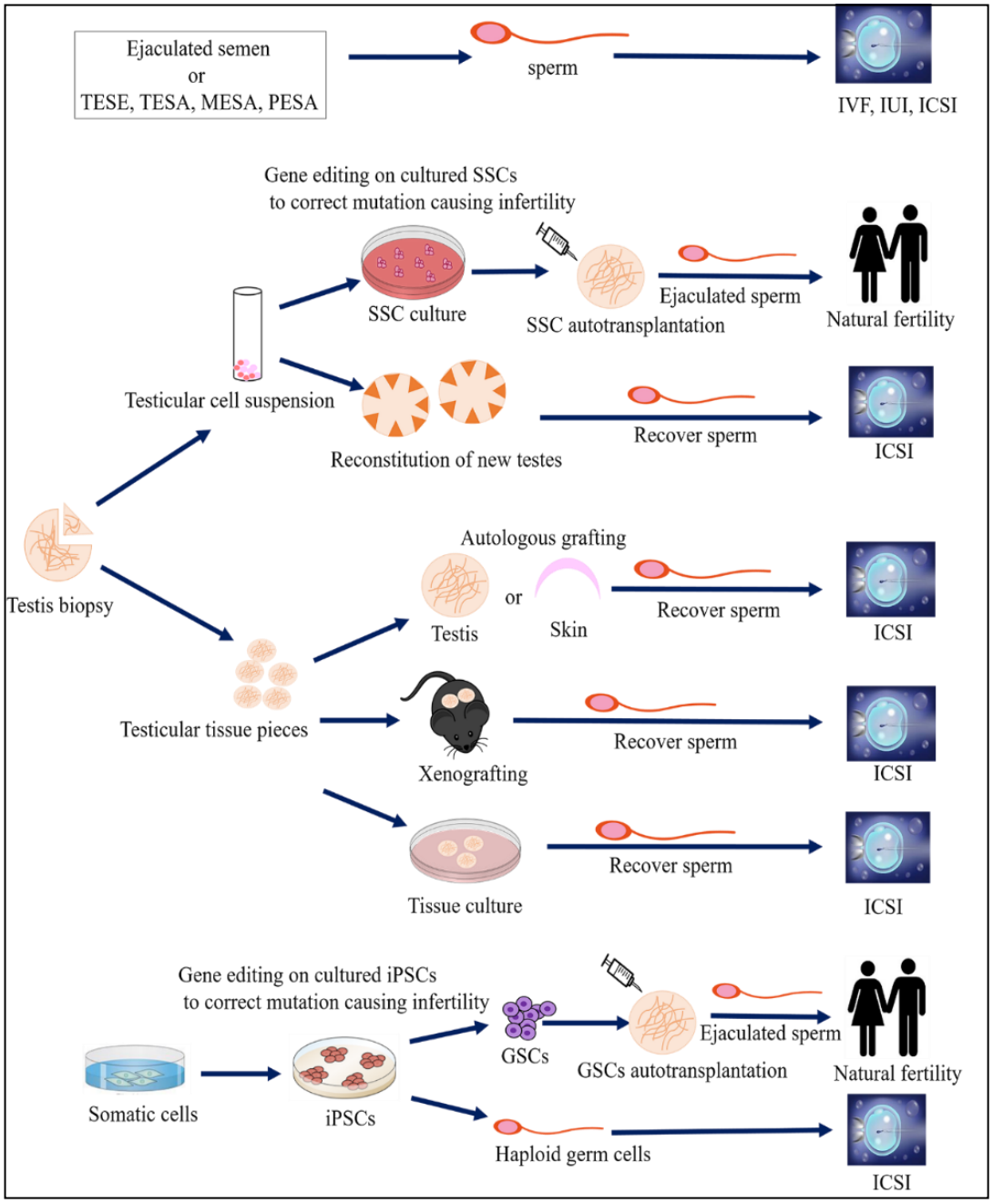

Figure 2.2. Standard (clinic) and experimental approaches are shown for treatment of male infertility. Figure was modified from reference (107).

2.3. Spermatogenesis and Testicular Niche

Spermatogenesis is a complex, productive, and ordered process that maintains the continuous generation of spermatozoa from SSCs (156). Testis-specific SSCs sustain germ stem cell pool by self-renewal, have differentiation abilities to generate

haploid germ cells, and play essential role to pass genetic information to the future generations (157).

In mice, primordial germ cells (PGCs) are precursors of male germline. They first become identifiable on embryonic day 7.5 (E7.5) as a cluster at the allantois bud. Migration of PGCs to settle in the gonadal ridges through hindgut endoderm (158, 159) and dorsal mesentery occurs at E11.5 (160). In the gonads, they become gonocytes at E12.5 that are surrounded by SCs form seminiferous cords, enter mitotic arrest at E13.5, and cease to proliferate until about postpartum day 1-2. By several days after birth, gonocytes resume proliferation and move from center area of the seminiferous cords to the basement membrane, and transit into the spermatogonia (161). Spermatogenesis occurs in three crucial phases: proliferation of spermatogonia, meiosis and spermiogenesis. During first phase of spermatogenesis, single A (A_s) spermatogonia divide, they either complete cytokinesis to give rise to two new A_s (self-renewal) or are linked by intracytoplasmic bridges to generate pair A (A_{pr}) spermatogonia. Subsequent divisions of A_{pr} give rise to chains composed of four A aligned (A_{al}) spermatogonia that also divide by one or more mitosis to generate chains containing 8, 16, and/or 32 A_{al} spermatogonia. Undifferentiated spermatogonia pool is created by A_s, A_{pr} and A_{al} spermatogonia (162). There is a controversy in this field about whether stem cell activity remain entirely in A_s spermatogonia or A_{pr} and A_{al} spermatogonia have committed for differentiation (163-165). Subsequently, the A_{al} spermatogonia differentiate without undergoing mitosis into A1 spermatogonia by induction of retinoic acid (RA). The A1 cells produce A2, A3, A4, intermediate and B spermatogonia which are termed as differentiating spermatogonia by sequential five mitosis. During second and last phase of spermatogenesis, the B spermatogonia divide into primary spermatocytes that generate secondary spermatocytes and round spermatids by two meiotic divisions. Round spermatids generate mature spermatozoa by undergoing a series of morphological transformation through spermiogenesis (166).

Human PGCs are first detected during the 4^{th} gestational week within the endodermal layer of yolk sac. Between 4 and 6 weeks, PGCs move from the yolk sac to hindgut endoderm and then reach to gonadal ridges through dorsal mesentery. After colonizing into the gonads, PGCs become gonocytes and remain mitotically inactive from the 6th week of embryonic development until after birth (167). Between birth

and postnatal 2 to 3 months, the gonocytes migrate to the basal membrane and differentiate to establish the pool of A_{dark} (A_d) and A_{pale} (A_p) of spermatogonia (168). In humans, A_d and A_p spermatogonia are termed as undifferentiated spermatogonia They can be distinguished from each other according to their nuclear morphology and staining intensity with hematoxylin. A_d spermatogonia and A_p spermatogonia are termed as reserve stem cells and renewing stem cells, respectively (169). During the prepubertal stage, A_p spermatogonia give rise to B spermatogonia and spermatozoa to maintain spermatogenesis under the normal circumstances (170).

The spermatogenesis is under the regulation of a number of essential signals provided by microenvironment or niche of the testis (171). Intratubular SCs and extratubular LCs, PMCs, endothelial cells (ECs) of blood vessels, peritubular (PMs) and interstitial macrophages (IMs), secreted soluble factors, and extracellular matrix components form the niche of testis (166) (Figure 2.3.). Differentiation and self-renewal of SSCs are dependent on testicular niche cells. The niche creates a suitable microenvironment and many specific factors secreted by niche cells determine fate of SSCs. Because SCs are in direct contact with SSCs within seminiferous tubules of testis, they play central role in their proliferation and differentiation by supplying physical and chemical support. The SCs produce and secrete GDNF that is one of the most essential regulators and responsible for proliferation and survival of SSCs while suppressing their differentiation (7). GDNF signaling pathway works for proliferative effect on SSCs through corresponding receptors Ret receptor tyrosine kinase and its co-receptor GDNF-GFRα1 (170). Also, SCs promotes the proliferation and maintenance of SSCs by FGF2, so these growth factors become indispensable of the culture medium for (171). Sertoli cells also secrete paracrine factors involved in differentiation of SSCs. Those are Bone Morphogenic Proteins (BMPs), Stem Cell Factor (KIT ligand) (SCF), and the retinoic acid (RA) (172). BMP4 exhibits its effects via ALK3 and SMAD5 receptors on differentiation of SSCs (173). Recently, it has been demonstrated that BMP4 may induce the differentiation of spermatogonia through KIT receptor expression (174). Stem cell factor induces differentiation of SSCs and KIT ligand/KIT pathway also is critical to enhance the number of differentiating spermatogonia (174). To distinguish differentiating spermatogonia from undifferentiated spermatogonia, KIT receptor is used as a marker (175). Retinoic

acid drives spermatogenesis by the differentiation of Aal into A1 spermatogonia (176). Moreover, factors secreted from SCs can affect each other by several mechanism resulting in differentiation of SSCs. Retinoic acid signaling may increase the expression of BMP4 in SCs and then BMP4 may induce KIT receptor expression on spermatogonia (174). The LC, PMCs as well as PM and IM produce colony-stimulating factor (CSF1) acting as enhancer for SSC self-renewal and SSCs have receptor for this factor (177). Elongated, spindle- shaped PMC form the cellular outer border of seminiferous tubules and these contractile cells are responsible for transporting sperm (178). The PMCs have a pivotal role in secretion of transferrin, inhibin, and ABPs by SCs (179). Moreover, PMCs secrets GDNF which is crucial growth factor of the renewal of SSCs (180). In addition to these niche cells, adipocytes located within the EWAT located around the testis contribute to modulation of spermatogenesis through locally secreted products including leptin and androgens. (26, 181, 182).

Extracellular matrix has a pivotal effect to modulate spermatogenesis. Collagen α1(IV), α2 (IV), α3 (IV) secreted by SCs and the PMCs contribute to formation of basement membrane with laminin, entactin and heparin sulfate proteoglycan. Laminin receptors α6- and β1-integrin are expressed by SSCs, providing their proper homing adjacent to the basement membrane (183).

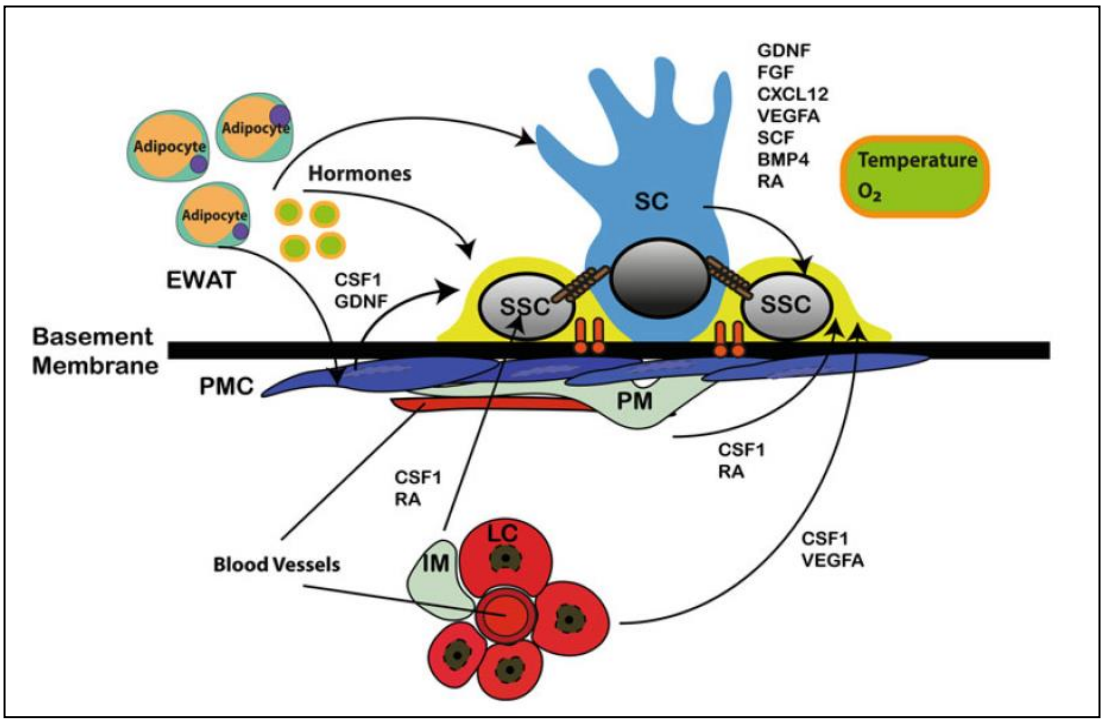

Figure 2.3. Testicular niche formed by germ cells and accessory somatic cells, secreted factors and ECM to determine fate of SSCs. SSC: Spermatogonial stem cell, SC: Sertoli cell, PMC: Peritubular myoid cell, LC: Leydig cell, PM: Peritubular macrophage, IM: Interstitial macrophage, EWAT: Epididymal white adipose tissue,

2.3.1. Isolation and Propagation of Mouse SSC *In Vitro*

Since testicular SSCs are low in number, their propagation and maintenance *in vitro* are important. However, the long term culture and expansion of SSCs have some challenges in terms of removal of somatic cells from TT to obtain a pure SSC population, determination of factors in medium, and protection of their stemness properties (11). Initial step is to isolate SSCs and remove somatic cells from heterogeneous TCS. SSC enrichment can be carried out by differential attachment (184-186), fluorescent-activated cell sorting (FACS) (10, 187, 188), and (magnetic-activated cell sorting) MACS (10, 11, 189-192) techniques. Differential attachment approach separates cells according to their attachment capabilities. Initial step is to plate the heterogeneous cell population from testis onto uncoated or matrix- coated dishes. After incubation, non-attached SSCs can be sorted via FACS or MACS by appropriate SSCs markers to obtain pure SSCs pool or BSA density gradient can be

apply to remove somatic cells and increase purity of SSCs (184-186). Various markers have been reported to enrich mouse SSCs (mSSCs). The antigenic profile of mSSCs has been detected to be ID4, PAX7, GFRa1, NANOS2, ITGA6, EPCAM, ITGB, THY1, CDH1, CD22, MCAM. A combination of determined surface markers can be used to obtain a uniform A_{undiff} spermatogonia population (162).

Second critical step is to determine appropriate culture condition in order to promote proliferation and protect stemness of the isolated SSCs. MEMα was better than DMEM for maintenance of SSCs. Specifically, GDNF was demonstrated as an essential growth factor to maintain and proliferate mSSCs in *in vitro* culture (9, 11, 189, 193). The successful long-term culture conditions for SSCs from DBA/2 gonocytes was achieved by supplementation of GDNF, LIF, EGF, FGF2 and 1% FBS on MEF (mouse embryonic fibroblast) feeder layer *in vitro* for up to 5 months. The cultured SSCs formed aggregates *in vitro* and colonizing potential of long term cultured SSCs was confirmed by transplantation into busulfan-treated sterile mice. Moreover, cultured SSCs were transplanted into infertile mice with c-kit gene defect mice. Offspring were obtained by ICSI or natural mating (7). The supplementation of media with GDNF, LIF, and 10% FBS (184) and 30% testicular interstitial fluid and 10% FBS (185) improved growth of the mSSCs obtained from ICR neonatal mice. Another research group reported the maintenance of SSCs more than 6 months by SFM conditions on STO feeder layer *in vitro*. In this study, SFM was used instead of medium supported by FBS to diminish proliferation of testicular fibroblast or the other somatic cells in testes. Furthermore, they indicated that while SSCs from DBA/2J strain mice continuously proliferated in the presence of GDNF, other mice strains required the supplementation of GFRα1 and bFGF2 to support replication (9). The doubling time of SSCs in mice was detected 5.6 day and cultured SSCs restored fertility in infertile recipient mice. Same research group compared effect of MEF, STO and MSC-1(mouse Sertoli cell line) feeder layers on C57BL/6 mSSCs in the presence of GDNF, GFRa1 and bFGF2. Even though germ cell clumps were supported initially by MEF, the growth of mSSCs on MEF was slower than mSSCs supported by STO. Survival and proliferation of SSCs were maintained on MSC1 poorly and most SSCs died on MSC-1 by 9 days (11). Testicular endothelial cells increased number and size of mSSCs colonies compared with STO co-cultures. Moreover, they maintained

neonatal mSSCs on testicular endothelial cells in the absence of GDNF and FGF for long term (194). Recently, it has been showed that mSSCs can also be maintained in feeder-free conditions. Matrigel feeder culture system supported long term of mSSCs maintenance; however, cells lost their proliferation capabilities on laminin and gelatin. Spermatogonial stem cells were cultured in medium containing 1% FBS, GDNF, LIF, EGF, bFGF. Furthermore, the cultured SSCs on matrigel were colonized after transplantation in testicular tubules (195). In another study, IGFBP-2, SDF-1, MIP-2, FGF-2 and GDNF supported expansion of mSSCs without feeder cells (194). The culture of mSSCs can be improved by reducing the atmosphere oxygen concentration. 10% O_2 significantly enhanced proliferation of mSSCs compared to atmosphere O_2 concentration *in vitro*. The size of cultured SSCs clumps with kit gene deficiency were larger in 10% O_2 condition compared to 21% O_2 condition. These cultured SSCs produced sperm after transplantation to W/W^v recipient testis and healthy offspring were born by natural mating (120).

2.4. Leptin and Its Mechanism of Action

Leptin, 16kDa polypeptide hormone, is encoded by obese (*ob*) or leptin (*LEP*) gene on chromosome 6 and 7 in mice and humans, respectively (25). Although leptin hormone is principally synthesized and secreted to the bloodstream by white adipocytes to regulate energy metabolism and control body mass, gastric mucosa mammary epithelium, bone marrow, pituitary, hypothalamus, bone, skeletal muscle placenta, and testes, have also been reported to be able to produce low amount of leptin (196) (197). Leptin not only has pivotal roles in regulating energy metabolism, but also it influences several physiological activities such as reproduction (23, 25, 198), angiogenesis (199), bone formation (200), immune regulation (201), and wound healing (202). However, the role of locally secreted leptin has not been yet determined (203).

Leptin shows its biological function via transmembrane OB-R receptors (204). To date, six isoforms OB-Ra-OB-Rf isoforms have been described as a result of alternative splicing of mRNA. Each isoform of OB-R receptor has an extracellular, a transmembrane, and an intracellular domain which is specific for each isoform (205). Based on the structural differences, isoforms can be subdivided into three classes: short

(OB-Ra, OB-Rc, OB-Rd and OB-Rf), long (OB-Rb) and secreted (OB-Re). The shorter isoforms with abbreviated intracellular domains have roles in transport of leptin across the blood–brain barrier The long one is functional isoform, responsible for cellular actions of leptin and the soluble isoform without both intracellular and transmembrane domains functions in its transport in the circulation and regulates its bioavailability (205).

Once leptin is secreted from white adipose tissue into the blood stream, it transports to the central nervous system (CNS) through the choroid plexus and circumventricular organs. Within the brain, leptin functions via the OB-Rb receptor which is expressed mainly on leptin-targeted neurons in particular nuclei of hypothalamus and brainstem (206). Binding to functional receptor of leptin initiates several pathways, including IRS/PI3K (207), JAK2/STAT3 (208), SHP2/ERK (209) (Figure 2.4.). These signaling pathways act coordinately for modulation of body weight, energy balance, and eating behavior (197). While the intracellular domain of all OB-R isoforms contains box1 motif, which is required for JAK binding, and activation, OB-Rb also includes the box2 motif which is important for STAT-binding (210). Since the functional OB-Rb isoform does not have intrinsic enzymatic activity, tyrosine kinases (mainly JAK2) phosphorylate both itself and tyrosine residues on the OB-Rb leptin receptor, after binding to receptor of leptin. Each phosphorylated tyrosine residue represents different ability for downstream signaling of leptin (197).

OB-Rb-expressing POMC and AgRP/NPY neurons are major targets of leptin action in the arcuate nucleus (ARC). Phosphorylated Tyr^{1138} by JAK2 kinase recruits the transcription factor STAT3 which facilitates transcriptional regulation of anorexigenic POMC and orexigenic AgRP, and NPY neuropeptides. Phosphorylated-STAT3 actives POMC expression, whereas suppress expression of AgRP and NPY transcription (197). Proopiomelanocortin is cleaved by prohormone convertases to generate anorexigenic a-MSH. The function of α-MSH to reduce body weight are mediated through MC3R and MCR4. Obesity phenotype and leptin resistance observed in MCR3 deficient mice (211) and MCR3 and MCR4 deficient rats (212). These findings imply that the central melanocortin system appears to play a specific function to promote leptin mediated weight loss. Both AgRP neuronal activity and the expression of orexigenic neuropeptides are inhibited by leptin hormone which results

in decreased food intake. AgRP shows its orexigenic function by acting both as a MC4R inverse agonist and an α-MSH antagonist. SOCS3 proteins via binding to p-JAK kinase or interacting directly with tyrosine phosphorylated Tyr^{985} receptors inhibit JAK/STAT3 signaling. Enhanced hypothalamic expression of SOCS3 in hypothalamus is a major mechanism in order to limit actions of leptin in obesity (213). The phosphorylation of Tyr^{985} allows binding of SHP2 to OB-Rb receptor and recruits the Grb2. It mediates activation of ERK pathway that induces expression of specific target genes participating proliferation and differentiation of cells. Leptin is also able to initiate the ERK signaling pathway independent of SHP2 (214). Moreover, leptin regulates PI3K signaling through IRS phosphorylation through independently of phosphorylation of tyrosine residues on OB-Rb receptor. PI3K integrates leptin and insulin signaling pathways in hypothalamic neurons. While PI3K activity is increased by leptin directly in POMC neurons and suppressed indirectly by leptin in AgRP neurons, it is activated by insulin in both POMC and AgRP neurons (215).

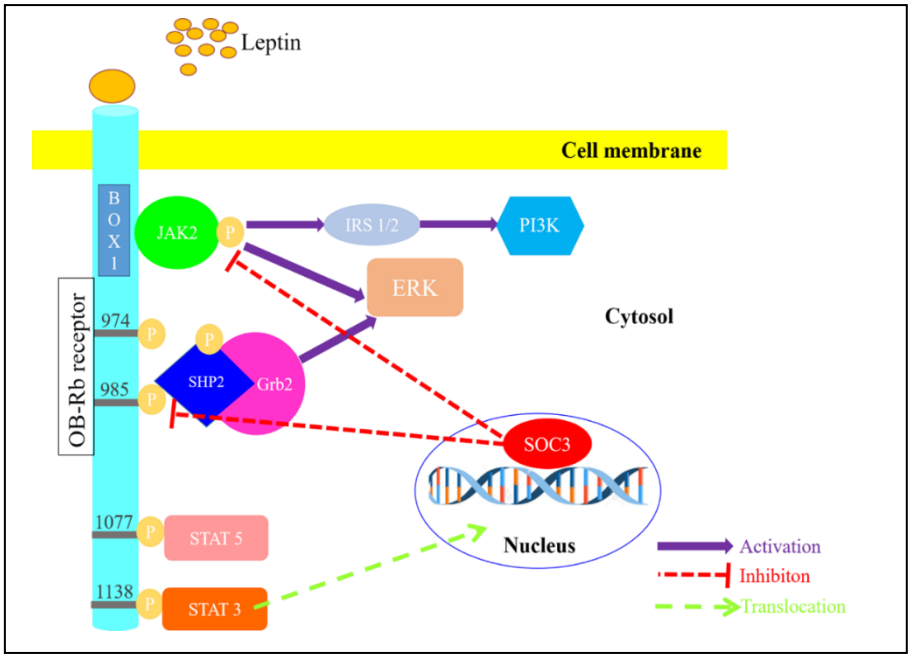

Figure 2.4. Leptin signaling via OB-Rb receptor. The binding to OB-Rb receptor of leptin induces auto-phosphorylation of JAK2 kinase which phosphorylates particular tyrosine residues on OB-Rb receptor. The phosphorylated Tyr^{1138} is required for activation of STAT3 and JAK/STAT3 pathway is inhibited by SOC3. Phosphorylated Tyr^{985} and Tyr^{1077} mediate initiation of ERK signaling pathway and activation of STAT5, respectively. JAK2 auto-phosphorylation mediates IRS- PI3K activation. Figure was modified from reference (197).

2.4.1. Effects of Leptin on Male Reproduction

In addition to role of leptin on the modulation of energy balance in the CNS by activating POMC neurons and suppressing AgRP nerouns, it serves as a signal for initiation of sexual maturation and modulation of reproduction by stimulating secretion of GnRH (24).

Puberty has been characterized the achievement of sexual development accompanied by growth of body size and behavioral changes. The sexual maturation differs from species to species in mammals and it is distinct for each sex. Changes in the GnRH are essential for regulation of reproductive function (216). Shortly after birth the hypothalamic-pituitary-gonadal (HPG) axis is activated. It is followed by a decrease in sex hormones and plasma gonadotropins levels until the onset of puberty (217). After this duration of quiescence of the HPG axis, puberty is initiated by GnRH secretion which increases gonadotropins and sex steroids and results in gonadal, somatic, and behavioral maturation (218).

Leptin's action in pubertal development and reproduction is important. Mutations of leptin receptor and congenital or acquired leptin deficiency lead to a failure to undergo pubertal maturation and infertility in human (219). Leptin serum concentrations are low in pre-pubertal period and change during pubertal development in mammals (220, 221). In woman, serum leptin levels show a continuous and progressive increase as pubertal development proceeds, whereas leptin levels increase shortly before and during the early stages of puberty in male and decline thereafter as a result of repressive effect of testosterone production on leptin synthesis by adipocytes (222). Leptin exerts its action on initiation of puberty through stimulating GnRH release in the hypothalamus (223, 224). Despite the fact that OB- Rb receptor is highly expressed in the specific nuclei of hypothalamus, GnRH neurons do not express leptin receptor (225). Leptin acts through other pathways in the brain to regulate GnRH release. In this regard, kisspeptins have been emerged as a major candidate for this essential function (224, 226). Leptin activates GnRH neurons via kisspeptin neurons in the ARC and modulates the HPG axis indirectly (227). Kisspeptins activate the receptor GPR54 and inactivation of Kiss1 or its receptor leads to pubertal initiation failure and infertility (228). Kiss1 neurons are found in the ARC and the rostral periventricular area of the 3rd ventricle (RP3V). In addition to kisspeptins, several

neuropeptides such as POMC, CART, NPY, and AGRP have been associated with leptin's function on GnRH neurons (229, 230). Furthermore, neurons in premammillary nucleus (PMN) express abundant leptin receptor and have projections on both GnRH and kisspeptin neurons. However, the other ways do not appear to have significant roles in leptin hormone activity on the HPG axis.

Besides the above-mentioned functions in the hypothalamus to initiate sexual maturation and regulation of reproductive functions, leptin may have local direct effects on the function of testis and spermatogenesis. The spermatogenic cells of mouse testis express leptin depending on the stage of spermatogenesis and cell-type during the PN period and type A spermatogonia, spermatocytes and the LCs express OB-Rb receptors (28). Human spermatozoa and spermatocytes secrete leptin; human LCs and spermatozoa carry OB-Rb receptors (27). The presence of leptin receptors on the cells of testes suggests that leptin may also have a direct role in spermatogenesis and testicular endocrine function.

Leptin deficient mice (*ob/ob* mice) are infertile (231-234). Gonadotropin levels are lower, testes are smaller with several morphological abnormalities, seminiferous tubules include fewer sperm and LCs are smaller with less cytoplasmic content in these animals comparing to wild type. Those animals show impaired spermatogenesis, increased spermatogenic cell apoptosis, shifts in enzymes related to spermatic activity and steroid pathway (231-233) . Replacement of leptin (daily 0.1-3 mg/kg for 12 weeks or 72 hour) improved function of LCs and restored spermatogenesis in *ob/ob* mice (234). Leptin treated type 1 diabetic mice (100 μg, subcutaneous, twice daily for 2 weeks) exhibited a larger body size, seminal vesicles, and testes than control group. Moreover, sperm could successfully fertilize ooctyes in leptin-treated mice (235). On the other hand, 0.1 μg/100μl (≈ 3 μg/kg) for 2 and 4 weeks intraperitoneal (IP) leptin administration reduced spermatogonial cell nucleus and seminiferous tubules diameter in mice (236). Daily 3 mg/kg IP leptin injection for 2 weeks reduced sperm concentration, motility and increased apoptotic germ cells, but leptin did not show negative effect at 0.1-0.5 mg/kg doses in mice (237). 5-60 μg/kg IP leptin for 6 weeks decreased sperm counts and disrupted sperm morphology in rats (196, 238).

2.4.2. Proliferative Effect of Leptin on Stem and Mature Somatic Cells

The effect of exogenous leptin has been shown on several somatic stem and differentiated cells at different doses and time intervals. Leptin stimulated porcine skeletal myoblast proliferation in a dose dependent manner (from 10 ng/ml to 80 ng/ml). The proliferative effect became saturated at 96–120 hours with supplementation of 20 ng/ml leptin. The proliferative effect of leptin were evaluated by MTT assay and cell cycle analysis showed that 20 ng/ml leptin for 48 h led to increased cell population in S+ G2/M phase (32). Wagoner et al (31) investigated effect of exogenous leptin on cultured rat stromal vascular cells (SVC) and preadipocytes from adipose tissue treated with 5, 50, 100, 250, or 500 ng/ml of leptin. 3H-thymidine incorporation assay revealed that while 50 ng/ml leptin stimulated proliferation of preadipocyte, 250 and 500 ng/ml leptin inhibited proliferation of SVCs and preadipocyte. Adipose rich stroma in human breast regulated breast stem cell pool via leptin. Leptin level of human mammary adipose tissue had the linear relationship with stem cell number in mammospheres derived from human breast tissue. When explants from adipose tissue were used directly, number of mammospheres increased with conditioned media prepared from explants. Furthermore, exogenous 100 ng/ml leptin treatment increased stem cell re-newal *in vitro* (33). Exogenous leptin at 1 to10 nM induced the generation of endothelial cells (ECs) promoting angiogenesis in embryonic vessels from embryonic stem cells (ESC). Leptin treated embryoid bodies (EBs) derived from ESC showed enhanced ECs markers and JAK/STAT3 acts on in this differentiation process (239). Leptin caused an increase in mouse embryonic mesenchymal stem cell (MEMSC) number demonstrated by increasing thymidine uptake. Leptin induced cell proliferation for 72 hours in a dose-dependent manner; the minimum stimulative dose was 50 ng/ml, and maximal stimulative effect of leptin occurred 100 ng/ml. Leptin treatment did not change cellular phenotypic features (30). Rat vascular smooth muscle cells (VSMC) from aorta were treated with a range of leptin doses (20-200 ng/ml) for 24, 48 and 72 hours. Cell cyle analysis by flow cytometry (FCM) and MTT assay revealed the maximal proliferative effect was 100 ng/ml and p-ERK1/2 expression was highest in 100 ng/ml leptin- treated cells (37). When rat aortic smooth muscle A10 cells were cultured with leptin doses (from 1 to 100 ng/ml) for 72 h; maximal effective dose of leptin to proliferate cells was 10 ng/ml

evaluated by CellTiter 96 AQueous One Solution kit. Phosphorylation of ERK1/2 in A10 cells was assessed 30 min after treatment with 1 and 10 ng/ml of leptin. Data showed that ERK1/2 phosphorylation was significantly induced the by leptin in a dose-dependent manner; maximal effective dose was 10 ng/ml (38). Human umbilical vein (HUVEC) and human microvascular endothelial cells (HMEC) were proliferated by 10 nmol/l leptin for 48 hours determined by 3 H-thymidine incorporation (35). Table 2.1. summarizes *in vitro* effect of leptin on stem and mature somatic cells.

Table 2.1. *In vitro* effects of leptin on stem and mature somatic cells.

Type of cell	Doses of leptin	Methods	Results	Effective signal pathway(s)	Reference
Porcine skeletal myoblast	10, 20, 40,80 ng/ml	MTT and cell cycle analysis by FCM	20 ng/ml for 48 h increased proliferation		(32)
Preadipocyte and SVCs	5, 50, 100, 250, 500 ng/ml	3H-thymidine incorporation	50 ng/ml increased proliferation, 250 and 500 ng/ml decreased proliferation		(31)
Rat VSMC	20, 40, 80, 100, 200 ng/ml	Cell cycle analysis by FCM and MTT	Maximal proliferative effect at 100 ng/ml	Expression p-ERK1/2 highest with 100 ng/ml	(37)
Human breast stem cells	Explant from adipose tissue	Formation of mammosphere	Number of mammosphere increased		(33)
Human breast stem cells	100 ng/ml		Increased stem cell renewal		(33)
Embryonic stem cells	1 nM or 10 nM	Endothelial cell markers	Promoted differentiation of ESCs to ECs	JAK/STAT3 played role in differentiation	(239)
MEMSCs (C3H10T1/2)		3H-thymidine incorporation	Stimulation at 50-100 ng/ml		(30)
Rat aortic smooth muscle cells (A10)	1, 10, 100 ng/ml	CellTiter 96 Aqueous One Solution kit	Maximal proliferative effect was at 10 ng/ml	Expression p-ERK1/2 highest with 10 ng/ml	(38)
HMEC and HVEC cells	10, 50 nmol/l	3 H thymidine incorporation	Proliferative effect at 10 ng/ml		(35)

2.5. Derivation of MGCs from iPSCs

Retroviral transduction of pluripotent genes (c-Myc, Sox2, Oct4, and KLf4) into somatic cells to establish iPSCs is the one of the important breakthroughs in stem cell research (140). Even though several strategies have been emerged to overcome male infertility problem, research is ongoing to iPSCs to differentiate into MGCs for infertile males who do not have sperm or SSCs of their own. Production of MGCs

from iPSCs provides new avenues to treat infertility and it may be an ideal model for understanding molecular mechanism modulating spermatogenesis (145).

Male germ cell development from iPSCs has been widely studied in mice models (Table 2.2.). Recently several differentiation protocols were carried out to obtain MGCs through various types of somatic cells. Imamura et al. (136) utilized two differentiation methods: EB formation from iPSCs in LIF free medium and induction by RA or suspension culture of iPSCs with BMP4, GDNF, SCF, and EGF-producing cells. Mouse iPSCs derived from adult hepatocytes were differentiated into PGCLCs marked by Oct4(+) and MVH(+) expression in co-aggregation culture system; however, the cells did not express late meiotic markers in this setup. On the other hand, Oct4(-) and MVH(+) round-shaped oocyte-like structures were reported in EB. Similarly, EBs were formed by hanging drop method and germ cell induction was performed by RA. Oct(+), c-kit(-) and MVH(+) PGCLCs were maintained for 3 months *in vitro* (137). In the other report, RA treated EBs derived from iPSC differentiated into meiotic germ cells expressed VASA, c-kit and SCP3 *in vitro* culture conditions. (138). In both studies, miPSCs were transplanted with neonatal mice TCS into backs of nude mice to ascertain differentiation of miPCS into MGCs. Although some iPSCs were observed in rebuilt seminiferous tubules; they were not able to differentiate into meiotic cells after transplantation. Neonatal mice TCS had supportive effect on iPSCs for their incorporation into new organized seminiferous tubules, but they were not enough to provide adequate environment for full spermatogenesis (137, 138). Zhu et al. (140) indicated that iPSCs can be differentiated into SSCs *in vitro*. Embryoid bodies were formed from iPSCs by LIF free medium and RA was used for male germ cell induction. The iPSCs were differentiated to GFRα1(+) and VASA(+) SSCs and the SSCs were subsequently transplanted into busulfan- treated mice and SCP3(+) late meiotic cells were shown in the recipient mice. Retinoic acid or testosterone administration induced the haploid MGCs differentiation from iPSCs combined with formation of EB. MVH(+), CDH1(+) and SCP3(+) cells were shown in the EBs (141). BMP4 supplementation promotes differentiation of iPSCs into MGCs. When EBs were treated with several doses of BMP4 or Noggin, BMP4 upregulated Vasa, c-kit, and Scp3 via Smad 1/5 pathway and activated Gata4, Id1 and Id2 pathways, whereas Noggin supplementation decreased expression of those

markers (139). The PGCLCs derived from miPSCs provided complete spermatogenesis in another study. After PGCLC induction, only 20D17 iPSC line differentiated into functional sperm *in vivo* which resulted in birth of healthy offspring. During this protocol, iPSCs initially were differentiated into epiblast like cells (EpiLCs) using EpiLC differentiation medium containing bFGF and activin A and then EpiLCs differentiated into PGCLCs by BMP4, BMP8b, SCF and EGF. The group also identified Integrin-β3 and SSEA1 as markers to isolate PGCLCs to regenerate spermatogenesis after transplantation to infertile mice (143). Another group generated PGCLCs from iPSCs derived from adult tail tip fibroblasts and MEFs using the previous method reported by Hayashi et al. (143). This group induced the PGCLCs to germline stem cell- like cells (GSCLCs) which were identical to SSCs and de-differentiated them back to embryonic germ cell-like cells. In this study, PGCLCs were cultured at least 16 day in presence of RA, BMP4 or by their combination differently from Hayashi et al. (143). Combination of BMP4 and RA not only proliferated PGCLCS but also induced PGCLCs to differentiate into GSCLCs (142).

Based on research in mice, different protocols (spontaneous differentiation, addition of cytokines, overexpression of male germ cell inducers, co-culture with gonadal stromal cells and xeno-transplantation) have been used to generate MGCs from human iPSCs (hiPSCs) (Table 2.3.) (2, 144-149, 151-153, 240). The co-differentiation of iPSCs on human fetal gonadal stromal cells isolated from gonadal ridges of 10-weeks- old fetus enhanced generation of PCGs *in vitro*. Several markers to characterize the PGCs were determined in the first trimester (5-9 weeks) of human development *in vivo* since human PGCs are known to be heterogeneous. While PGCs were positive for VASA, c-kit, PLAP and SSEA1 from 5 to 9 weeks, PLAP expression diminished at 7 weeks of development and its expression is absent by 9 weeks of development. This report showed that iPSCs became PGCs after 7 days of differentiation *in vitro*; which corresponds with developmental window of human gestation *in vivo* (145). Although supplementation of BMP4, BMP7 and BMP8b induced MGCs differentiation by increasing expression of VASA and DAZL in iPSCs derived from fetal and adult fibroblasts, the number of meiotic cells did not substantially increase. Overexpression of VASA, BOULE, DAZ, and DAZL stimulated differentiation of hiPSCs into acrosin (+) post-meiotic haploid cells (151,

152). Post-meiotic germ cells can also be generated from hiPSCs without genetic manipulation. Eguizabal et al. (153) succeeded differentiation of hiPSCs reprogrammed from cord blood and keratinocytes into haploid germ cells *in vitro*. In this differentiation protocol, hiPSC initially were maintained with hESC media without FGF. Subsequently, cells were treated with RA for 3 further weeks. At the end of this period, sorting was performed and cells were treated with Forskolin, LIF, FGF and CYP26 inhibitor R115866 for 2,3, and 4 more weeks. However, imprinting re-establishment was not complete in the differentiated cells. It has also been demonstrated that using standardized mouse SSC culture conditions, hiPSCs can be differentiated into spermatid-like cells (240). In this protocol, hiPSCs were initially differentiated into spermatogonia and then these cells gave rise to post-meiotic round spermatids. Moreover, the haploid spermatid cells presented uniparental genomic imprints similar to human sperm on two loci: H19 (paternally imprinted) and insulin like growth factor 2 (IGF2) (maternally imprinting) (240). Zhao et al. (2) utilized similar protocol with Easley et al. (240) to assess developmental potential of spermatogonial like cells (SLCs) from iPSCs derived from NOA patients. Standardized mouse SSC culture condition was optimized by removal of 2-mercapthoethanol and addition of vitamin C and xeno-free serum replacement was used instead of BSA. In addition, SLCs were efficiently cultured without any feeder cells. Induced pluripotent stem cell lines from NOA patients with Sertoli cell-only syndrome showed reduced SLC and haploid cell formation. By contrast, the number of SLCs formed by iPSC lines from NOA patients with AZFc microdeletion was normal and they exhibited slightly fewer haploid cell (2). The Fragile X male patient-derived iPSC lines were grown in medium (4i medium) including four inhibitors in addition to TGF-β1, LIF, and bFGF. Primordial germ cells like cells were generated by two steps. To preinduce, iPSCs were cultured for 2 days in FGF, TGF-β1 or Activin A and ROCK inhibitor. After preinduction, they were plated on ultra-low cell attachment well in the presence of BMP4 or BMP2, LIF, SCF EGR, ROCK inhibitor. Moreover, they showed that CD38/TNAP were consistent markers for hPGCLCs isolation differentiated from hiPSC without any reporters (144). The hİPSCs derived from peripheral mononuclear blood cells (PMBCs) can be differentiated into mesoderm/primitive streak like-cells (MeLCs) by WNT signaling agonist and Activin

A, and then generate PGCLCs in response to BMP4. Induction, proliferation and survival of PGCLCs required different signal molecules. While BMP4 was essential for induction, SCF, LIF, and EFG were essential for maintenance of PGCLCs. Transcriptomes of the PGCLCs were identical to PGCs of non-human primates (148). It has been also reported that defined and stepwise differentiation system with different cytokine combinations induced differentiation of PGCLCs from hiPSCs. The iPSCs differentiated into a heterogenous mesoderm-like cell population by combination of BMP4, activin A and bFGF. To induce PGCLCs, BMP4, LIF, and ROCK inhibitor Y-27632 were added into culture medium. Additionally, epigenetic reprogramming in the generated PGCLCs was globally identical to PGCs *in vivo* (149).

Since germ cell niche is required to promote successful meiosis *in vivo,* transplantation of MGCs derived from hiPSC into human testis is critical step before clinical applications. However, transplantation has not been applied yet in human testis because of ethical and safety issues. Durruthy-Durruthy et al. (146) and Ramathal et al.(147) transplanted hiPSC into sterile murine in order to evaluate their differentiation potential. Integration-free iPSCs were generated via mRNA-based reprogramming with Yamanaka factors alone (OSKM) or combination of Yamanaka factors with VASA (OSKMV). The appearance of OSKMV reprogrammed colonies was similar to that of OSKM colonies. Both the transplanted OSKMV and OSKM iPSCs differentiated into PGCs, but GFRα1 staining was limited to only OSKMV cells and OSKM cells formed tumors outside of the seminiferous tubules (146). The researchers also transplanted hiPSCs produced from fertile and infertile men to mouse seminiferous tubules. Although AZF-intact and AZF-deleted derived hiPSCs could produce PGCLCs, AZF-deleted iPSC lines produced fewer germ cells-like cells (GCLCs) with shifted expression of specific proteins and were restricted to produce PGCLCs following transplantation. In addition, AZF deleted and AZF intact iPSCs formed embryonal carcinoma or yolk sac tumors outside of the seminiferous tubule (147).

Table 2.2. *In vitro* or *in vivo* differentiation of MGCs from miPSCs.

Sources of stem cells	Source donor cells	Methods	Derived cells	References
Mouse iPSCs	Adult hepatocytes/retroviral transduction	EB formation and RA induction or suspension culture (with BMP4, GDNF, SCF, and EGF-producing cells (M15-4GF cells).	Oct4(+) and MVH(+) PGCLCs No expression of late meiotic markers	(136)
Mouse iPSCs		2-step induction (EpiLCs and PGCLs)	PGCLs Spermatozoa in vivo Healthy offspring	(143)
Mouse iPSCs	Neural progenitor cells/retroviral transduction	EB formation and RA induction, in vitro Transplantation iPSC derived MGCs with neonatal TCS	VASA(+), c-kit(+) and SCP3(+) meiotic germ cells, in vitro VASA (+), SCP3 (-) MGCs in reconstituted seminiferous tubules	(138)
Mouse iPSCs	Neural progenitor cells/retroviral transduction	EB formation and RA induction, in vitro Transplantation of GFRα1 (+) and VASA (+) cells , in vivo	GFRα1(+) and VASA (+) cells, in vitro SCP3 (+) late meiotic cells, in vivo	(140)
Mouse iPSCs	Mouse embryonic fibroblast/retroviral transduction	EB formation and RA and/or testosterone induction	MVH (+), CDH (+) and SCP3 (+) cells	(141)
Mouse iPSCs	Mouse embryonic fibroblast and adult tail–tip fibroblast/retroviral transduction	2-step induction (EpiLCs and PGCLs)	Recovery of spermatogenesis, SCP3(+) spermatocytes after transplantation of PGCLCS Induction of PGCLCS into GSCLCs in vitro by combination of BMP4 and RA	(142)
Mouse iPSCs	Neural progenitor cells/retroviral transduction	EB formation and RA induction, in vitro Co-transplantation of mİPSCs with neonatal TCS, in vivo	PGCLCs, in vitro MVH(+) iPSCs in reconstituted seminiferous tubules structures, in vivo	(137)
Mouse iPSCs	Neural progenitor cells/retroviral transduction	EB formation and BMP4	Upregulation of Vasa, c-kit and Scp3 protein and gen levels	(139)

Table 2.3. *In vitro* or *in vivo* differentiation of MGCs from hiPSC

Sources of stem cells	Source donor cells	Methods	Derived cells	References
Human iPSCs	Dermal fibroblast	Co-culture with human fetal gonadal stromal cells	PGCs Identifying and isolating human PGC during the first trimester in vivo	(145)
Human iPSCs	Human fetal-derived İPSC line (IMR90) Human adult-derived iPSC line (iHUF4) lentiviral transduction	BMP4, BMP7, BMP8b Overexpression of BOULE, DAZ, and DAZL	PGCs Meiotic cells and haploid cells (acrosin (+) spermatid)	(151)
Human iPSCs	Keratinocytes and cord blood/retroviral transduction	3-step method 3 weeks in absence of any growth factor 3 weeks in presence of RA 4 weeks in presence of LIF, FRSK, bFGF and CYP26 inhibitor	PGCs, haploid acrosin(+) spermatid	(153)
Human iPSCs	Foreskin fibroblast	Standardized mouse SSC culture condition	Spermatogonia-like cells: CDH1(+), UTF1(+), and PLZF(+) Spermatocyte-like cells: HILI(+) and HIWI(+) Haploid cells : Acrosin(+)	(240)
Human iPSCs	Fetal and adult fibroblast	Overexpression of DAZL and /or VASA	Acrosin (+) haploid cells	(152)
Human iPSCs	Dermal fibroblasts	mRNA-based reprogramming with Yamanaka and VASA xeno-transplantation	PGCLCs and pre-meiotic germ cells, GFR1a(+) cells	(146)
Human iPSCs	Dermal fibroblasts from fertile and azospermic men lentiviral reporgramming	BMP4, BMP8, RA, LIF in vitro xeno-transplantation	PGCLCs and gonocyte-like cells	(147)
Human iPSCs	Fragile X male patient somatic cells	To preinduce: FGF, TGF-β1 or Activin A and ROCK inhibitor To induce: BMP4 or BMP2, SCF, EGF, LIF, and ROCK inhibitor,	PGCLCs	(144)
Human iPSCs	iPSC lines (393.2 and SA8/25)	To obtain mesoderm-like cell population: BMP4, ActA, bFGF To obtain PGCLCs: BMP4, LIF	PGCLCs	(149)
Human iPSCs	PMBCs	Activin A, Wnt signaling antagonist CHIR99021, BMP4, SCF, EGF, LIF	PGCLCs	(148)
Human iPSCs	Skin fibroblast or PMBCs from non-obstructive azoospermia patients /retroviral transduction or non-integrated episomal plasmid	Standardized mouse SSC culture condition (without 2-mercaptoethanol, with C vitamin, xeno-free serum)	PLZF+/GPR125+/CD90+ spermatogonium–like cells, haploid cells	(2)

2.6. Gene Editing Technology with CRISPR/Cas9

Recent developments in gene editing technologies with programmable nucleases, especially CRISPR/Cas9 system, have opened up new avenues in both fundamental research and clinical therapies (241). Gene editing technology is a mechanism that creates dsDNA at a desired location via a sequence-specific nuclease and edits by repair mechanisms (242). There are two major types of site specific nucleases to edit the genome: protein guided tools (TALEN, ZFN) and RNA inducible nucleases (CRISPR/Cas9) (243). The protein guided tools consist of a DNA binding domain and a DNA cleaving domain. FokI dimer induces cleavage of genomic DNA, when the complex links to the defined position, the Zing finger nucleases consist of tandem repeating DNA-binding domain that recognizes a 3- to 4-bp DNA sequence. On the other hand, series of repeated 33-35 amino acid sequence constitute DNA-binding domain of TALE proteins. The 12^{th} and 13^{th} amino acids within a TALE repeat known as repeat variable di-residues (RVDs) have essential roles in DNA recognition. Each RVD specifically recognizes a single bp (244). On the other hand, CRISPR/Cas9 tool recognizes the target region by sgRNA and the Cas9 nuclease creates a DSB underneath the RNA/DNA hybrid complex (245). While protein guided systems need complex vector constructions for creating fusion proteins at each desired location, RNA molecule that is complementary to the gene of interest provides CRISPR/Cas9 specifity (242). In addition to being easy to use and cheap, the efficiency of CRISPR/Cas9 tool is equal to or greater than the ZFN and TALEN genome editing methods, especially in mammalian cells.

CRISPR was first discovered as an adaptive immune system to protect bacteria from invasive phages or other genetic elements (246). In the bacteria CRISPR locus, protospacers (from invasive DNA sequences) are inserted as spacers and serve as specific recognition in order to destroy any foreign DNA sequences matching the protospacers (247). Invasive DNA is firstly cleaved into small pieces and then incorporated into the CRISPR locus. In the next step, incorporated sequence is transcribed into precursor CRISPR RNA (pre-crRNA) and processed into small CRISPR RNA (crRNA). In the last step, crRNA forms a complex with the Cas9 endonuclease assisted by trans-activating crRNA (tracrRNA). This complex then detects and destroy target DNA including 20-nucleotide crRNA complementary

sequence next to the PAM sequence (248). The PAM sequence is distinguished by a NGG sequence- any nucleotide (N) and two guanines (GG)- after approximately 20 bp of invasive DNA and Cas9 cleaves the DNA 3 bp before the PAM sequence. DNA cleavage is carried out by two domains to destroy invasive DNA: the HNH domain, which cuts the strand complementary to the crRNA-guide sequence, and the RuvC-like domain, which cuts the non-complementary strand (249). Although three types of CRISPR-Cas system have been discovered so far, type II system has been identified as a tool for genome editing (241). Cleavage of both DNA strands are corrected via two main pathways: NHEJ pathway or HR. In the absence of a donor template, DSBs are re-ligated via NHEJ pathway, which results in insertions and deletions (indels) (250). On the other hand, HR pathway is activated to induce specific insertions, deletions or mutations in the presence of a donor template (Figure 2.5.). Induction DSBs by Cas9 nuclease at desired location under the guidance of custom sgRNA performing function of tracrRNA:crRNA duplex in designed CRISPR system allows introduction or correction of mutations in cells by using donor template (251, 252).

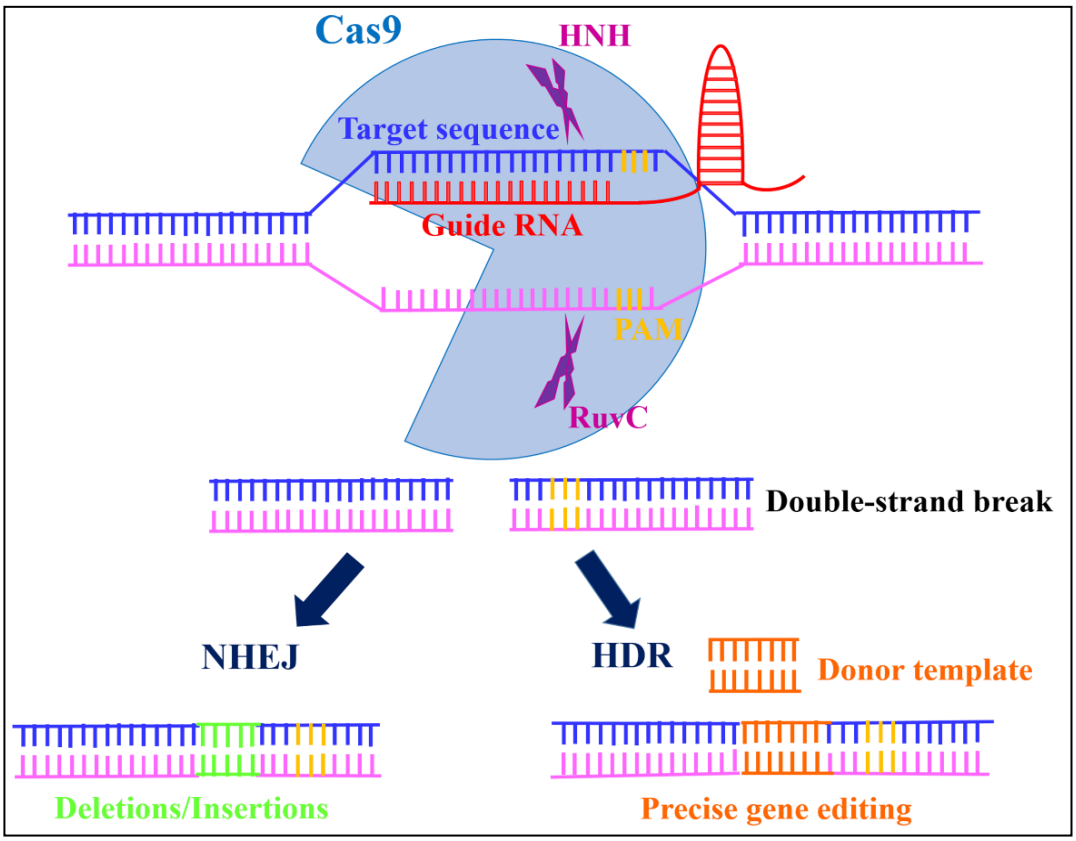

Figure 2.5. Mechanism of CRISPR/Cas9 gene editing.

2.7. Utilization of CRISPR/Cas9 in hiPSCs to Treat Single Gene Disorder

In recent years, CRISPR/Cas9 gene editing tool could be applied for deletion or correction of deleterious mutation that causes of the disease in mammalian cells (253). Creation of hiPSCs from somatic cells and then correction of the mutation by gene editing tool is the possible strategy for clinical applications. Until now, correction of mutation in hiPSCs using nucleases has been succeeded in various single gene disorders including, sickle cell disease (SCD) (254), β-thalassemia (255, 256) Duchenne muscular dystrophy (DMD) (257) , hemophilia A (258) and B (259), cystic fibrosis (CF) (260) either via correction of mutated endogenous gene or via insertion of an efficient gene into a safe harbor locus. In addition to single gene disorders, CRISPR/Cas9 could be used viral mediated infections such as HIV.

In gene therapy, mutation in the cells can be corrected via two main approaches: *ex vivo* and *in vivo* gene editing. Target cells are removed from the body,

edited using a designer nuclease to correct mutation and then auto-transplanted into the host which prevents complications because of immune rejection in *ex vivo* gene therapy. On the other hand, *in vivo* gene editing approach involves direct transfer of designer nucleases and donor templates into the body (261). Each approach has advantages and disadvantages and they are performed differently to cure particular diseases. There have been several attempts of therapeutic applications for single gene disorders with genome editing using iPSCs.

Mutations in the CFTR gene encoding epithelial chloride anion channel cause chronic and progressive auotosomal recessive disorder CF. Mutations in CFTR leads to fluid transport defect resulting in thicker mucus which brings about obstructions in the multiple organs (262). Firth et al (260) accomplished to correct mutation in iPSCS from patients with homozygous phenylalanine deletion at position 508 in CFTR gene using CRISPR/Cas9 tool combined with piggyBac system. The mutation corrected iPSCs were differentiated into lung epithelial cells. Moreover, the chloride channel function restoration and normal CFTR expression were shown in differentiated lung epithelial cell

Mutations in the dystrophin gene found on the X chromosome cause DMD. This gene consists of 79 exons and several types of mutation in exon sequences cause DMD (263, 264). Three ways were tested to correct mutation in DMD patients diagnosed with a deletion of exon 44 in dystrophin gene. These are skipping of exon 45, frameshifting in exon 45, and exon 44 knock-in. Furthermore, the gene corrected iPSCs were successfully differentiated into skeletal muscle cells expressing functional DMD protein. Differentiated skeletal muscle cells derived from mutation corrected iPSCs had dystrophin protein expression with all three approaches. However, the last of these strategies was the most effective to restore full-length dystrophin protein (257).

Genetic mutations in coagulation factors VIII and IX cause X linked recessive inherited bleeding disorders hemophilia A and B. Nearly half of all hemophilia A cases are caused by two gross chromosomal inversions 140 kbp or 600 kbp in introns 1 and 22 of the F8 gene, respectively (265). CRISPR/Cas9 tool was used to revert 140 kb and 600 kb inversions to WT situation in iPSCs derived from hemophilia A patients. Epithelial cells generated from inversion-corrected iPSCs exhibited expression of the

F8 gene *in vitro* and transplantation of endothelial cells to hemophilic mice functionally rescued F8 deficiency (258). In the other study, to cure hemophilia B, AAVS1- Cas9-sgRNA plasmid targeted AAVS1 locus and AAVS1-EF1a-F9 cDNA-puromycin donor plasmid was incorporated into the AAVS1 locus. They were transfected via electroporation into iPSCs derivated from PMBCs. Hepatocytes were generated from iPSCs successfully and they were transplanted into (NOD/SCID) mice. Antigen hFIX could only be detected in the short term (259).

β-thalassemia (266) and SCD (267) are autosomal recessive inherited disorders both resulted from mutations in the HBB gene. Correction of mutations in HBB by designer nucleases using patient specific iPSCs from somatic cells, differentiation of iPSCs into hematopoietic stem cells, and then transplantation of hematopoietic stem cells into patients provides an ideal therapeutic solution for this patients. This strategy has already been carried out using CRISPR/Cas9 gene editing tool in both SCD (254) and β-thalassemia patients (255, 256) . Huang et al. (254) corrected one allele of the SCD HBB gene in hiPSCs reprogrammed from blood cells of SCD patient with a homozygous missense point mutations in the HBB gene via HR pathway with a donor template. Erythrocytes were differentiated from gene corrected iPSCs expressed high level of HBB mRNA. CD17 (A-T) homozygous point mutation in HBB was corrected in iPSCs using CRISPR/Cas9 based on HR method. Mutation corrected iPSCs showed higher hematopoietic differentiation efficiency when compared to uncorrected iPSCs (256). To correct mutation of -28A/G and TCTT deletion in exon 2 of HBB gene in the iPSCs derived from patient with β-thalassemia, CRISPR/Cas9 gene editing tool was combined with the piggyBac transposon. Differentiated erythrocytes from gene edited iPSCs restored HBB gene expression (255).

The advent of genome editing technologies, especially CRISPR/Cas9 tool, could offer new doors for male infertility treatment. Genetic anomalies could be corrected by genome editing technologies in iPSCs from infertile male, edited iPSCs could be differentiated into germ cells, and then transplanted back to testes of patients to obtain mature sperm.

3. MATERIALS and METHOD

3.1. Assessment of Time and Dose Dependent Proliferative Effect and Mechanism of Action of Leptin Supplementation on Cultured Neonatal SSCs

3.1.1. Experimental Design

This first experimental set up of the thesis study has been conducted in Hacettepe University Faculty of Medicine Department of Histology and Embryology under the supervision of Prof. Petek Korkusuz. Hacettepe University Animal Experimentations Local Ethics Board (#2016/59/1) approved the use of animal material. A prospective randomized study with control and leptin-treated experimental SSC groups is designed in order to ascertain the proliferative potential effect of this agent. The testes were obtained from 6 day old neonatal male C57BL/6 mice. First, 6 day old testicular tissue has been characterized morphologically and SSC enriched testicular cell suspension was obtained by 30% Percoll gradient and MACS separation using CD90.2 microbeads. Cultured SSCs were treated with four different leptin concentrations (R&D Systems) (10, 50, 100, 200 ng/ml in 20mM Tris-HCI) according to the literature (37, 268-270). In this study, we assessed the dose dependent colony forming and proliferative capacity of leptin on SSCs by using colony assay, WST-1 and xCELLigence RTCA assays on days 3, 5 and 7 of culture. Flow cytometry was carried out to characterize SSCs after leptin treatment to demonstrate their stemness features. Western blot analysis was performed to study the molecular signaling mechanism related to leptin administration. (Figure 3.1.).

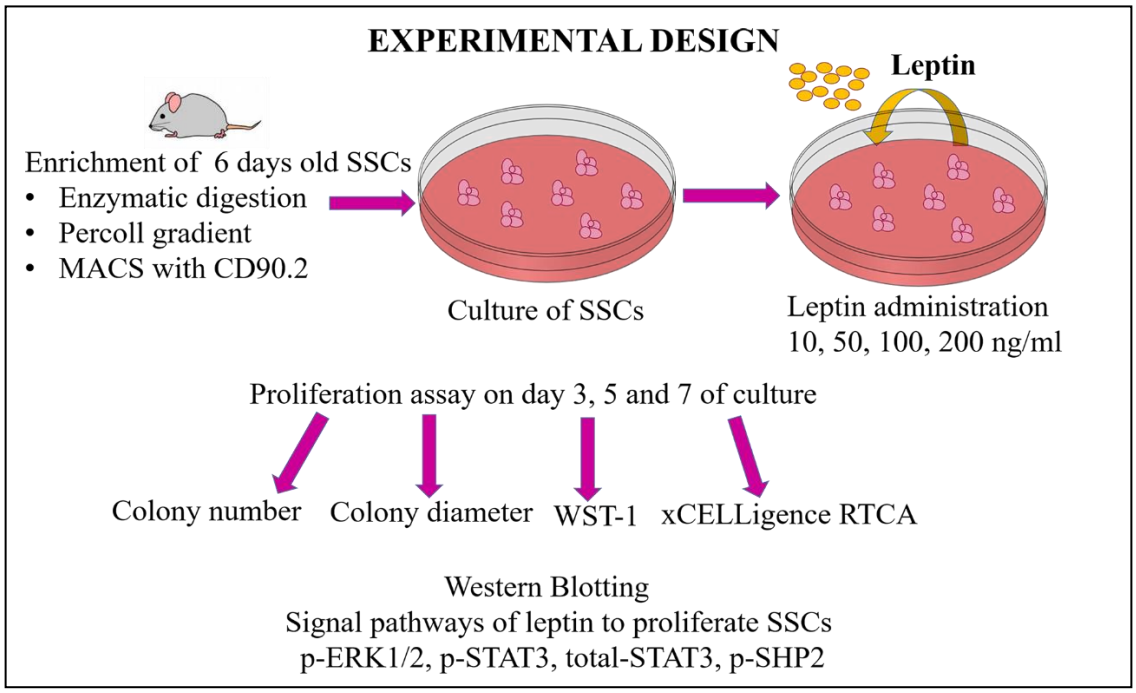

Figure 3.1. Experimental design for the assessment of time and dose dependent proliferative effect and the mechanism of action of leptin supplementation on cultured 6 day old mice mSSCs.

3.1.2. Histological Characterization of SSCs in Neonatal Testis

The presence of undifferentiated spermatogonia has been reported in testes of 5-8 day-old male C57BL/6 mice (184, 185, 189, 271). For the efficient cell isolation and culture, detection of the SSCs were undertaken by screening testicular sections obtained from 6 day old mice prior to experiments. Based on the preliminary studies we performed, we have decided to proceed all experiments using 6-days-old male C57BL/6 mice.

Bright Field Microscopy

For paraffin embedding, fixed tissues were washed and processed in an automated tissue-processing machine (Leica TP 1020 Nussloch, Germany) Table 3.1. demonstrates the tissue processing protocol.

Table 3.1. Protocol of tissue-processing for neonatal mouse testes.

Process	Solution	Time (minute)
Dehydration	70% alcohol	45
Dehydration	70% alcohol	45
Dehydration	95% alcohol	45
Dehydration	95% alcohol	45
Dehydration	Absolute alcohol	45
Dehydration	Absolute alcohol	45
Clearing	Xylene	30
Clearing	Xylene	45
Clearing	Xylene	45
Infiltration	Paraffin Wax	30
Infiltration	Paraffin Wax	45
Infiltration	Paraffin Wax	45

After processing, tissues were embedded in a paraffin station (Leica Eg1150H, Nussloch, Germany). Five-micrometer thick sections were stained with hematoxylin & eosin manually using following protocol: Initially, they were kept in the incubator at 60^{o}C overnight (ON) and deparaffinized with xylol for totally 45 min. In the next step, they were rehydratated with a series of alcohol solutions (100%, 96%, 80%, 10 min each) and stained with Harris hematoxylin for 15 min. Subsequently, differentiation and bluing were performed for 30 seconds in 1% acid alcohol and in 0.2% ammonia water, respectively. In the last step, sections were counterstained by eosin with phloxine (SelecTech Eosine with Phloxine 515, Surgipath 3801606) for 30 seconds, dehydratated with alcohol, and cleared with xylene. After stained sections were covered with Entellan, they were analyzed and imaged using a bright field microscope attached with a digital camera (Leica DM 6000 Wetzlar, Germany).

Transmission Electron Microscopy

For plastic-embedding*;* after initial fixation by 2.5% glutaraldehyde, at room temperature (RT) for 2 hours, post-fixation was performed with 1% osmium tetroxide in dark for an additional 1 hour. After washing with buffer solution, testes were processed in Leica EM TP Tissue-processor. Briefly, samples were dehydrated in a

graded series of ethanol and cleared in propylene oxide. Tissues were then infiltrated with a 3:1, 1:1, 1:3 mixture of propylene oxide:epoxy resin for 2, 2, and 8 hours, respectively They were embedded in epoxy resin and polymerized at 60ºC for 48 hours followed by 10 hours infiltration in 100% epoxy resin. Plastic blocks were cut into semi-thin and ultrathin sections that were stained with methylene blue- azure II in 1% borax solution, uranyl acetate & lead citrate, respectively. The sections were examined and imaged using JEOL-JEM 1400 (Tokyo, Japan) transmission electron microscope attached with a CCD camera (Gatan Inc., Pleasanton, CA, USA).

Immunoflourescence (IF) Microscopy

Sections from frozen tissues of neonatal testes were fixed in chilled acetone at 4ºC for 15 min. After drying, permeabilization was performed by 0.1% Triton- X solution. The sections were stained with PE-Armenian hamster anti-mouse PLZF antibody (BioLegend) at RT for 1 hour. After washing, DAPI staining was performed for 2 min. The sections were visualized and photographed by fluorescence microscope (Leica DM 6000 Wetzlar, Germany).

3.1.3. Isolation, Characterization and Culture of SSCs

Cell Isolation and MACS Separation

The testes obtained from neonatal (6-day-old) C57BL/6 mice were collected in Hank's balanced salt solution (HBSS) (Sigma-Aldrich) and tunica albuginea was removed under a dissecting microscope. The testes were digested with 0.25 % Trypsin-EDTA (4.5 ml) (Gibco) and 7 mg/ml DNase I (0.5 ml) (Sigma-Aldrich) at 37°C, for 4-5 min to generate cell suspension. After first incubation, tubules were digested for an additional 2-3 min at 37°C and enzymatic digestion was stopped with the addition of fetal bovine serum (FBS) (Gibco). Filtration of suspension was performed through a 40µm-pore nylon cell-strainer (Thermo Fisher Scientific) and centrifuged at 1400 rpm for 7 min. The pellet was re-suspended in 10 ml of PBS (Calbiochem) supplemented with 1% FBS, 10 mM HEPES (Sigma- Aldrich) MO, USA), 1mg/ml glucose (Sigma- Aldrich) 1mM pyruvate (Sigma- Aldrich), 1% penicillin and streptomycin (Hycolen). Enrichment of SSCs were done through a 30% Percoll

(Sigma- Aldrich) gradient and collected using Thy-1.2 antibody-conjugated magnetic microbeads (Miltenyi Biotec, 130-049-101). In brief, after Percoll gradient, suspension was centrifuged at 1400 rpm for 7 min and pellet was re-suspended in 180 µl of PBS-MACS including 1mg/ml glucose, 10 mM HEPES, 1% FBS, 1mM pyruvate, 1% penicillin and streptomycin and. 20 µl of CD90.2 (Thy1) magnetic microbeads were added to 180 µl of cell-suspension and mixture was incubated for 1 hour at 4°C. The mixture was washed by 2 ml of PBS-MACS and centrifuged and re-suspended in serum-free medium (SFM). Then, the suspension was loaded onto a column to collect CD90.2(+) cells. CD90.2(+) cells were further cultured on STO feeder cells.

Preparation of STO Feeder Layer

The mouse embryonic fibroblasts (STO cell line, ATCC CRL-1503) were maintained in Dulbecco's modified Eagle's medium (DMEM) with high glucose (Sigma-Aldrich) including 1% L-glutamine (Hyclone), 10% FBS, 1% penicillin-streptomycin. Growth-arrested feeder layer was prepared using mitomycin-C (Sigma-Aldrich). Inactivated STO cells were cultured as $2x10^5$ per well in 0.1% gelatin (Sigma- Aldrich) coated 12 well plate. Following isolation, SSCs were co-cultured with STO feeder cells.

Culture of SSCs

The number of CD90.2(+) testis cells and the mitotically inactivated STO feeder fibroblastic cells per well of 12-well plate were designated as $7x10^4$ and $2x10^5$ respectively. CD90.2+ testis cells were maintained in serum-free MEM-α medium (Gibco) supplemented with 0.2% bovine serum albumin (BSA) (Sigma-Aldrich), 2mM L-glutamine, 10 µg/ml holo-transferrin (Sigma-Aldrich), $3x10^{-8}$ M sodium selenite (Na_2SeO_3) (Sigma- Aldrich), 50µM mercaptoethanol (Sigma- Aldrich), 5µg/ml insulin (Sigma- Aldrich) MO, USA), 10mM HEPES (Sigma- Aldrich), 1% MEM non-essential amino acid (NEAA) solution (Sigma- Aldrich), 60 µM putrescine dihydrochloride (Sigma- Aldrich), 20 ng/ml GDNF (Biolegend), 150 ng/ml (GFRα-1 (R&D Systems), and 1 ng/ml human bFGF (Biolegend). Medium was replaced every other day.

Characterization of Isolated and Cultured SSCs

Flow Cytometry (FCM)

The SSC enriched testicular cell suspension was characterized by FCM prior to and after MACS separation. Briefly, the sample was treated with FITC conjugated rat anti-mouse CD90.2 (BioLegend) and APC conjugated c-kit (BioLegend) at 4ºC for 20 min after washing in wash buffer and centrifugation. The True-Nuclear Transcription Factor Buffer Set (BioLegend) was used for fixation and permeabilization. The sample was then labeled with PE conjugated Armenian hamster anti-mouse PLZF at 4ºC for 20 min in the dark. On day 7 of the culture, FCM was carried out by CD90.2 antibody to demonstrate whether SSCs maintain their stemness properties after leptin treatment. In brief, SSC cell suspensions were labeled with CD90.2 antibody in the dark at 4ºC for 30 min. After washing with wash buffer, samples were analyzed. Death cells were excluded by gating and; analysis was carried out by BD FACS-Diva software version 6.1.2 with 100.000 list mode events recorded for each sample. Isotype controls were used for each antibody to rule out the background labeling.

IF Labeling for PLZF and Leptin Receptor in Cultured SSCs

Ten microliter of the cultured cell suspension ($5x10^6$/ml) was placed on (+) charged slides and fixation was carried out with cold- methanol. After rinsing two times with PBS, slides were blocked with a blocking buffer including 3% BSA and 0.1% Triton- X 100 to eliminate non-specific binding. Slides were incubated for 2 hours at RT with PLZF (1:100, Santa Cruz) or leptin receptor (1:100, Novus Biologicals) primary antibody. Isotype matched normal IgG (1:50, BD Biosciences) was used as negative control. After washing with PBS, slides were treated with anti-rabbit AlexaFluor-488 or AlexaFluor-568 conjugated secondary antibody (1:200, Invitrogen) for 45 min at RT. The slides were rinsed with PBS and covered by mounting medium containing DAPI. Immunofluorescence staining was observed with a fluorescence microscope (Nikon Eclipse E600).

3.1.4. Dose-Dependent Proliferative Effect of Leptin on SSCs

Colony Forming Assay

The SSCs and the STO feeder cells were plated onto 12 well plates as $7x10^4$ and $2x10^5$ per well, respectively. Totally 3 sets of experiment were performed with 4 different concentrations of leptin in each well (0, 10, 50, 100, 200 ng/ml). The SSC colony number was calculated and the diameters of all SSC colonies were measured in control and leptin-treated groups on day 3, 5 and 7 of culture by using an inverted microscope (Leica DM6B, Westlar, Germany) attached with a computerized digital camera (Leica DFC 480, Wetzlar, Germany). All colony micrographs were captured, analyzed and the largest diameter of each colony was measured in micrometer by using an image analyzing Leica Las X software (Wetzlar, Germany) (185).

WST-1 Assay

Feeder cells were plated at $2x10^4$ cells/well in 96-well plate and they were treated with mitomycin-C (Sigma-Aldrich) for 4 hours at 37°C to inhibit cell proliferation after 2 days. Spermatogonial stem cells were placed at a density of $4x10^3$ cells in 200 µl serum-free MEM-α media into the wells of the 96-well plate and then SSCs were treated with 10- 200 ng/ml leptin to analyze possible proliferative effect. For WST analysis, the SSCs were treated with 10µl/well cell proliferation reagent WST-1 (Roche) for 2 hours at 37°C on days 3, 5 and 7 of culture. Absorbance measurement was performed at 460nm. Experiment were repeated four different times (184).

xCELLigence Real-Time Cell Analysis

To investigate dose and time dependent effect of leptin, proliferation of SSCs after leptin treatment was observed via the xCELLigence RTCA DP instrument (Roche, Switzerland). Firstly, $2x10^4$ STO feeder cells were added to 96-well e-plates (Roche, Basel, Switzerland). The STO cells were treated with mitomycin-C for 4 hours to inactivate cell proliferation. Spermatogonial stem cells were seeded into the wells of the e-plate at a density of $4x10^3$ cells and treated with medium containing different concentration of leptin (10-200 ng/ml). Each treatment condition

was measured in 6 wells and the medium was changed every other day. The impedance value of each control and leptin-treated well was monitored by xCELLigence every 1 hour for totally 7 days. A 100-µl medium was added to e-plate 96 for measurement of background values. The cell index values were normalized before addition of leptin doses. The RTCA Software v1.2.1 (OLS) was used to analyze data and calculate temporal dynamics of cellular attachment and half-maximal effective concentration (EC50) (272-274).

3.1.5. Assessment of Leptin's Proliferative Mechanism of Action on SSCs

Western Blotting Analysis

Protein levels of p-SHP2, total- STAT3, p-STAT3, p-ERK1/2 were evaluated by western blot in accordance with the literature (37, 38). Initially, SSCs were treated 114 ng/ml leptin for 30 min. Proteins were extracted by lysis buffer including protease and phosphatase inhibitors and samples were centrifuged at 4°C 10000xg for 15 min to obtain supernatant. Amount of protein was calculated by a Pierce BCA Protein Assay kit (Thermo Fisher Scientific) and 15 micrograms of protein was loaded into the gels. After samples were mixed with sample buffer, mixtures were boiled at 95°C. In the next step, samples were run on SDS-PAGE gel and transferred to PVDF membranes (Thermo Fisher Scientific). In order to prevent unspecific binding, the blocking was performed by 5% non-fat milk in PBS for 1 hour. Membranes were incubated ON with specific primary antibodies: p-SHP2 (1:2000) (Cell signaling 3751), total- STAT3 (1:2000) (Direct-Blot HRP anti STAT3, BioLegend), p-STAT3 (1:2000) (Direct-Blot HRP anti STAT3 Phospho (Tyr 705), BioLegend) and p-ERK1/2 (1:2000) (Direct-Blot HRP anti ERK1/2 Phospho (Thr202/Tyr 204), BioLegend) and secondary antibody (Goat Anti-Rabbit IgG, Secondary Antibody, HRP Conjugate (Boster) for 1 hour. Immune detection was carried out by the Super Signal West Femto Maximum Sensitivity Substrate (Thermo Fisher Scientific). The membranes were striped for incubation with anti- β-actin (Biolegend) antibody. In order to quantify protein expressions, densitometry analysis was performed utilizing Image J. Three replicates of experiments were performed for each protein.

3.1.6. Statistical Analysis

We evaluated the normality of the distribution of variables by Shapiro–Wilk test. The comparisons between multiple groups were assessed by repeated measure ANOVA with one fixed factor differences. The pair comparison was done by Sidak correction. Descriptive statistics were presented as mean ± SEM. The p values < 0.05 were considered statistically significant.

3.2. Germline Gene Editing in A *Mcm8*$^{-/-}$ Mouse Model of Azoospermia Using CRISPR/Cas9-Directed Gene Repair in iPSCs Followed by Differentiation to PGCLSs

3.2.1. Experimental Design

This experimental set up of the study has been conducted in Pittsburgh University Magee-Womens Research Institute under the supervision of Prof Kyle E. Orwig. Institutional Animal Care and Use Committee, Pittsburgh University approved the study (Protocol#: 17050289), The aim of the chapter was to transplant PGCLCs from gene corrected *Mcm8*$^{gc/-}$ iPSCs to obtain functional sperm and offspring. For this aim, illustrated working packages in Figure 3.2. were performed. Initially, *Mcm8*$^{-/-}$ iPSCs were generated from *Mcm8*$^{-/-}$ fibroblasts and they were characterized for morphological appearance, pluripotency markers and teratoma formation. Karyotype analyses were carried out to evaluate genomic stability.

For gene editing CRISPR/Cas9 tool was applied to induce DSB in *Mcm8*$^{-/-}$ iPSCs. Four different sgRNAs were designed and their efficiencies were tested in vitro and in *Mcm8*$^{-/-}$ iPSCs. Transfection methods electroporation and lipid-mediated transfection were tested and best condition to deliver Cas9 protein/guide RNA ribonucleoprotein (RNP) complex was determined in *Mcm8*$^{-/-}$ iPSCs. To induce HDR repair pathway, after DSB, repair templates consisting of 60 bp or 90 bp homology arms on each side flanking the cutting were designed. Also, SCF7 was used to inhibit NHEJ repair pathway and increase HDR pathway. After transfection, mCherry(+) single colonies were separately extended and genotyped to select *Mcm8*$^{gc/-}$ colonies. A validated *Mcm8*$^{gc/-}$ line was differentiated into PGCLCs.

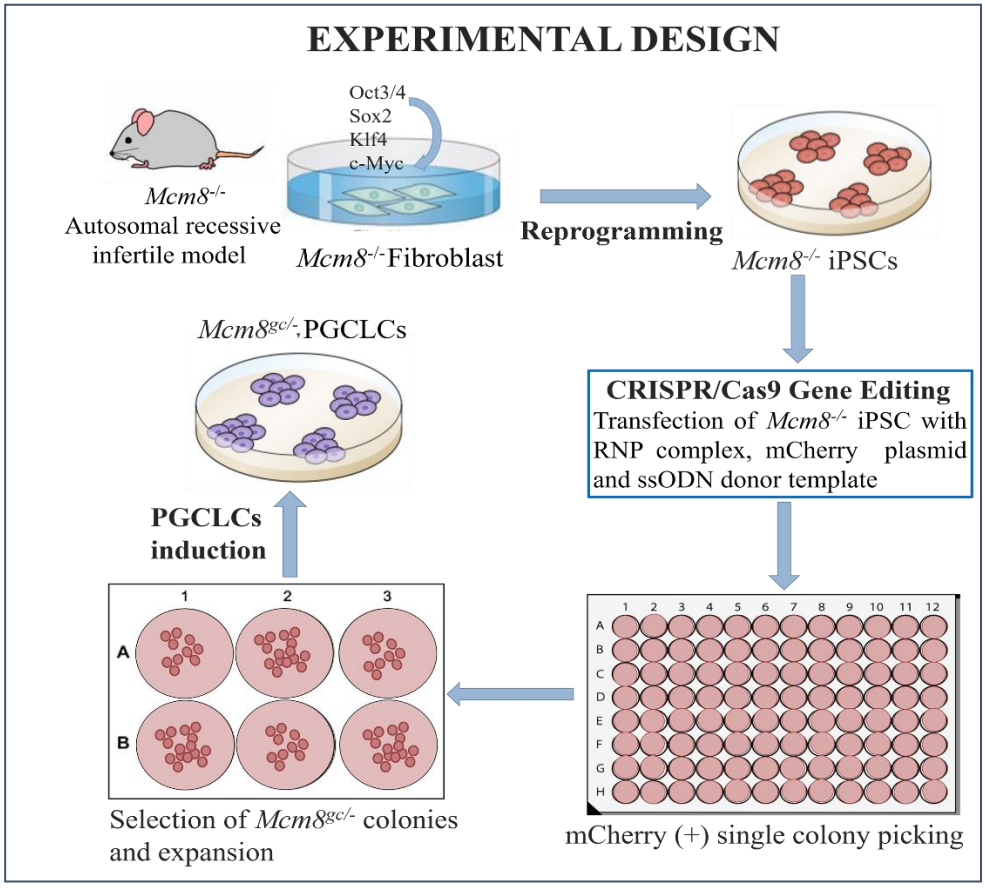

Figure 3.2. Experimental design of germline gene editing in a *Mcm8*$^{-/-}$ mouse model of azoospermia using CRISPR/Cas9-directed gene repair in iPSCS followed by differentiation to PGCLCs.

3.2.2. Histological Examination of *Mcm8*$^{+/+}$, *Mcm8*$^{+/-}$ *and Mcm8*$^{-/-}$ Testes

Testis tissues were fixed in Bouin's fixative solution, washed with 70% ethanol, and processed in a tissue processor (Tissue- Tek VIP). Table 3.2. demonstrates the tissue processing protocol.

Table 3.2. Protocol of tissue-processing for *Mcm8*$^{+/+}$, *Mcm8*$^{+/-}$ and *Mcm8*$^{-/-}$ testes.

Process	Solution	Time (minute)
Dehydration	70% alcohol	45
Dehydration	70% alcohol	45
Dehydration	95% alcohol	45
Dehydration	95% alcohol	45
Dehydration	Absolute alcohol	45
Dehydration	Absolute alcohol	45
Clearing	Xylene	30
Clearing	Xylene	45
Clearing	Xylene	45
Infiltration	Paraffin Wax	30
Infiltration	Paraffin Wax	45
Infiltration	Paraffin Wax	45

After tissue processing, tissues were embedded in paraffin using a station (Thermo Electron Corporation Shandon Histocentre 3), five micrometer thick sections were obtained with a sliding microtome. Five-micrometer thick sections were stained with hematoxylin & eosin manually using following protocol: Sections were kept in the incubator at 60ºC overnight (ON) and deparaffinized with xylene for totally 20 minutes. They were rehydrated with a series alcohol dilution (100%, 96%, 80%, 70%, 5 min each). They were stained with hematoxylin (SelecTech Hematoxylin 560, Surgipath 3801571) for 5 min, differentiated by SelecTech Define MX-aq, Surgipath 3803598 for 1 min, and bluing was performed in SelecTech Blue Buffer 8, Surgipath 3802918 for 1 min. Subsequently, sections were counterstained by eosin with phloxine (SelecTech Eosine with Phloxine 515, Surgipath 3801606) for 30 seconds and dehydratated with alcohol series. Finally, sections were cleared with xylene and mounted with mounting medium using Leica CV5030. The stained sections were analyzed and photographed using a bright field microscope.

3.2.3. Generating Primary Fibroblast Culture from Adult *Mcm8* $^{-/-}$ Mouse Tail and Genotyping

To generate fibroblast, tail of adult *Mcm8*$^{-/-}$ mouse was excised after de-capitation and then rinsed with 70% ethanol in a sterile eppendorf tube. Tail was cut into smaller pieces and digested with 2 ml 0.25 % Trypsin-EDTA 37ºC for 15 min in a shaker. Enzymatic digestion was stopped with 4 ml DMEM with sodium pyruvate, L-Glutamine, and 4.5 g/L glucose (Fisher Scientific) containing 10% FBS and %1 pen-strep and cell suspension was centrifuged 600x*g* for 5 min. After centrifugation, re-suspended pellet was counted to determine cell number. The tail fibroblasts were cultured at $2x10^5$ cells per well of a 12 well plate. The medium was changed every other day. The *Mcm8*$^{-/-}$ mouse tail fibroblasts at passage 3 were used to generate iPSCs.

Genotyping

Mcm8$^{-/-}$ fibroblasts were harvested by 0.25 % trypsin-EDTA and centrifuged 600x*g* for 5 min. The pellet was re-suspended by 150 µl lysis buffer (20 mM EDTA, 200 mM NaCI, 40 mM Tris HCL pH=8, 0.5% β-mercaptoethanol, and 0.5% SDS) and 10 µl Proteinase-K and incubated at 55ºC for 2 hours in shaker. After incubation, precipitation was done by adding 1 ml 100% ethanol and the mixture was centrifuged at 13000x*g* for 13 min. After centrifugation, supernatant was removed, the pellet was re-suspend by adding 1 ml 100 % ethanol, and centrifuged 13000x*g* for 13 min. In the next step, supernatant was removed and pellet was dried at 60ºC. 100 µl dH_20 was added and DNA concentration was determined by Nano Drop 200 spectrophotometer.

For genotyping following primers were used for genotyping by PCR:

Forward

TTTGAGGAGCTAGTGAGCGTG

Reverse- WT

ACACGCCAGTGTTTCTC

Reverse-KO

AGCCCCATACACGCCAGG

Table 3.3. demonstrates components of PCR for genotyping of *Mcm8*$^{-/-}$ fibroblasts.

Table 3.3. Components of PCR for genotyping of *Mcm8*$^{-/-}$ fibroblasts.

Component	Amount (µl)
ddH_20	7
Forward primer (10µM)	1
Reverse primer (WT or KO)	1
Long Amp Taq DNA polymerase	10
DNA	1

The PCR was carried out in a thermocyler by using the following parameters: 98ºC 5'/(98ºC 20''/66ºC 30''/72ºC 60'')$_{35}$/72ºC 10'/ 4ºC∞. PCR products were loaded onto a polyacrylamide gel and the gel electrophoresis was run at 115V for 25 min.

3.2.4. Generation of iPSCs from *Mcm8*$^{-/-}$ Fibroblasts

Mcm8$^{-/-}$ fibroblasts at passage 3 were reprogrammed using the CytoTune®-iPS 2.0 Sendai Reprogramming Kit (Thermo Fisher) according to manufacturer's instruction. Initially, fibroblasts were seeded at a density of 30-60% confluency two days before transduction. The calculated volume of each CytoTune 2.0 Sendai virus (SeV) vector was added to in a total volume of 1 ml fibroblast medium (Table 3.4.). The cells were incubated in medium including pluripotency vector at 37ºC for 24 h and following day, medium was replaced with fresh fibroblast medium in order to remove the SeV vectors. The transduced cells were continuously cultured for another 6 day in fresh fibroblast medium. On day 7 post-transduction, the cells were harvested by TrypLE Express enzyme and plated onto MEF treated with mitomycin-C. The next day, fibroblast medium was replaced with iPCS medium supplemented with 10 ng/ml LIF recombinant mouse protein (Table 3.5.). To expand colonies, at least 10 distinct colonies were chosen. At day 20 after transduction, individual colonies were picked up using a pipette tip and treated with 0.25% trypsin-EDTA for 2-3 min at RT. The colonies were dissociated into single cells and transferred to wells in 48-well plates coated MEF. Each iPSC colony was further expanded in separate 6-well plates coated with MEF.

3.2.5. Preparation of the Mitomycin-C Treated MEF Feeder Layer

Mouse embryonic fibroblasts were cultured in DMEM with L-glutamine, 4500 mg/L glucose and without sodium bicarbonate (Sigma) supplemented with 15% FBS and 0.15% sodium bicarbonate. The MEFs at passage 7 were treated 5 µg/ml mitomycin-C at 37ºC for 2 hours. After treatment, cells were washed with HBSS, harvested via trypsinization, and frozen in basal medium containing 10% DMSO and 40% FBS. Before using, frozen MEFs were thawed by incubation in a 37ºC water bath and cultured on 0.1% gelatin (Sigma-Aldrich) coated 6 well plate in fibroblast medium. Reprogrammed iPSCs were maintained on MEF.

Table 3.4. Medium components for tail fibroblasts from *Mcm8*$^{-/-}$ mice.

Component	Source	Volume
DMEM, high glucose, GlutaMAX Supplement, pyruvate	Thermo Fisher Scientific	439.75 ml
FBS	Thermo Fisher Scientific	50 ml
MEM NEAA Solution (100X)	Thermo Fisher Scientific	5 ml
2- Mercaptoethanol (7µl in 1ml medium)	Sigma- Aldrich	250 µl
Penicilin-Streptomycin	Sigma- Aldrich	5 ml

Table 3.5. Medium components for *Mcm8*$^{-/-}$ iPSCs.

Component	Source	Volume
DMEM/F12,GlutaMAX Supplement	Thermo Fisher Scientific	394.25ml
KnockOut Serum Replacement-Multi Species	Thermo Fisher Scientific	100 ml
MEM NEAA Solution (100X)	Thermo Fisher Scientific	5 ml
2- Mercaptoethanol (7 µl in 1 ml medium)	Sigma- Aldrich	250 µl
LIF Recombinant Mouse Protein, 10 µg/ ml	Thermo Fisher Scientific	500 µl

3.2.6. Characterization of iPSCs

Characterization of iPSCs (574, 591) were performed by Fluorescent Mouse ES/iPS Cell Characterization Kit (Milipore, SCR077) after passage 5.

Alkaline Phosphatase (AP) Staining

Reprogrammed iPSCs colonies were cultured for 3-5 days prior to analyzing activity of AP. Fixation was performed by 4% paraformaldehyde (Sigma-Aldrich) for 1-2 min at RT. After fixation, colonies were washed with Rinse Buffer (20 mM Tris-HCL, pH 7.4, 0.05% Tween 20, 0.15 M NaCI). The colonies were stained with staining solution ((fast red violet: naphthol AS-BI phosphate: water (2:1:1)) for 30 min in the dark at RT. After incubation, colonies were washed with rinse buffer and each well was covered with 1XPBS. The colonies were examined under an inverted microscope.

IF Labelling

Fixation was performed with 4% paraformaldehyde at RT for 30 min. Nonspecific binding was blocked by using 3% donkey serum, 0.05% NaN_3, and 0.2% Triton X-100 in 1X PBS for intracellular gene targets, Oct-4, Sox-2 and Nanog. Non-permeable blocking solution (3% donkey serum in 1XPBS) was used for cell surface epitope, SSEA-1. Colonies were incubated ON at 4^{o}C with specific antibodies Oct-4 (dilution 1:100), SSEA-1 (dilution 1:100), Sox-2 (dilution 1:100) and Nanog (dilution 1:25) (Merck Millipore). After several washes in PBS, iPSCs colonies were stained with DAPI (1:1000) and viewed by an inverted fluorescence microscope.

Teratoma Formation

To evaluate the differential potential of mouse *Mcm8*$^{-/-}$ iPSCs cells were injected into testis of 6-8-week-old NOD-SCID mice ($5x10^5$ per mouse testis) and animals observed once a week for tumor growth. Six weeks after injection, teratomas were dissected and fixed in 4% paraformaldehyde. Paraffin embedded blocks were cut into 5 µm sections that were stained with hematoxylin & eosin and examined.

Karyotype Analysis

Before karyotype analyses, about $3x10^6$ cells were placed onto matrigel coated T25 flask. Following day, cells were sent to Cincinnati Children's Hospital Medical Center Mouse Cytogenetics Core for analysis.

3.2.7. Correction of Mutation by CRISPR/Cas9

Even though CRISPR/Cas9 components can be delivered into cells in different, in this study, protein-based delivery approach was used. Four sgRNAs sgRNA1, sgRNA2, sgRNA3 and sgRNA4 were designed crispr.mitt.edu to target mutant DNA sequence and direct Cas9-mediated double strand breaks. To induce the HDR pathway an ssODN template containing 60 bp or 90 bp homology arms flanking the cutting site in either sense or antisense orientation relative to the gRNA sequence were designed. Moreover, in order to reduce activity of nucleases, ssODNs containing 60 bp homolog arms were chemically modified with phosphorotiate near both 5 prime and 3 prime ends. The incidence of HDR-mediated DNA repair is very low in mammalian cells and even in the presence of repair template, NHEJ is the more frequent repair mechanism. To overcome this challenge, some approaches have been developed to increase efficiency of HDR repair way and inhibit NHEJ. For this reason, in our study, Scr7 that inhibits NHEJ component DNA ligase IV was used at different concentrations in some trials to increase HDR efficiency (Figure 3.3.).

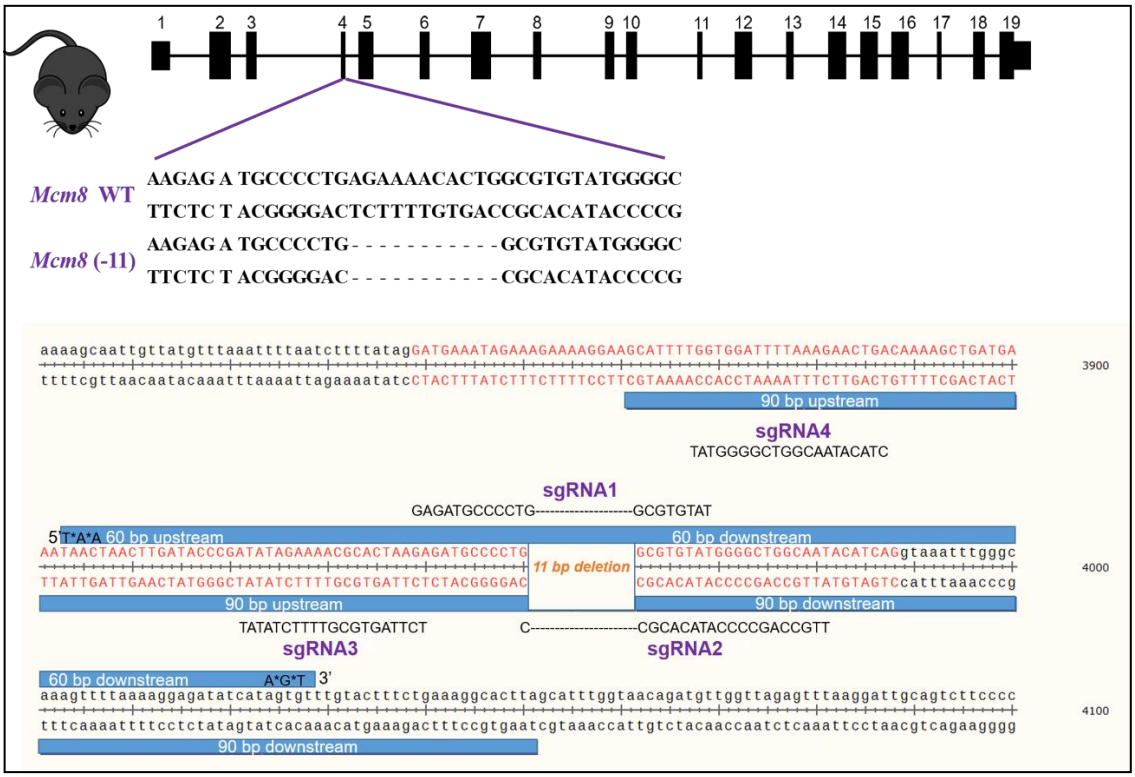

Figure 3.3. Demonstrative picture of mutation in mouse *Mcm8* gene and designed sgRNAs and ssODNs to correct mutation.

Transcription of Designed SgRNAs for Protein Delivery Method

Four different sgRNAs targeting the *Mcm8* gene were synthesized using the Guide-it sgRNA In Vitro Transcription Kit (Takara). The PCR fragments containing the sgRNA target sequence were mixed with recombinant Cas9 protein and each sgRNA. The cleavage efficiency was tested for each different sgRNAs and assessed by agarose gel electrophoresis and measured using densitometry. The efficiency was calculated by following formula:

$$\text{Cleavage efficiency (\%)}: \frac{b+c}{a+b+c} \times 100$$

a: Uncleaved DNA

b: I. Cleaved DNA

c: II.Cleaved DNA

Designing a 56 to 58- nt Forward Primer to Create DNA Template for sgRNAs

sgRNA1

CCTC TAATACGACTCACTATA G GAGATGCCCCTGGCGTGTAT GTTTAAGAGCTATGC

sgRNA2

CCTC TAATACGACTCACTATA GG TTGCCAGCCCCATACACGCC GTTTAAGAGCTATGC

sgRNA3

CCTC TAATACGACTCACTATA GG TCTTAGTGCGTTTTCTATAT GTTTAAGAGCTATGC

sgRNA4

CCTC TAATACGACTCACTATA GG TATGGGGCTGGCAATACATC GTTTAAGAGCTATGC

Table 3.6. and Table 3.7. demonstrate components of PCR to amplify sgRNA-encoding template and components of *in vitro* transcription reaction for each sgRNA-encoding template

Table 3.6. Components of PCR to amplify sgRNA-encoding template.

Reagent	**Amount (µl)**
PrimeSTAR Max Premix (2X)	12.5
Guide-it Scaffold Template	1
Forward primer (10 µM)	0.5
RNase Free Water	11
Total	25

The PCR was carried out in a thermocyler by using the following parameters (98ºC 10'', 68ºC 10'')$_{33}$/4ºC∞

PCR products and DNA ladder was analyzed on 2% agarose gel.

Table 3.7. Components of *in vitro* transcription reaction for each sgRNA-encoding template.

Component (For each sgRNA)	Amount (µl)
sgRNA PCR template (Step 1)	5
Guide-it In vitro Transcription Buffer	7
Guide-it T7 Polymerase Mix	3
RNase Free Water	5
Total	20

Following program was run: 37 C for 4 hour/ 4ºC forever

After incubation, 2 µl of Recombinant DNase I /RNase-Free was added to the 20 µl reaction and incubated at 37ºC for 15 min.

Purification of Transcribed sgRNAs

For each designed sgRNA, 78 µl of RNase free water was added to 22 µl reaction mixture for a total volume 100 µl and transferred to a 1.5 ml micro centrifuge tube. 30 µl of binding buffer and 130 µl isopropanol were added and vortexed for 5 sec. RNA clean-Up spin column was placed in a collection tube, samples were added, and centrifuged at 11000x*g* for 1 min. The flow through was removed and column was placed back in the collection tube. Subsequently, 500 µl of wash buffer was added and centrifuged at 11000xg for 1min. After discarding flow through, column was placed back, 600 µl of wash buffer was added, and centrifuged at 11000x*g* for 2 min. RNA Clean-up Spin Column was placed in a new 1.5 ml micro centrifuge tube. 20 µl of RNase Free water put onto the silica membrane of the spin column, incubated for 1 min at RT, and centrifuged at 11000x*g* for 1min. Concentration of sgRNAs was determined by NanoDrop Spectrophotometer.

Evaluation of In Vitro Cleavage Efficiency in Mcm8$^{-/-}$ iPSCs DNA

PCR amplicons containing a sgRNA target site were synthesized from genomic *Mcm8*$^{-/-}$ iPSCs DNA by using following primers.

350 Forward primer: AAC TGG ACA ATG TTT GAG GAG C

850 Forward primer: GCA AGT GGC AGT TTG GAC TA

300 Reverse primer: CAT ACG GGA CTC AGT GGG GA

500 Reverse primer: CTG TGT CCA GAT TGT ACC CCC

650 Reverse primer: TGG GTG ATT GGA TGA GGC TG

Six candidate primer pairs were tested for cleavage efficiency of designed sgRNAs

350 Forward primer- 300 Reverse primer

350 Forward primer- 500 Reverse primer

350 Forward primer- 650 Reverse primer

850 Forward primer- 300 Reverse primer

850 Forward primer- 500 Reverse primer

850 Forward primer-650 Reverse primer

98 ^{0}C 3'/(98 ^{0}C 10''/60 ^{0}C 15''/68 ^{0}C 2')$_{35}$/ 4 ^{0}C∞

Table 3.8. demonstrates components of PCR reaction to amplify target *Mcm8*$^{-/-}$ iPSCs DNA

Table 3.8. Components of PCR reaction to amplify target *Mcm8*$^{-/-}$ iPSCs DNA.

Reagent	**Amount (µl)**
2X Terra PCR Direct Buffer (with Mg2, dNTP)	25
Forward primer (10 µM)	1.5
Reverse primer (10 µM)	1.5
Terra PCR Direct Polymerase Mix (1.25 U/ µl)	1
RNase Free Water	20
DNA from *Mcm8*$^{-/-}$ iPSCs	1
Total	50

DNA ladder (ThermoFisher Scientific, GeneRuler DNA Ladder Mix, SM0333) was loaded into the first lane of the gel and the samples with gel loading dye (ThermoFisher Scientific, Gel Loading Dye, Purple (6X) into the rest of the wells. The gel electrophoresis was run at 120V for 15 min.

Cleavage Assay with Cas9 and Designed sgRNAs

Target-specific sgRNA (50 ng/µl) or control sgRNA (50 ng/µl) were mixed and incubated at 37^{o}C for 5 min. Target fragment (6 different PCR products) or control fragment was incubated with each designed sgRNA/Cas9 mix using a thermal cycler

with the following conditions: 37°C for 1 hour, 80°C 5 min, 4°C forever. Table 3.9. demonstrate components of components of cleavage assay with each designed sgRNA/Cas9 mix.

Table 3.9. Components of cleavage assay with each designed sgRNA/Cas9 mix.

Component	Amount (µl)
PCR reaction solution (100-250 ng) or Control fragment	5
15X Cas9 Reaction Buffer	1
15X BSA	1
RNase Free Water	6.5
Cas9/sgRNA mix	1.5
Total	15

3.2.8. Optimization of Transfection Method

Isolation of mCherry Plasmid

pAAV CAG mCherry plasmid was used to select colonies after transfection. Transformed E.coli was grown in the 200 µl LB broth including convenient antibiotics for 2.5 hours with shaking. After incubation, 200 µl LB broth was divided into 2 X 250 ml LB broth containing convenient antibiotic (250 ml + 100 µl; 250 ml + 100 µl). After ON culture, the LB broth (totally 500 ml) was split into 10 tubes (50 ml each). Manufacturer's instructions were followed to isolate plasmid (Invitrogen PureLink HiPure Plasmid Midiprep Kit) The cells were sedimented by centrifugation at 3500x*g* for 10 min. The supernatants were removed and pellets were resuspended in 5 ml of resuspension buffer. Each two suspensions were combined and 10 ml of lysis buffer was added, incubated for 5 min. After incubation, precipitation buffer (10 ml) was added to each tube and centrifuged at 3000x*g* for 4 min. The columns were equilibrated by 15 ml of equilibration buffer and supernatants were loaded onto the equilibrated columns. The columns were washed with 10 ml of wash buffer. After discarding inner filtration cartridge, the columns were washed by 20 ml of wash buffer. Sterile 50 ml tubes were placed under the columns and 5 ml of elution buffer was added to the

columns. After 27 ml of isopropanol was added to each tube, total volume was transferred into centrifuge tubes and centrifuged at 12000x*g* for 30 min at 4ºC. After centrifugation, the supernatants were discarded. The pellets were washed 3 ml of absolute ethanol and centrifuged at 13000x*g* for 13 min. The supernatants were discarded and pellets were dried at 55ºC for 15-20 min. 100 µl of dH_20 was added to each pellet and DNA concentration was determined by Nano Drop 200 spectrophotometer.

Electroporation

In order to determine which electroporation condition is best for iPSCs, the following 6 different conditions were tested (Table 3.10.). Electroporated cells were plated on treated MEF inactived by mitomycin-C, and mCherry (+) cells were selected by FACS sorting on day 3 after electroporation. Since efficiency of electroporation was low, after FACS sorting these cells were seeded on feeder cells, expanded, and harvested for surveyor assay, when the number of cells for DNA isolation was enough.

Table 3.10. Six different conditions are presented for optimizing the electroporation-based transfection.

Condition	Voltage (ms)	Length (ms)	Interval	No	D. Rate (%)	Polarity
1.Poring pulse	115.0	5	50.0	2	10	+
Transfer pulse	20.0	50.0	50.0	5	40	+/–
2. Poring pulse	125.0	2.5	50.0	2	10	+
Transfer pulse	20.0	50.0	50.0	5	40	+/–
3. Poring pulse	125.0	5	50.0	2	10	+
Transfer pulse	20.0	50.0	50.0	5	40	+/–
4. Poring pulse	135.0	2.5	50.0	2	10	+
Transfer pulse	20.0	50.0	50.0	5	40	+/–
5.Poring pulse	135.0	5	50.0	2	10	+
Transfer pulse	20.0	50.0	50.0	5	40	+/–
6.Poring pulse	150.0	5	50.0	2	10	+
Transfer pulse	20.0	50.0	50.0	5	40	+/–

Before analyses, about $5x10^5$ cells were placed onto each of 12 wells of two sets of matrigel coated 6 well plates. Two days later, cells were harvested by

trypsinization. Next, the cell pellet was resuspended in the 5 ml Opti-MEM medium and centrifuged at 600xg for 5 min. This step was repeated to wash medium containing serum and supplements completely off the cells. Resuspended cell pellet in Opti-MEM medium was counted to determine cell density. The total volume for electroporation was 100 µl and DNA concentration (mCherry) was 10 µg/100 µl. To electroporate the cells, 100 µl of mixture was transferred into cuvettes and electroporation parameters were set. The cuvette for each condition was placed into the CU500 Cuvette Chamber and the ð button of NEPA21 was pressed. The start button was pressed to execute the electroporation program and values of currents and joules displayed in the measurement frame were noted. The cuvette for each condition was taken out of the chamber and about 900 µl of the iPSC culture medium was added into the cuvettes. The cells were completely pipette-out from the cuvettes and placed onto MEF coated 6-well plate (0.5 x10^6/ well/6 well plate) (500 µl cell suspension/well/6 well plate).

Lipofectamine

In order to determine whether which lipofectamine condition is best for iPSCs, following 4 different conditions were tested (Table 3.11.).

Table 3.11. Four different conditions are presented to optimize lipofectamine-based transfection.

Mixture	Component	1	2	3	4
Mixture 1	Opti-MEM medium	25 µl	25 µl	25 µl	25 µl
	Lipfectamine Stem reagent	1 µl	1 µl	2 µl	2 µl
Mixture 2	Opti-MEM medium	25 µl	25 µl	25 µl	25 µl
	mCherry plasmid (0.8 µg/µl)	250 ng	500 ng	250 ng	500 ng

Firstly, the diluted mCherry plasmid (mixture 2) was added to the diluted Lipofectamine Stem Reagent (mixture 1) and it was incubated in RT for 10 min. After incubation, 50 µl of mixture was added to 500 µl media without serum gently. After overnight incubation at 37ºC, 500 µl regular media was added into each well. 72 hours after transfection, the cells were collected for analysis.

Evaluation of Viability and Transfection Efficiency by FCM

For flow cytometry, cells from each condition were trypsinized on day 3 after electroporation. Cell numbers for each condition were determined. The cell suspensions were centrifuged at 600x*g* for 5 min and media were decanted. The cell pellets were re-suspended with 1xPBS and centrifuged at 600x*g* for 5 min. After centrifugation, based on the cell count, volumes for 0.1% BSA and DAPI were calculated considering the following:
Cells need to be at a concentration < 20 million cells/ml
Volume needs to be >200µl

3.2.9. Evaluation of Cleavage Efficiency of Designed sgRNAs in *Mcm8*$^{-/-}$ iPSCs

Electroporation

Before analyses about 5x10^5 cells were placed onto each of 12 wells of two sets of matrigel coated 6 well plates. Two days later, cells were harvested by trypsinization. The cell pellet was resuspended in the 5 ml Opti-MEM medium and centrifuged at 600xg for 5 min. This step was repeated to wash medium containing serum and supplements completely off the cells. The cell pellet was resuspended in Opti-MEM medium and cells were counted to determine cell density. The total volume for electroporation was 100 µl, DNA concentration (mCherry) was 10 µg/100µl, sgRNA concentration was 1.2 µg/100µl, and Cas9 protein (Invitrogen True Cut Cas9 Protein V2) concentration was 5 µg/100µl.

Surveyor Assay

mCherry(+) cells were harvested by 0.25% trypsin-EDTA and DNA was extracted Initially, cells were centrifuged 600xg for 5 min, pellet was re-suspended 150 µl lysis buffer (200 mM NaCI, 20 mM EDTA, 40 mM Tris HCL pH=8, 0.5 % SDS, 0,5% β-mercaptoethanol) and 10 µl proteinase-K, and incubated at 55ºC for 2 hours in shaker. Precipitation was performed by adding 1ml 100 % ethanol and the mixture was centrifuged at 13000x*g* for 13 min. After centrifugation, pellet was re-suspend by adding 1 ml 100% ethanol, and centrifuged 13000x*g* for 13 min. Next,

pellet was dried at 60ºC. 100µl dH_20 was added and DNA concentration was determined by Nano Drop 200 spectrophotometer.

PCR for Surveyor Assay

The PCR products of the targeted regions were produced using high-fidelity PCR master mix with primers (Table 3.12.).

Table 3.12. Components of PCR for surveyor assay.

Component	Amount (µl)
ddH_20	11.8
350 Forward primer (10µM)	1
500 Reverse primer (10µM)	1
Phusion High Fidelity reaction buffer (BioLabs)	4
PCR nucleotide mix (Roche)	0.4
DMSO	0.6
Phusion High Fidelity DNA polymerase (BioLabs)	0.2
DNA	1

The PCR was carried out in a thermocyler by using the following parameters: 98ºC 5'/(98 ºC 20''/60ºC 30''/72ºC 60'')$_{35}$/72ºC 10'/ 4ºC∞. The gel electrophoresis was run at 110V for 30 min. The products were gel purified by gel purification kit.

Gel Purification

Gels were purified by Nucleospin Gel and PCR clean-up following the manufacturer's instruction with some modifications. Initially, binding buffer was added to each tube containing PCR products according to weight of the gels (for each 200mg of gel, 200µl binding buffer) and incubated at 55ºC for about 10 min. In the next step, columns were placed into collection tube, samples were loaded, and centrifugated at 13000x*g* for 1 min. For each sample, flow through was discarded, 700 µl of washing buffer was added and centrifuged at 13000x*g* for 1 min. The washing step was repeated twice. To remove buffer wash buffer completely, the sample was centrifuged for 2 min at 13000x*g*. The column was placed into new eppendorf tube. 20µl warmed dH_20 was added to each column, incubated at RT for 2 min, and

centrifuged at 13000x*g* 1 min. The step was repeated and DNA concentration was determined.

Heteroduplex Formation

200 ng of PCR products were mixed 19 µl annealing reaction mixture (annealing buffer and dH_2O) Samples were denatured by heating at 99°C for 5 min. Heteroduplexes were formed by cooling down to 65°C for 30 min and to 23°C for 30 min. After re-annealing, samples were incubated 1µl T7 endonuclease (BioLabs) for 45 min at 37°C. Reaction was stopped by adding 1.5 µl 0.1 M EDTA and then digested PCR products were analyzed by 1.5% agarose gel.

3.2.10. Transfection of iPSCs with RNP Complex and ssODN Donor Template Using Electroporation-Based Approach

To target DNA and induce HDR pathway efficiently after cleavage of strands, ssODN donor templates containing flanking sequences of 60 or 90 bp on each side that were homologous to target region were used. The total volume was 100 µl for $1x10^6$ cells in Opti-MEM. Concentration of mCherry plasmid and ssODN was 5 µg/100µl, sgRNA1 concentration 1.2 µg/100 µl, Cas9 protein (Invitrogen True Cut Cas9 Protein V2) concentration was 5 µg/100 µl. Firstly, Cas9 and sgRNA in opti-MEM were incubated for 10 min at RT. After incubation, plasmid, ssODN and cells were added and the mixture was electroporated. After transfection, mCherry(+) colonies were picked up manually and expanded for genotyping and DNA sequencing.

3.2.11. Transfection of iPSCs with RNP Complex and ssODN Donor Template Using Lipofectamine-Based Approach

One day prior to lipofectamine-based transfection, cells were placed onto 6-well MEF coated plates at $4x10^5$ cells per well. On the day of transfection, 5 µg Cas9 protein and 1.2 µg sgRNA1 were incubated in 125 µl of Opti-MEM at RT for 5 min to form Cas9 RNPs complex. After incubation, 2 µg 60 bp ssODN donor template and 3 µg mCherry plasmid were added to the mixture of Cas9 RNPs. 5 µl of Lipofectamine Stem Cell was added to 125 µl of Opti-MEM and mixture were incubated at RT for 5 min. The Cas9 RNPs were added to the Lipofectamine Stem Cell solution. The final

mixture was incubated at RT for 10–15 min to form Cas9 RNPs and Lipofectamine Stem Cell complexes and then added to the medium. After incubation 24 hour, medium was replaced with fresh iPSC medium to remove mixture. After transfection, mCherry(+) colonies were picked up manually and expanded for genotyping and DNA sequencing.

3.2.12. DNA Sequencing

To find heterozygous gene corrected colony, genotyping and DNA sequencing were performed after transfection. For DNA sequencing, DNA was extracted, PCR was performed, and PCR products were purified by Nucleospin Gel and PCR clean-up according to instruction of manufacturer. 300 µl of binding buffer was added to each eppendorf tube containing PCR products (45 µl products + 55 µl ddH20). The NucleoSpin® Gel and PCR Clean-up Column was placed into collection tube and mixture was loaded. After centrifugation at 13000x*g* for 1 min, flow through was discarded, 700 µl of washing buffer was added and centrifuged at 13000x*g* for 1 min. The washing step was repeated twice. To remove wash buffer completely the sample was centrifuged for 2 min at 13000x*g*. The column was placed into new eppendorf tube. 20 µl warmed dH20 was added to column, incubated at RT for 2 min, and centrifuged at 13000x*g* for 1 min. The step was repeated and DNA concentration was determined. Reaction mixture was prepared and samples were analyzed in Genomic Research Core of University of Pittsburgh.

3.2.13. Generation of PGCLCS

To generate PGCLCs, we mimicked the step of PGCLC development by *in vitro* culture system. Initially, gene corrected iPSC line was maintained in N2B27 medium containing LIF and two inhibitiors and then they were differentiated into epiblast like cells (EpiLCs) using EpiLC differentiation medium containing 20 ng/ml activin A (Peprotech) and 12 ng/ml bFGF (Invitrogen) and then EpiLCs differentiated into PGCLCs in response to 500 ng/ml BMP4, 500 ng/ml BMP8b, 100 ng/ml SCF, 50 ng/ml EGF, and 1,000 U/ml LIF. These differentiated cells were characterized by FCM using and SSEA1 and CD61 antibodies.

4. RESULTS

4.1. Assessment of Time and Dose Dependent Proliferative Effect and the Mechanism of Action of Leptin Supplementation on Cultured Neonatal SSCs

4.1.1. Characterization of SSCs by PLZF Labelling and Morphologically in Neonatal Testis

The 6-day-old-mouse testes exhibit lobular parenchyma and surrounding stroma with interstitial tissue and tunica albuginea. All the lobules consist of seminiferous cords under the light microscope (Figure 1 A-B.). Sertoli cells with perpendicular orientation to the basement membrane and the basally located spermatogonia form the seminiferous cords in the lobules as been observed in semi thin section micrographs (Figure 1.C-D.). Undifferentiated spermatogonia including the SSCs that are located at the basal compartment present large spherical euchromatic nuclei with small clumps of heterochromatin at the ultrastructural level. Those cells have little amount of cytoplasm with numerous mitochondria (Figure 1.E-F.). The 6-day-old-mouse testes that contain PLZF(+) undifferentiated spermatogonia including SSCs were demonstrated by immunofluorescence staining in frozen sections (Figure1 G-H.).

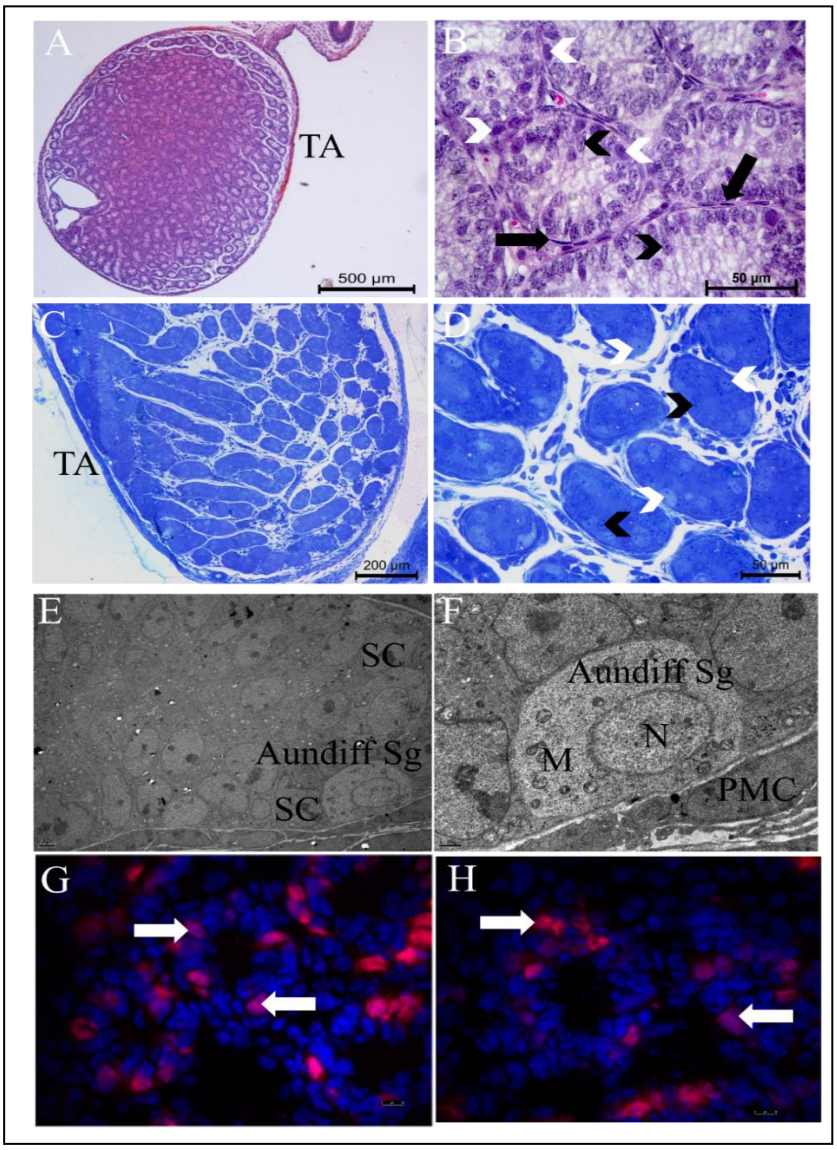

Figure 4.1. Morphological characterization of 6 day old mouse testis. A and B) The micrographs of paraffin sections show the testicular lobules consisting of seminiferous cords and the tunica albuginea (TA) that surrounds the testis. Seminiferous cords are surrounded by monolayer of PMCs (black arrows) cotain spermatogonia (white arrowheads) and Sertoli cells (black arrowheads) C and D) The semi-thin plastic section micrographs show the presence of the basally located spermatogonia (white arrowheads) and Sertoli cells (black arrowheads) inside the seminiferous cords. E and F) The undifferentiated spermatogonia (Aundiff Sg) at the ultra-structural level within the cords. Note the high amount of mitochondria (M) in the cytoplasm and small heterochromatin clumps inside the nucleus (N) of the Aundiff Sg and peritübüler miyoid cells (PMCs). G and H) The frozen sections stained with PLZF show the presence of PLZF(+) undifferentiated spermatogonia (white arrows) in the seminiferous cords. A, B: Hematoxylin & eosin 100x, 600x; C, D: Methylene Blue Azur II 100x, 400x, E, F: Uranyl acetate-Lead citrate 4000x, 20000x. G, H: IF labelling for PLZF 1000x.

4.1.2. Isolation, Characterization of SSCs by FCM and PLZF and OB-Rb Labelling by IF in Cultured SSCs

Spermatogonial stem cells enriched testicular cell suspension was successfully obtained from 6 day-old prepubertal mice by isolation protocol containing enzymatic digestion, 30% Percoll gradient and MACS separation (Figure 4.2.A). The total testis cell population comprised 8.18% CD90. 2(+), 14.9% PLZF(+) and, 57.4% c-kit(-) cells by FCM. MACS selection revealed the presence of CD90.2 and PLZF immune labeled cells as 44.1% CD90.2(+), 57.2% PLZF(+) and 83.7% c-kit(-) by FCM (Figure 4.2.B). Therefore, the MACS separation with CD90.2 micro beads provided SSC enriched testicular cell suspension. The cultured SSCs exhibited intense nuclear immune labeling for PLZF and membranous labeling pattern for OB-Rb receptor by IF (Figure 4.2.C).

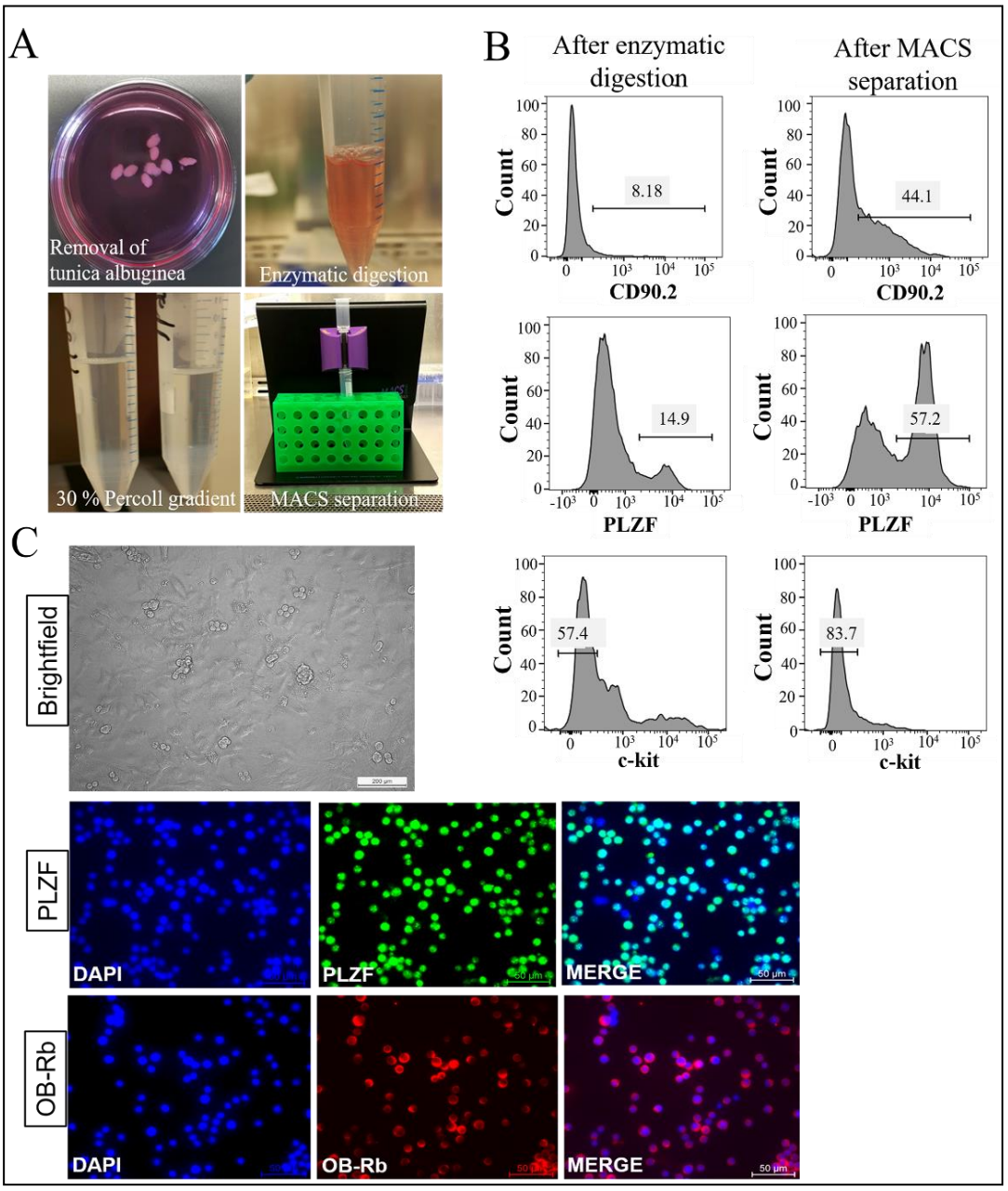

Figure 4.2. Isolation and enrichment protocol of SSCs from 6 day old C57BL/6 mice and characterization of cultured SSCs. A) The protocol consists of four steps: removal of tunica albuginea, enzymatic digestion of seminiferous tubules, enrichment of SSCs by 30% Percoll gradient, and MACS using CD90.2 microbeads B) FCM analysis of SSCs performed using the CD90.2, PLZF and c-kit antibodies from whole testis after enzymatic digestion and after MACS separation with CD90.2 C) Passage 2 SSCs and IF labelling of SSCs for PLZF and OB-Rb DAPI; nucleus.

4.1.3. Dose and Time Dependent Proliferative Effect of Leptin on SSCs

Number and the diameter of the colonies increased significantly from day 3 to day 7 in both the control and all leptin-treated groups ($p < 0.05$, Figure 4.3.A). There was no statistical difference in the mean diameter and the mean number of colonies among the control and leptin groups on 3rd day of the culture. The colony number did not change between groups; however, the mean colony diameter was significantly higher in 100 ng/ml leptin-treated SSCs compared to control on 5th day of the culture ($p=0.043$). The mean diameter and the number of colonies were significantly higher in 50 and 100 ng/ml leptin-treated groups when compared to control on day 7 ($p=0.022$ and $p=0.001$ for the diameter and $p=0.023$ and $p=0.001$ for number of colonies, respectively). 100 ng/ml of leptin treatment provided the largest colony diameter rate when compared to other doses of leptin ($p=0.001$, each), and it initiated a better colony number comparing to 200 ng/ml leptin treatment on day 7 of culture ($p=0.006$) (Figure 4.3.B and C).

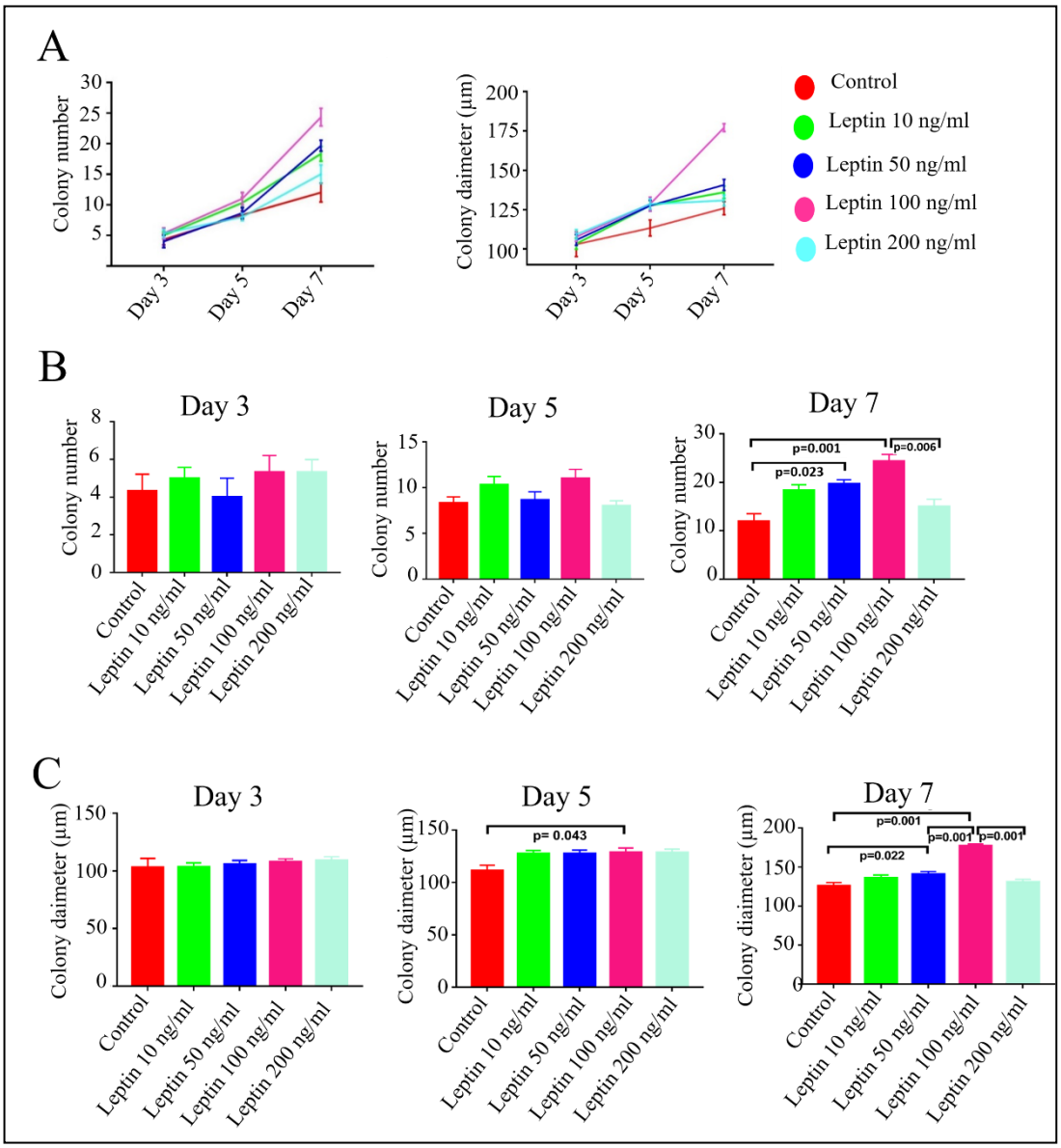

Figure 4.3. Evaluation of dose and time dependent proliferative effect of leptin on SSCs by colony number and colony diameter. A) Colony number and diameter in control and leptin treated groups from day 3 to day 7 B) The mean colony number in control and leptin-treated groups on 3rd, 5th and 7th of SSCs culture C) The mean colony diameter in control and leptin-treated groups on 3rd, 5th and 7th of SSCs culture.

The WST-1 assay and xCELLigence RTCA indicated proliferative effect of leptin in a dose and time –dependent manner on SSCs (Figure 4.4.). The addition of 100 ng/ ml leptin promoted proliferation of SSCs on day 7 of culture comparing to control in WST-1 assay (p=0.009) (Figure 4.4.A). 50 ng/ml (p=0.003, p=0.019 and p=0.04 on days 3, 5 and 7, respectively) and 100 ng/ml (p=0.028 and p=0.033 on days

5 and 7, respectively) leptin-treatment significantly increased SSC growth curve from day 3 to 7 comparing to control by xCELLigence RTCA. 10 ng/ml and 200 ng/ml leptin treatment did not significantly promote the growth curve in any of the time points comparing to control by xCELLigence RTCA. Leptin's proliferative effect sustained on SSCs, at the concentration of 100ng/ml, from 104 to 135 hours when compared to control and other experimental groups. The growth curves remained unchanged from 135 hours in all groups (Figure 4.4.B and C) The real time analysis revealed the EC50 dose for leptin as 114 ng/ml for 7 days of SSCs culture (Figure 4.4.D).

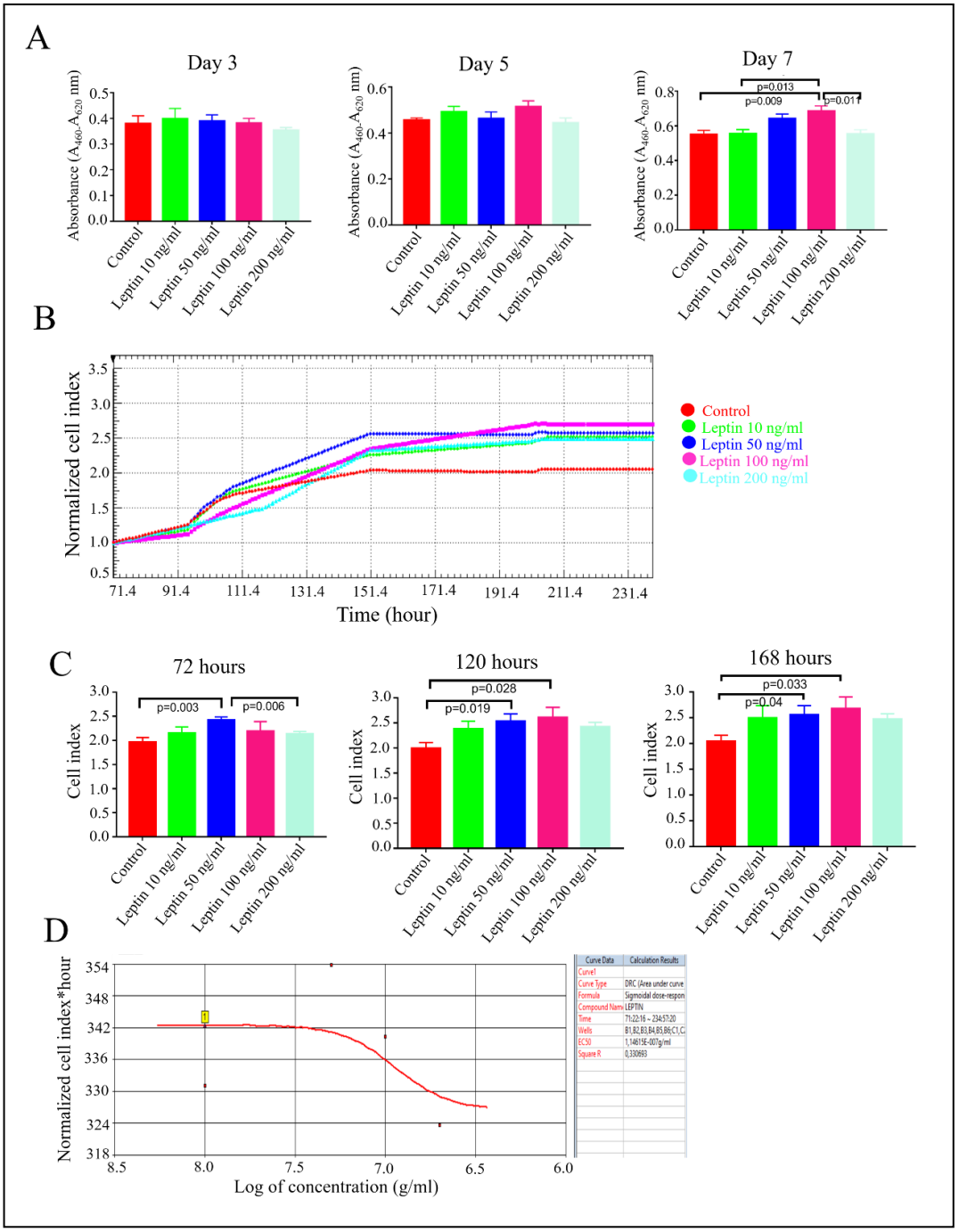

Figure 4.4. The proliferation analysis of leptin supplementation on SSCs with WST-1 assay and xCELLigence RTCA. A) Note that the maximum proliferative effect is observed at a concentration of 100 ng/ml on day 7 of SSCs culture B) xCELLİgence RTCA analysis: Growth curve shows dose dependent proliferative effect of leptin on SSCs compared to control, in time. Analysis was performed real time for totally 7 days and results were expressed as a cell index (CI) value. C) Statistical analysis of CI calculated from six repeated experiments D) The EC50 of leptin was calculated approximately as 114 ng/ml based on the dose-response curves of cell index during 7 days in SSCs and calculated from repeated experiments (n=6) by the RTCA software 1.2.1 (ACEA Bioscience).

4.1.4. Characterization of Cells After Leptin Treatment by FCM

The total number of CD90.2(+) testis cells was calculated as 75.1%, 77.9%, 80.8% and 71% with 10, 50, 100 and 200 ng/ml of leptin treatment, respectively. The highest rate of CD90.2 positivity was detected in 100 ng/ml leptin group, insignificantly (Figure 4.5.). The findings showed that most of cultured cells retained CD90.2 expression after culture with leptin treatment independent of the leptin concentration.

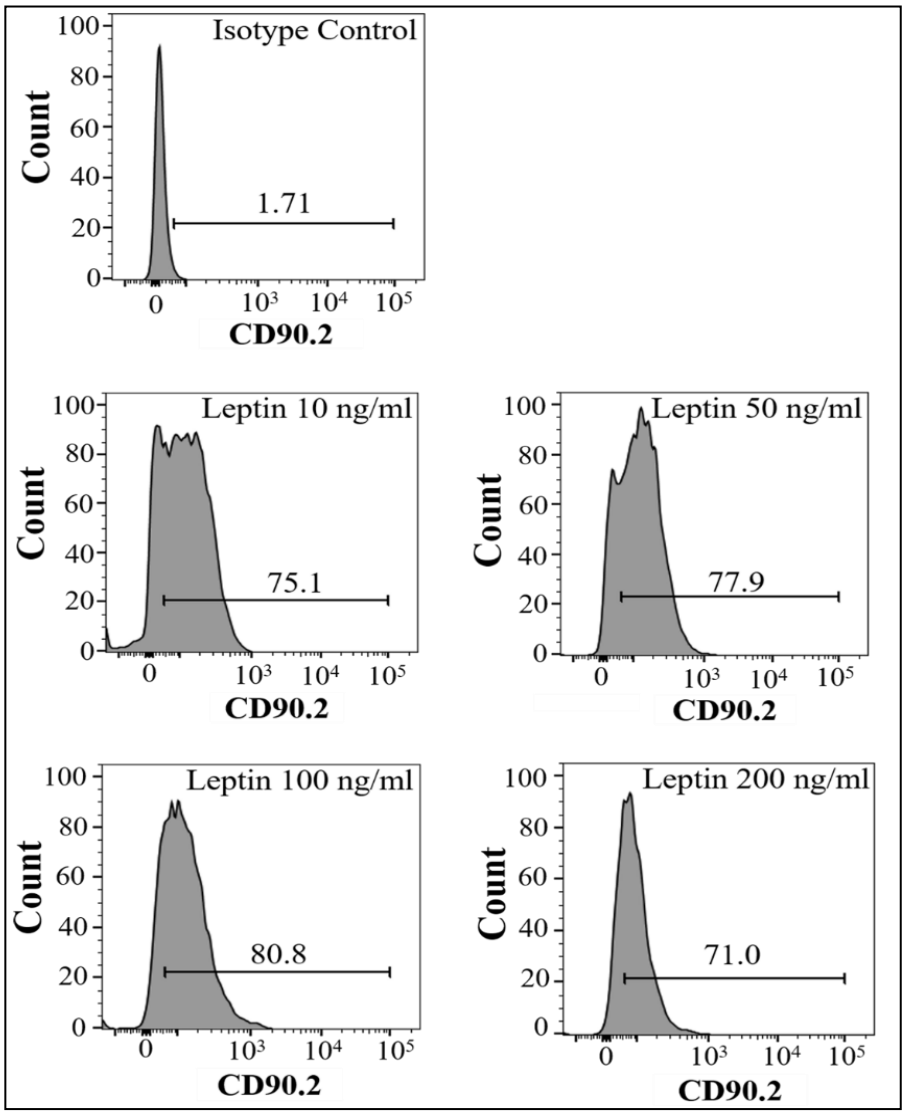

Figure 4.5. Evaluation of the percentage of CD90.2(+) SSCs after leptin treatment by FCM. Note that 100 ng/ml of leptin provides highest percentage.

4.1.5. Leptin-Induced Signaling Pathways

Densitometric analysis of the bands demonstrated that 114 ng/ml leptin treatment increased level of p-ERK1/2 (p=0.009), p-STAT3 (p=0.023) and decreased p-SHP2 level (p=0.008) when compared to control. Leptin treatment did not change total STAT3 protein expression level (Figure 4.6.).

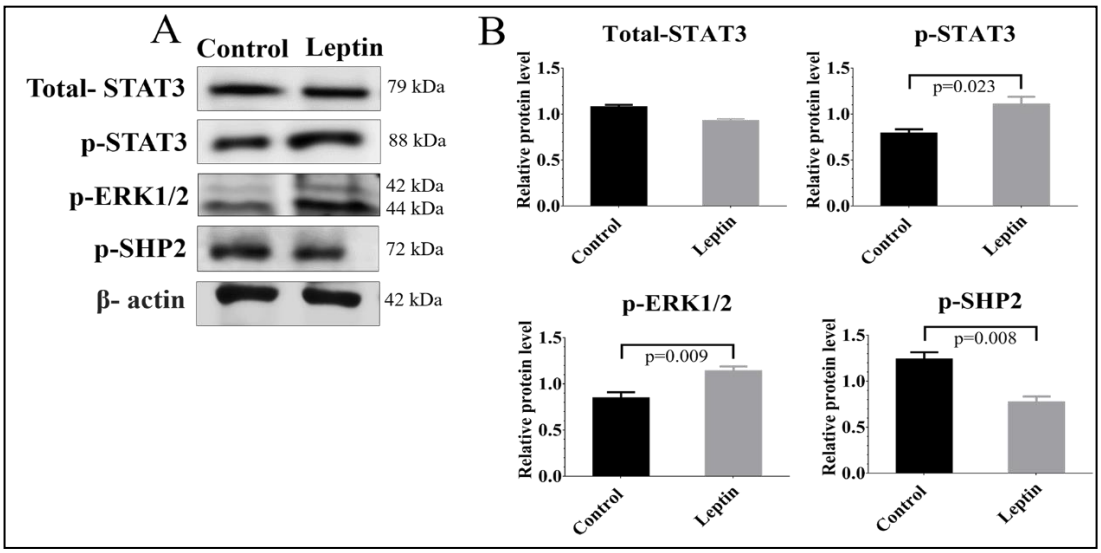

Figure 4.6. The level of p-STAT3, total-STAT, p-ERK1/2 and p-SHP2 protein in control and leptin-treated group examined using western blot analysis. A) Representative images for total-STAT3, p-STAT3, p-ERK1/2, and p-SHP2 expression B) Statistical analysis of p-SHP2, p-ERK1/2, total-STAT3, and p-STAT3 protein levels, Mean±SEM, n=3 replicates were done.

4.2. Germline Gene Editing in A *Mcm8*$^{-/-}$ Mouse Model of Azoospermia Using CRISPR/Cas9-Directed Gene Repair in iPSCs Followed by Differentiation to PGCLCs

4.2.1. Histological Evaluation of Testes from *Mcm8* Wild type, Heterozygous and Knock-out

Histologic evaluated showed that while wild type and heterozygous mice had complete and normal spermatogenesis, KO mice had atrophied seminifereous tubules and no sperm. One wild type allele in heterozygous mice is sufficient to restore spermatogenesis in this autosomal recessive infertile model.

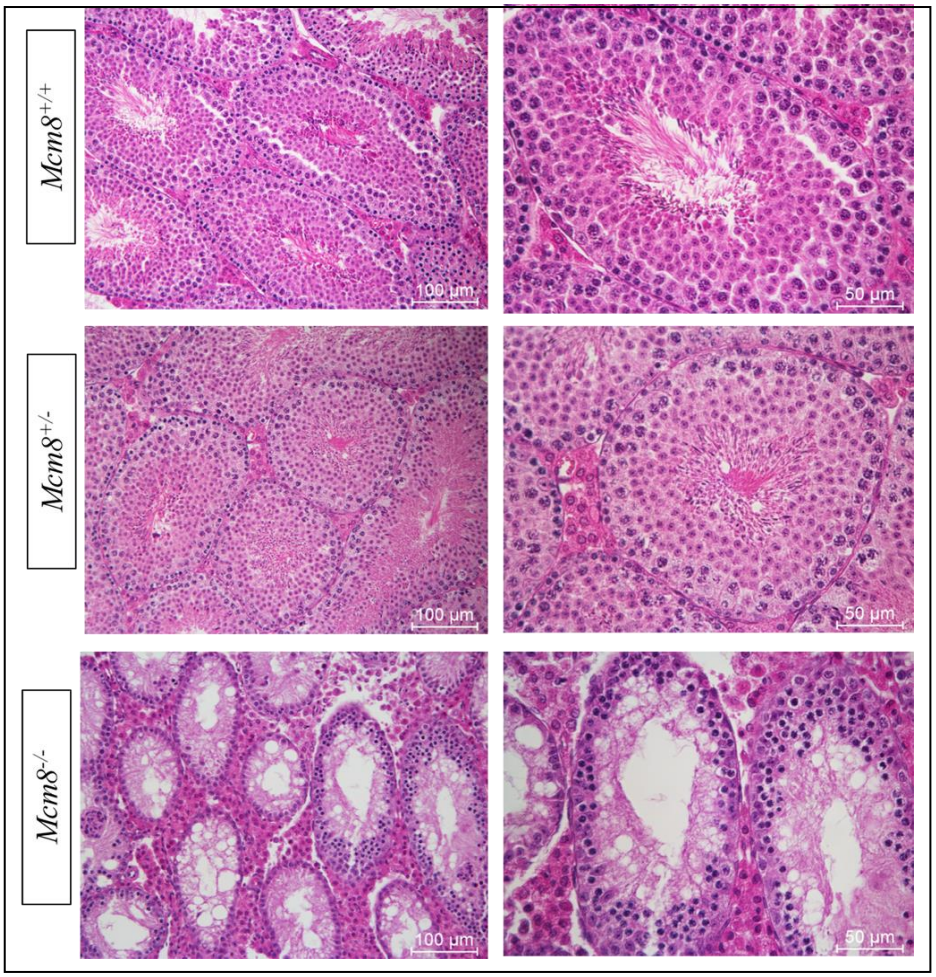

Figure 4.7. Histological examination of testes from *Mcm8* wild type, heterozygous and knock out mice. Wild type and heterozygous testes exhibited completed spermatogenesis. Knock out mice were sterile because of impaired spermatogenesis.

4.2.2. Isolation of *Mcm8*$^{-/-}$ Tail Fibroblasts and Genotyping

Fibroblast were isolated from *Mcm8*$^{-/-}$ adult mouse tail and cultured successfully and genotying results confirmed that fibroblasts had 11 bp deletion in *Mcm8* exon4 (Figure 4.8.).

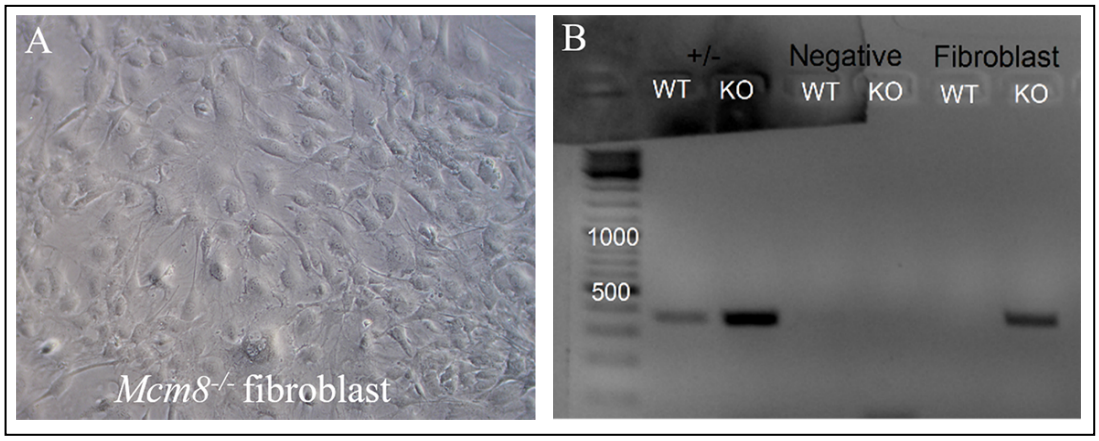

Figure 4.8. Micrograph of cultured *Mcm8*$^{-/-}$ fibroblasts at passage 3 and genotyping result. A) *Mcm8*$^{-/-}$ fibroblasts from adult mice at a lower magnification (X10) B) Genotyping result of *Mcm8*$^{-/-}$ fibroblasts. *Mcm8*$^{-/-}$ fibroblasts have only one band amplified by KO specific reverse primer.

4.2.3. Reprogramming of *Mcm8*$^{-/-}$ Fibroblast into iPSC and Genotyping

The *Mcm8*$^{-/-}$ fibroblast cells at passage 3 were co-transduced with Oct4, Sox2, Klf4, and c-Myc. On day 4 after transduction, morphological changes were observed. The small clumps between the *Mcm8*$^{-/-}$ fibroblasts indicated of reprogramming cells. On day 25, individual colonies were picked up and placed onto MEF coated 48 well plate to establish cell lines (Figure 4.9.).

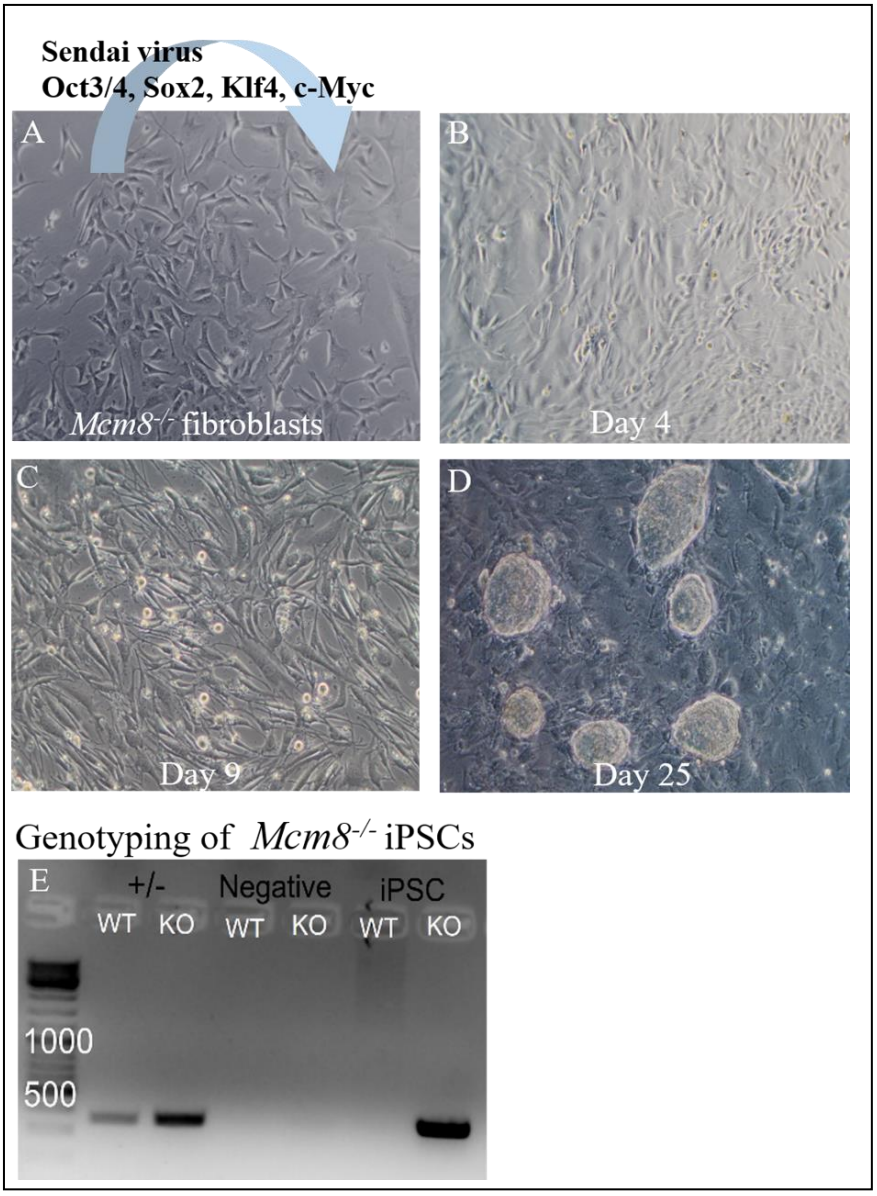

Figure 4.9. Representative phase contrast photographs of the iPSC generation process from *Mcm8*$^{-/-}$ fibroblasts and genotyping result for *Mcm8*$^{-/-}$ iPSCs. A) Primary cultures of adult *Mcm8*$^{-/-}$ fibroblasts were transduced with a Sendai virus encoding Oct3/4, Sox2, Klf4 and c-Myc and were subsequently treated with LIF on MEF treated with mitomycin-C B) Small clusters with altered morphology on day 4 following transduction. C) On day 9, small colonies with altered iPSC- like morphology on the MEF D) On day 25, individual colonies were picked up and placed onto MEF coated 48 well plate to establish cell lines E) Genotyping result of *Mcm8*$^{-/-}$ iPSCs. *Mcm8*$^{-/-}$ iPSCs have only one band amplified by KO specific reverse primer.

4.2.4. Characterization of *Mcm8*$^{-/-}$ iPSCs Lines

The iPSC lines (591 and 574) expressed pluripotency markers Oct-4, Sox-2, Nanog, and SSEA-1.and exhibited positive staining for AP. They formed teratomas including ectoderm (neural rosette, epidermis), mesoderm (bone and cartilage) and endoderm (gut-like epithelium) differentiation. (Figure 4.10.B and Figure 4.11.B) For karyotyping, 20 cells were analyzed in 591 iPSC line. Eleven (55%) showed a normal karyotype with 40 chromosomes or 40, XY and nine (45%) had an abnormal chromosome composition, including three cells with a translocation between the Y and the 19, two cells with an extra copy of the 19, random chromosome loss and single cell anomalies (Figure 4.10.). Ten (50%) showed a normal karyotype with 40 chromosomes or 40, XY and ten (50%) had an abnormal chromosome composition, including five cells missing the Chromosome Y, three cells with a translocation between the Y and the 9, and single cell anomalies in 574 iPSC line (Figure 4.11).

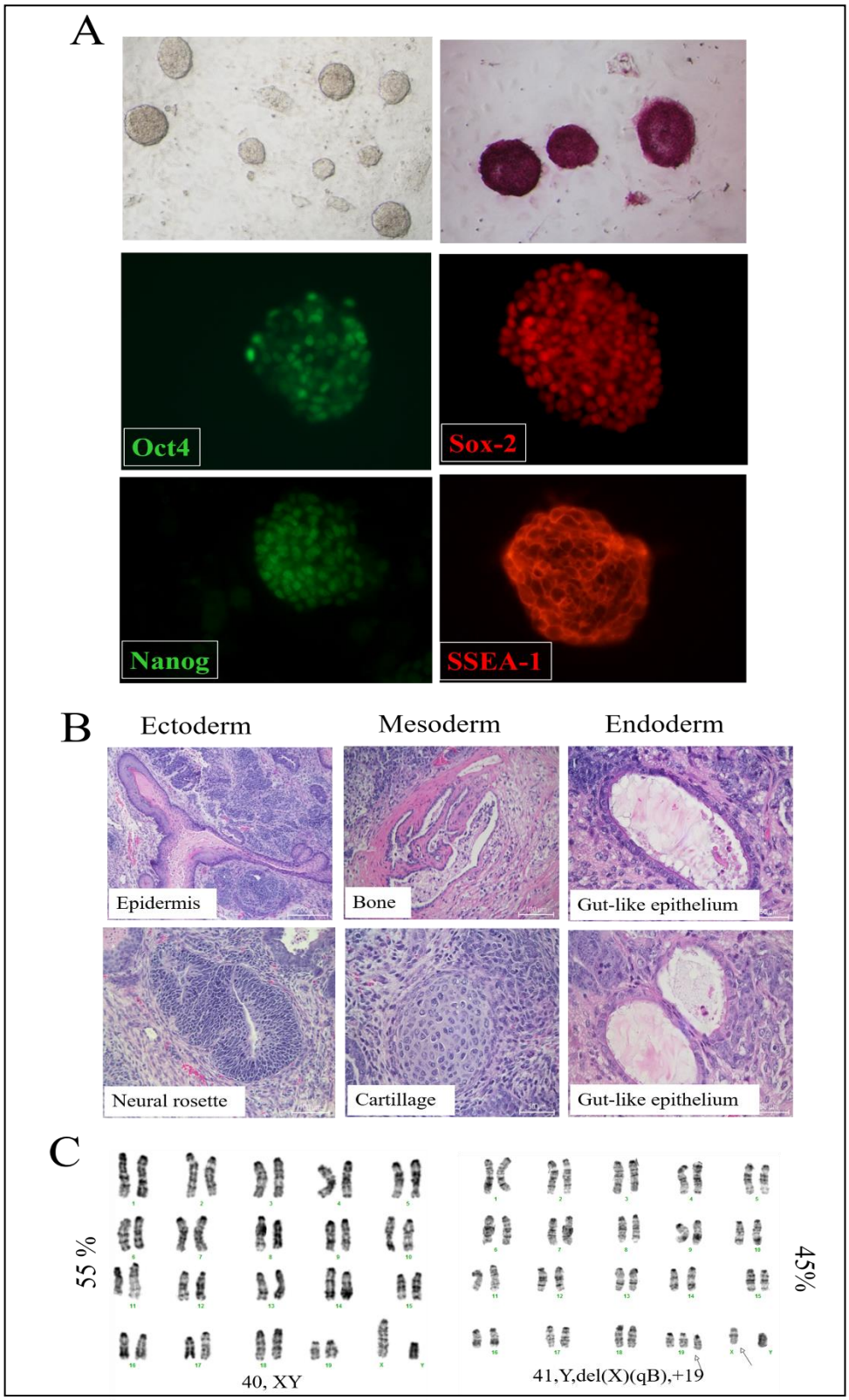

Figure 4.10. Characterization of *Mcm8*$^{-/-}$ 591 iPSCs at passage 12. A) AP staining and IF labelling for pluripotency markers Oct-4, Nanog, Sox-2 and SSEA-1 B) Teratoma formation C) Karyotype analysis.

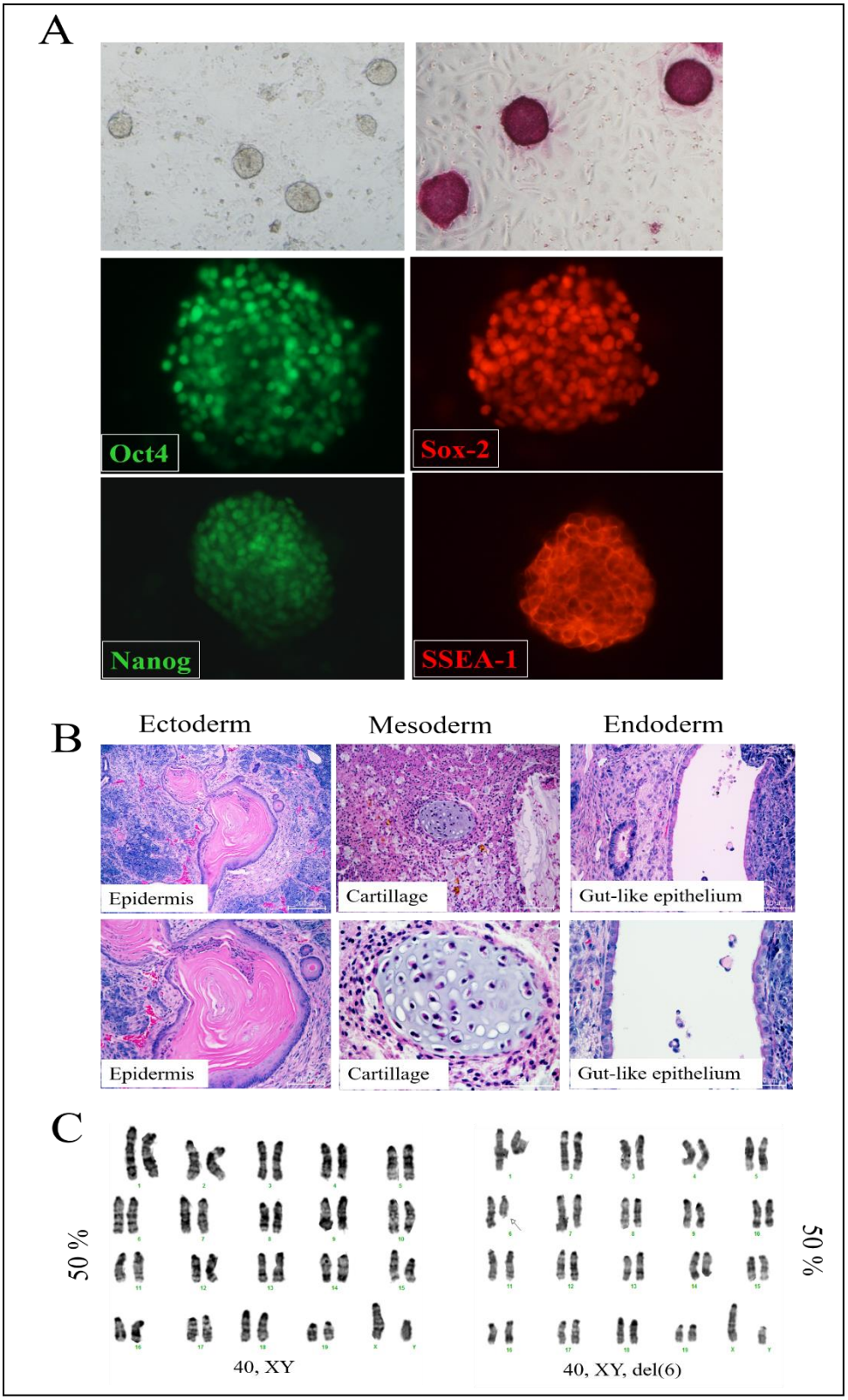

Figure 4.11. Characterization of *Mcm8*$^{-/-}$ 574 iPSCs at passage 7. A) AP staining and IF labelling for pluripotency markers Oct-4, Nanog, Sox-2 and SSEA-1 B) Teratoma formation C) Karyotype analysis

4.2.5. *In vitro* Cleavage Efficiency of Designed sgRNAs Using DNA Isolated from *Mcm8*$^{-/-}$ iPSCs

The *in vitro* assay results showed that sgRNA2 had the lowest cleavage efficiency (23.5%) and sgRNA3 had the highest cleavage efficiency (91.4%). Cleavage efficiency of sgRNA1 and sgRNA4 were 55.4% and 46.2%, respectively (Table 4.1. and Figure 4.12.). According to these in vitro results, to determine sgRNAs efficiency in cells 350 forward and 500 reverse primers were used to amplify targeted regions.

Table 4.1. *In vitro* cleavage efficiency of designed sgRNAs using DNA isolated from *Mcm8*$^{-/-}$ iPSCs.

	sgRNA1 Densitometry (%) (a-b-c) Cleavage efficiency	**sgRNA2 Densitometry (%) (a-b-c) Cleavage efficiency**	**sgRNA3 Densitometry (%) (a-b-c) Cleavage efficiency**	**sgRNA4 Densitometry (%) (a-b-c) Cleavage efficiency**
Uncleaved Control	100	100	100	100
Cleaved Control	14.5 - 54.5 - 31.0 85.5	35.7 - 52.3 - 12.0 64.3	13.3 - 46.8 - 39.9 86.7	16.6 - 46.4 - 37.0 83.4
Uncleaved350-300	100	100	100	100
Cleaved350-300	45.1 - 25.7 - 29.2 54.9	72.8 -13.8 -13.4 27.2	5.4 - 58.2 - 36.4 94.6	76.9 - 14.1 – 9.0 23.1
Uncleaved350-500	100	100	100	100
Cleaved350-500	38.5 - 34.1 - 27.4 61.5	61.6 - 24.9 - 13.5 38.4	9.6 - 51.3 - 39.1 90.4	53.4 - 27 - 19.6 46.6
Uncleaved350-650	100	100	100	100
Cleaved350-650	45.0 - 31.3 - 23.7 55	74.7 - 16.8 - 8.5 25.3	6.2 - 61.5 - 32.3 93.8	48.7 - 30.9 - 20.4 51.3
Uncleaved850-300	100	100	100	100
Cleaved850-300	42.6 - 38.9 - 18.5 57.4	84.8 - 14.4 - 0.8 15.2	5.6 - 61.7 - 32.7 94.4	50.1 - 37.7 - 12.2 49.9
Uncleaved850-500	100	100	100	100
Cleaved850-500	43.8 - 35.8 - 20.4 56.2	82.3 - 11.9 - 5.8 17.7	8.5 - 52.1 - 39.4 91.5	45.1 - 32.2 - 22.7 54.9
Uncleaved850-650	100	100	100	100
Cleaved850-650	52.6 - 24.5 - 22.9 47.4	82.7 - 10.8 - 6.5 17.3	15.9 - 46.8 - 37.3 84.1	48.6 - 27.6 -23.8 51.4
Average of efficieny for each sgRNA	55.4	23.5	91.4	46.2

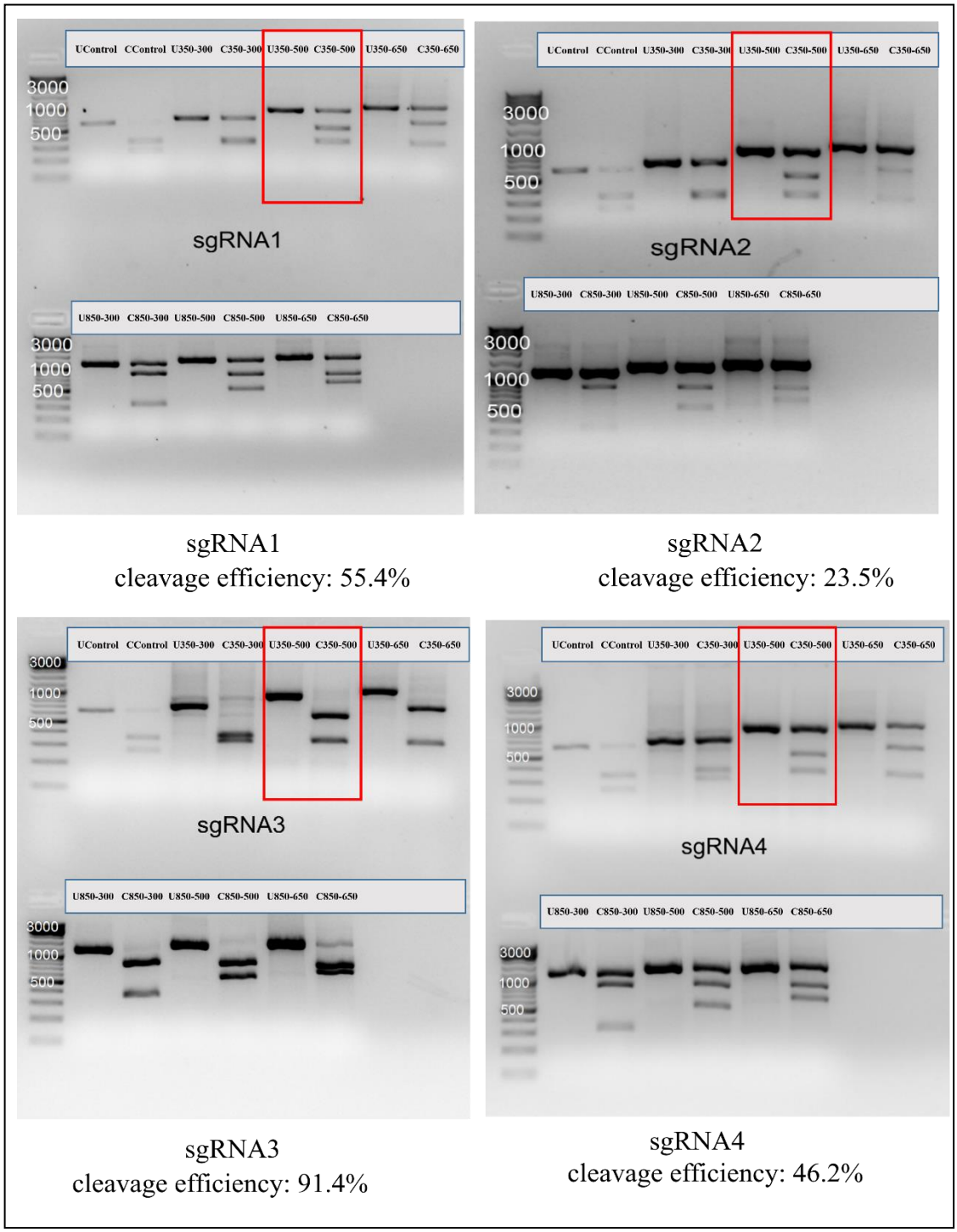

Figure 4.12. Cleavage efficiency of designed sgRNAs *in vitro*. PCR fragment (different size of PCR fragments) containing the sgRNA target sequence was mixed with recombinant Cas9 protein and each sgRNA. The cleavage reaction was analyzed by agarose gel electrophoresis.

4.2.6. Optimization of Transfection Methods

Electroporation

Six conditions were evaluated to determine which electroporation condition has highest viability and transfection efficiency. The results showed that first condition 115V-5S had highest transfection efficiency compared with the other conditons. Viability of negative non-transfected control, first condition and second condition were higher than last condition. Based on the results, first condition 115V-5S was used for electroporation-based transfection in iPSCs (Figure 4.13.).

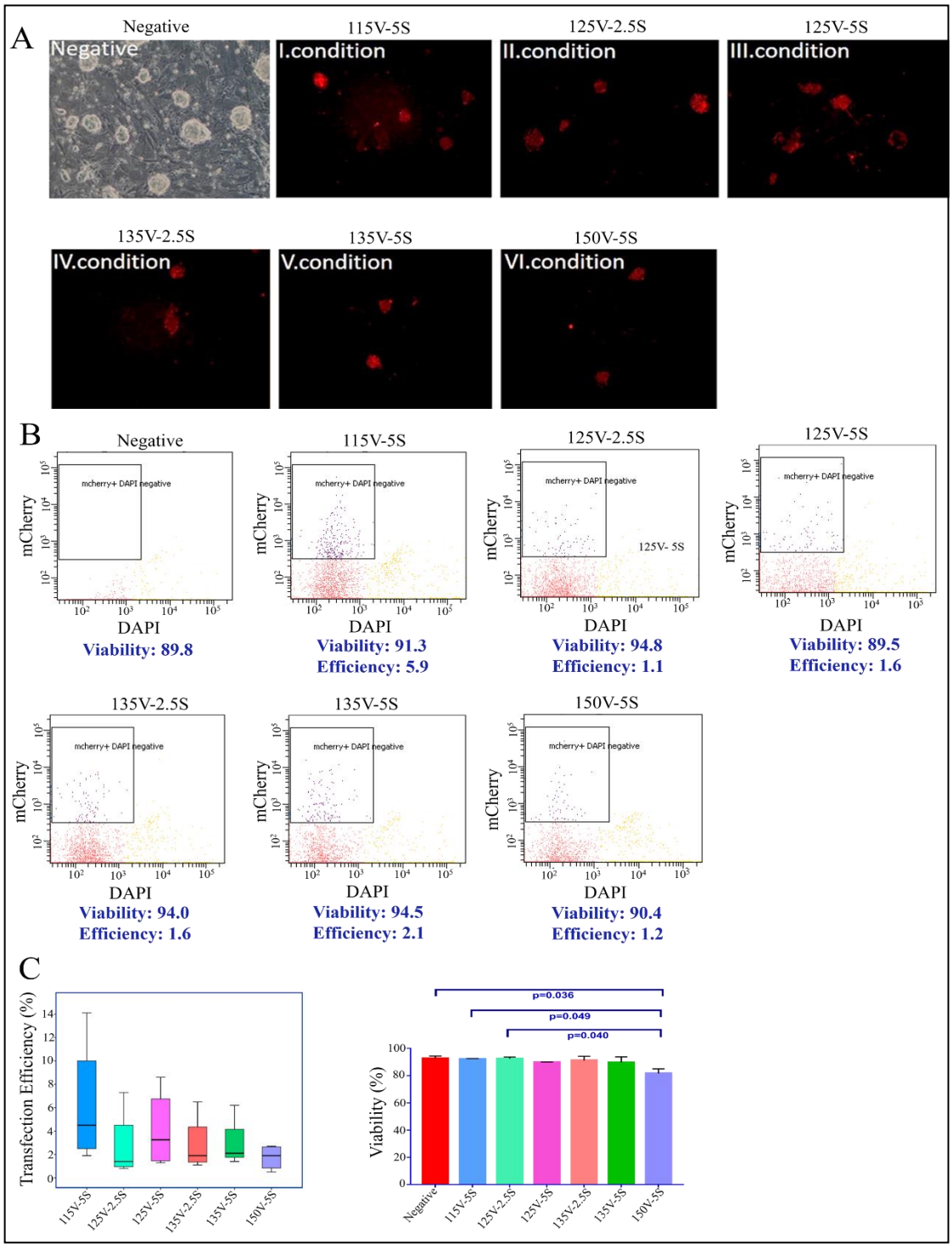

Figure 4.13. Optimization of electroporation-based transfection. A) Micrographs show mCherry (+) iPSC B) Representative FCM analysis shows that 115V-5S condition has higher viability and transfection efficiency compared with other conditions C) Statistical analysis for viability and electroporation-based transfection efficiency according to the FCM results, n=4.

Lipofectamine

For this approach four different conditions by feeder free and feeder-dependent conditions using different cell number were evaluated and viability and transfection efficiency for each condition was determined by flow cytometry. Lipofectamine based transfection method has higher transfection efficiency than electroporation-based method while viability is similar in these two approaches. Higher amount of lipofectamine led to decrease of transfection efficiency in feeder dependent and feeder free conditions. Based on these results, to deliver CRISPR/Cas9 components as a RNP complex, feeder free and feeder dependent approach with lower amount of lipofectamine using 50000 cells on MEF and 75000 cells on matrigel were chosen for this approach (Figure 4.14.).

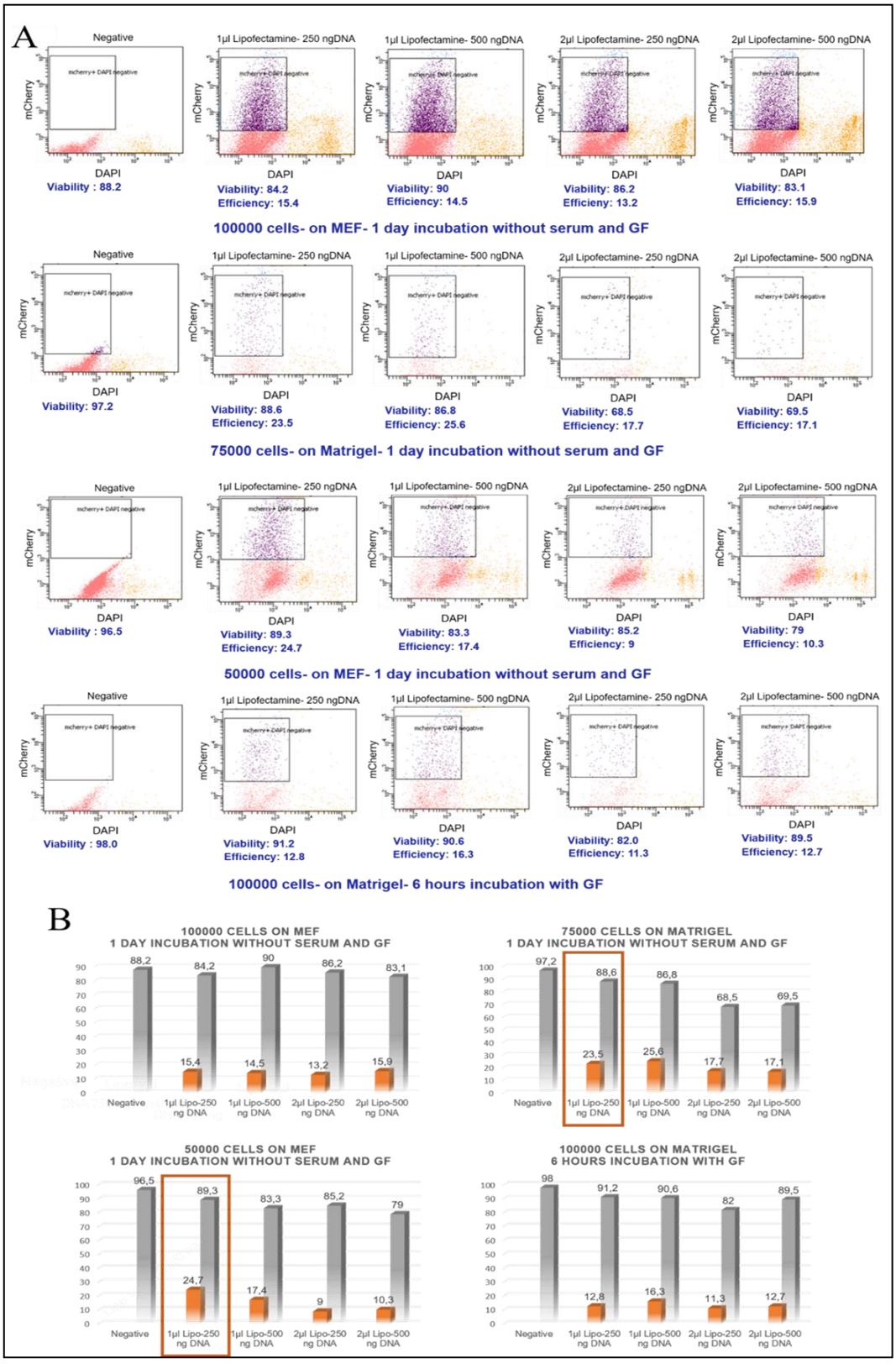

Figure 4.14. Optimization of lipid-based transfection. A) Flow cytometry analysis results for each condition B) Graphical demonstration of FCM results for viability and transfection efficiency in each condition.

4.2.7. Cleavage Efficiency of Designed sgRNAs in *Mcm8*$^{-/-}$ iPSCs

Cleaveage efficiency of designed four sgRNAs was tested in iPSCs by surveyor assay. Red arrows indicate the detected cleavage products. The cleavage products should be around 350 bp and 500 bp. sgRNA1 was highest efficiency compared with the other sgRNAs in cells. However, for sgNA4 in addition to expected bands extra bands indicated by white arrows were seen. The results showed that while sgRNA1 and sgRNA2 efficiency results were consistent with *in vitro* cleavage efficiency, efficiency of sgRNA3 in iPSCs cells were lower than *in vitro* cleavage efficiency (Figure 4.15.). To induce HDR repair pathway with ssODN template, sgRNA1 was used to target mutant gene.

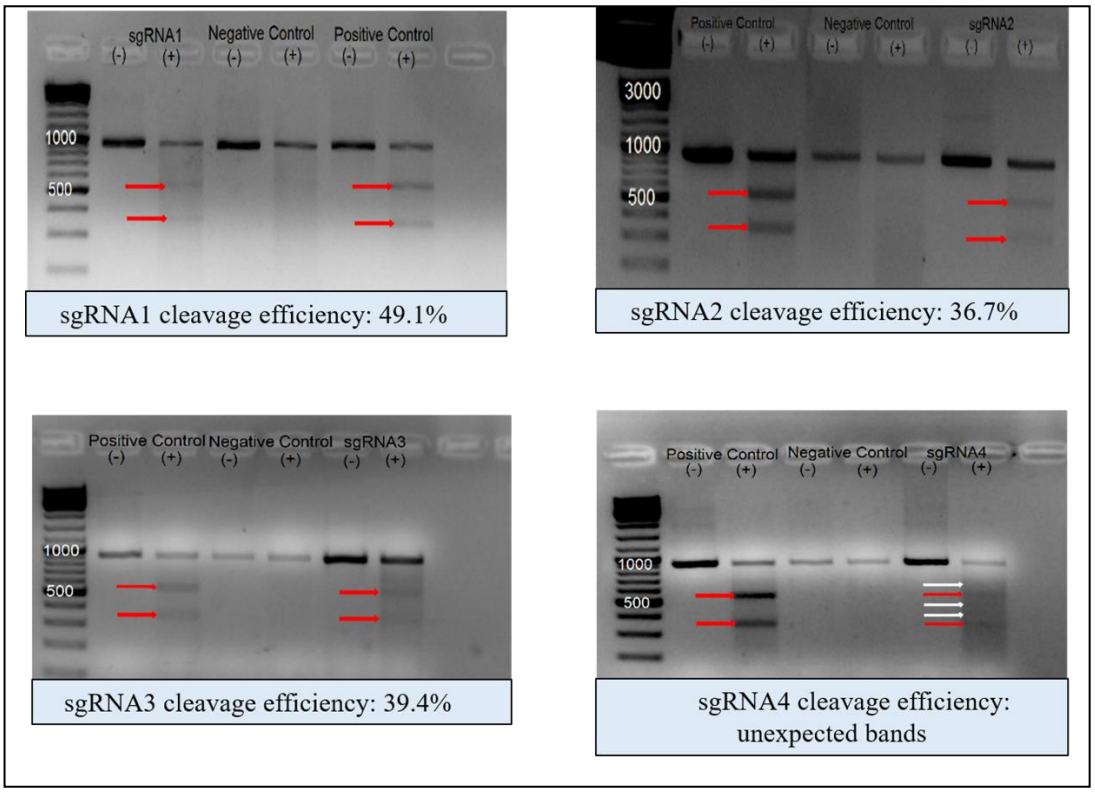

Figure 4.15. Cleavage efficiency of designed sgRNAs in *Mcm8*$^{-/-}$ iPSCs.

4.2.8. Correction of Mutation by Homologous Recombination Pathway

To induce DSB sgRNA1 was used to target mutant gene with 60 bp or 90 bp ssODN. Electroporation and lipofectamine transfection methods were carried out and

to increase efficiency of HDR pathway, DNA ligase inhibitor SCR7 was used in some trials. *Mcm8* 11 bp deletion was corrected (one gene corrected allele and one KO allele) successfully corrected using 90 bp ssODN without SCR7 inhibitor delivered by electroporation transfection method and 60 bp ssODN with chemical modification and SCR7 delivered by lipofectamine transfection method. Initially, genotyping was performed to select heterozygous colony (Figure 4.16.) and the DNA sequencing was confirmed that electroporated colony with sgRNA1 and ssODN containing 90 bp homology arms was heterozygous (Figure 4.17.A). Also, after establishing heterozygous colony, genotyping and karyotyping were performed. The line (591-14) was heterozygous (4.17.B) and showed a normal karyotype in 90% of cells analyzed (Figure 4.17.C).

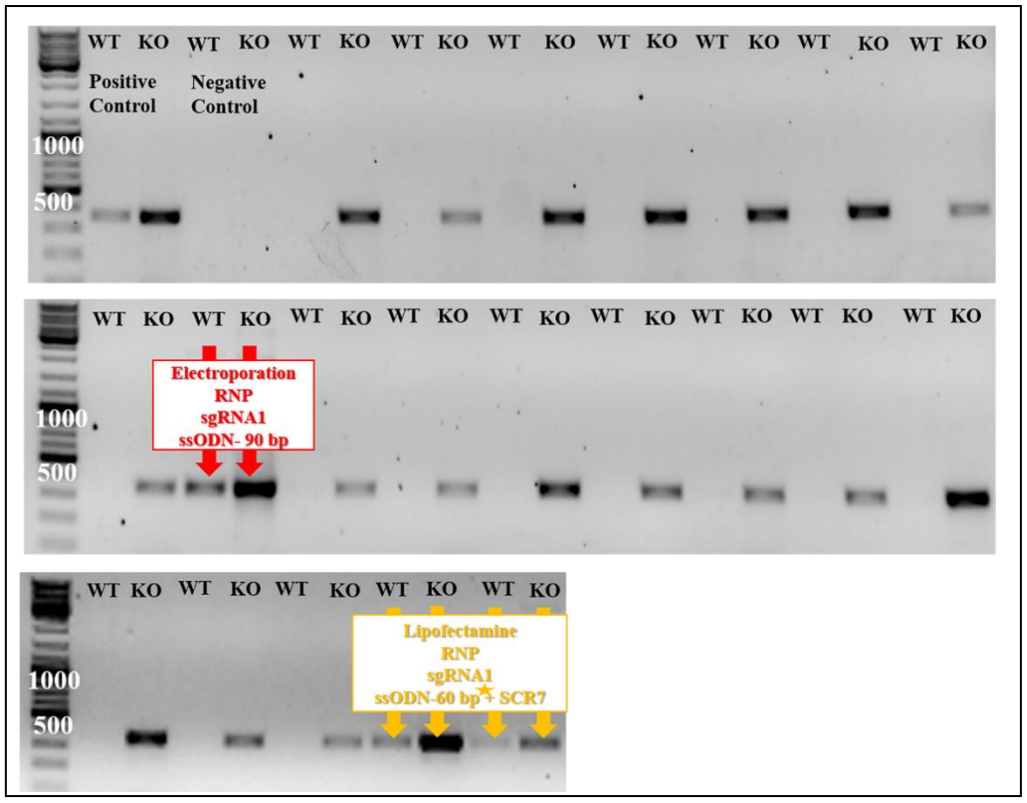

Figure 4.16. Demonstrative genotyping results from mCherry (+) single colonies. After transfection, mCherry (+) single colonies were picked up and expanded on MEF coated 48 well plate. *Mcm8*$^{gc/-}$ colonies was selected by genotyping.

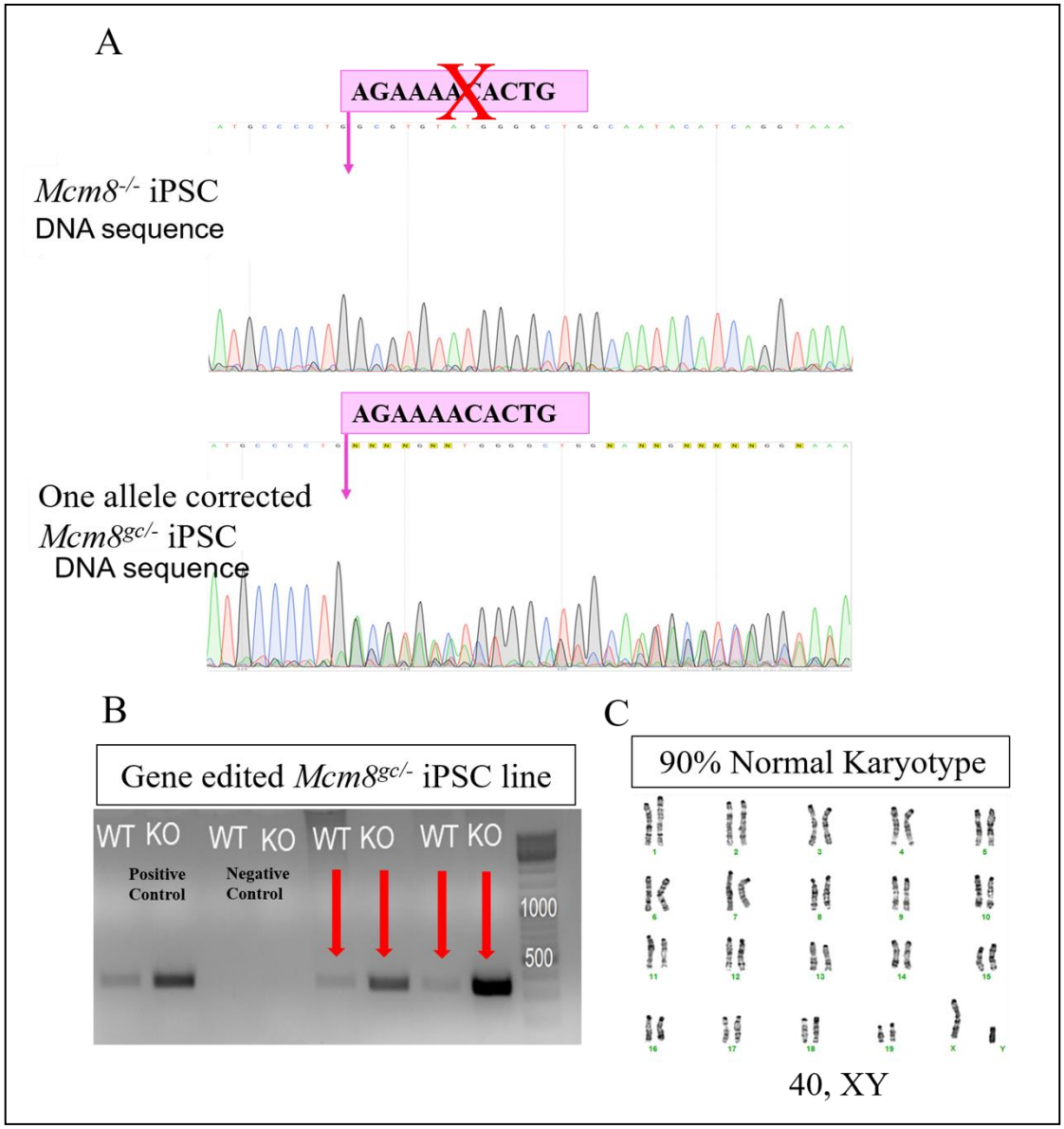

Figure 4.17. DNA sequencing and karyotyping in gene edited *Mcm8*$^{gc/-}$ colony (591-14) transfected by electroporation. A) DNA sequencing results showed presence of one gene edited allele and one KO allele in this heterozygous colony B) Genotyping result confirmed that *Mcm8*$^{gc/-}$ cell line (591-14) was heterozygous. C) The line showed a normal karyotype in 90% of cells analyzed.

4.2.9. Generation and Characterization of PGCLCs

Gene corrected iPSC line was differentiated into flat and simple epithelium like that morphologically resemble epiblast by EpiLCs differentiation medium containing ActA, bGFG and KSR. When EpiLCs were cultured with BMP4, BMP8a, SCF, LIF

and EGF, these cells formed aggregates. After PGCLC induction, surface markers CD61 and SSEA1were used to quantify these cells by FC analysis and 65.32% of cells induced PGCCLs were double positive for these markers (Figure 4.18.).

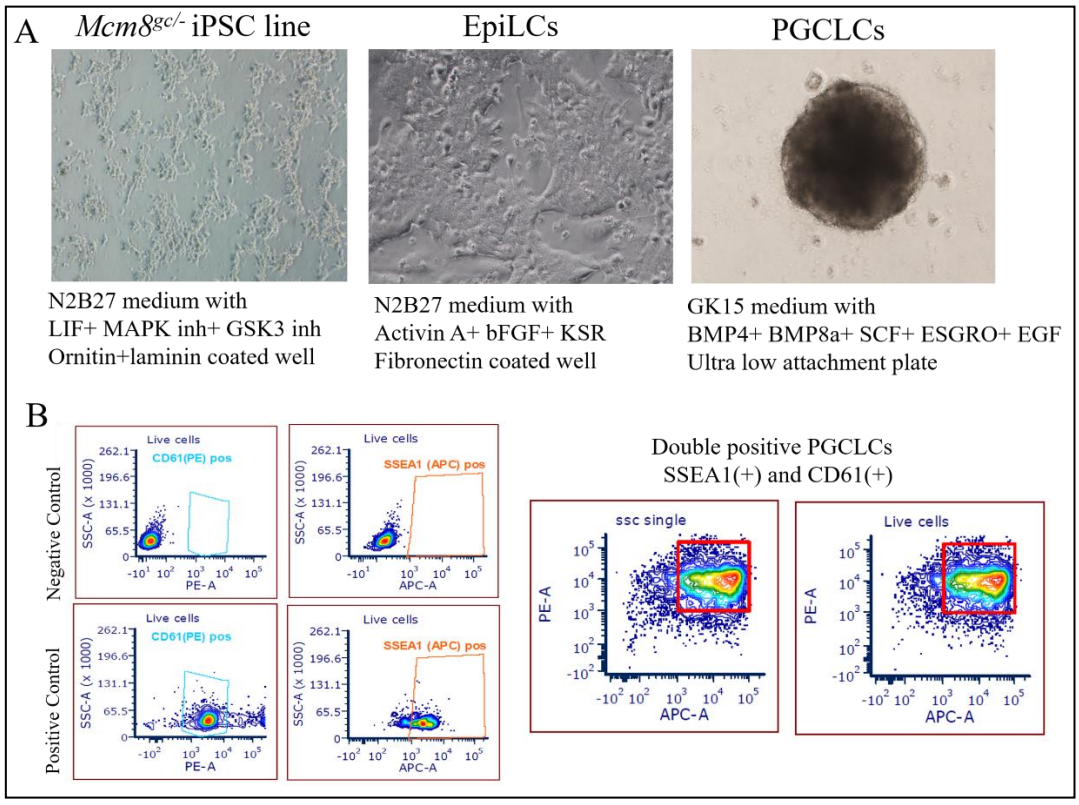

Figure 4.18. Generation and characterization of *Mcm8*$^{gc/-}$ PGCLCs. A) PGCLCs induction from gene edited 591 p6 *Mcm8*$^{gc/-}$ colony transfected by electroporation method B) Flow cytometry analysis to determine SSEA1(+)/CD61(+) PGCLCs derived from gene edited *Mcm8*$^{gc/-}$ iPSC line.

5. DISCUSSION

In this thesis we demonstrated that leptin induces proliferation neonatal male C57BL/6 mouse SSCs. Moreover, we corrected the mutation via CRISPR/Cas9 gene editing in *Mcm8*$^{-/-}$ mouse fibroblast-derived iPSCs and further generated *Mcm8*$^{gc/-}$ PGCLCs *in vitro*. Those two chapters data will be discussed separately and a final conclusion will be done at the end.

Chapter 1. Isolation, Characterization of Neonatal Male C57BL/6 SSCs and to Assessment of Time and Dose Dependent Proliferative Effect and the Mechanism of Action of Leptin Supplementation on Cultured SSCs *In vitro*

In this thesis, neonatal mouse SSCs were isolated successfully and proliferative effect of leptin in a dose and time dependent manner on cultured SSCs was shown. Our findings indicated that leptin hormone at 100 ng/ml concentration promoted proliferation in SSC cultures on day 5 and 7 compared to control by colony number, colony diameter, WST-1 assay and xCELLigence RTCA. Moreover, 114 ng/ml of leptin was determined as ED50 to proliferate SSCs for 7 days. Flow cytometry results showed that 100 ng/ml leptin administrated group had the highest percentage of CD90.2 positive cells. Our findings also suggested that STAT3 and ERK1/2 signaling pathways might contribute to proliferative effect of leptin in SSC cultures evaluated by western blot analysis.

We initially mapped neonatal SSCs within the testes of 6-days-old male C57BL/6 mice by IF labeling, histologic and ultrastructural morphologic assessment. Subsequently, seminiferous tubules were digested by enzymes and fractionation by 30% Percoll and MACS technique by CD90.2 microbeads were carried out to get highly enriched SSCs and eliminate other cell contamination. Several approaches such as extracellular matrix selection, differential plating, FACS and MACS have been used to enrich SSCs and maintain the viability and spermatogenic potential (10, 11, 184-190, 192, 275, 276). The percentage of PLZF(+) CD90.2(+) and c-kit(-) cells was checked with FCM following MACS separation. Additionally, cultured SSCs were evaluated for PLZF by IF labeling. These findings clearly indicated that the MACS separation method was an effective and appropriate technique to enrich undifferentiated stem and progenitor spermatogonia prior to *in vitro* culture. Our

results related to fractionation by Percoll and MACS separation utilizing CD90.2 positivity were consistent with previous research in the literature.(11, 189, 192).

Here we report the existence of the functional leptin receptor (OB-Rb) on cultured SSCs by qualitative IF labelling. The OB-Rb of leptin presented diffuse membranous labeling pattern within the SSCs in our study. El- Hefnawy et al. (29) and Herrid et al. (28) indicated the presence of leptin and its receptors in neonatal testis tissue of mice using IHC and RT-PCR. Their IHC assessment revealed membranous labeling pattern for OB-Rb and, our data is consistent with both studies (28, 29). Leptin is endogenously produced by EWAT (26) and it is capable of crossing BTB to act in paracrine manner on type A spermatognia (277). Taken together, the OB-Rb labeling suggests leptin supplementation might target the SSCs in the neonatal testis to exert its potential proliferating effect.

Our proliferation assay results indicated that leptin hormone at 100 ng/ml concentration promoted SSCs proliferation on day 5 and 7 of culture compared to control by colony number, colony diameter, WST-1 assay and xCELLigence RTCA. Exogenous leptin's proliferative effect terminates and reaches to the control values when used at a dose of 200 ng/ml. The proliferating effect of exogenous leptin on several somatic stem (30-34) and differentiated (35-38) cells has been reported at a range of 10-500 ng/ml at various time intervals *in vitro*. 10- 100 ng/ml leptin supplementation induces derivation rate of mouse ESCs from blastocysts in embryo culture media (34). In the same study leptin-treated, embryo-derived ESCs exhibited Oct-4, Nanog, SSEA-1 pluripotency markers and positive staining for alkaline phosphatase (34). Leptin stimulated porcine skeletal myoblast proliferation by MTT assay at a dose range of 2- 20 ng/ml for 48 hours (32). It induced and inhibited pre-adipocyte and stromal vascular cell proliferation by 3H-thymidine incorporation assay at a dose range 50-100 ng/ml and 250-500 ng/ml, respectively (31). Those results suggest dose dependent specific effect of leptin on cellular proliferation of pre-adipocytes. Exogenous 100 ng/ml leptin treatment increased human breast stem cell (33) and mouse embryonic mesenchymal stem cell number (30) by secondary mammosphere formation and 3H-thymidine uptake respectively, and it did not change phenotypic features of those stem cells (30). Leptin proliferated HUVECs and HMECs at a dose of 10 nmol/l for 48 hours by 3 H-thymidine incorporation (35). Rat smooth

muscle cells were proliferated with exogenous leptin at a dose range of 10-200 ng/ml when supplemented into culture (38). While a single injection of 1 to 10000 ng/ ml leptin for 24 hours stimulated H-thymidine incorporation in cultured rat glomerular endothelial cells, it failed to stimulate proliferation of syngeneic rat mesangial cells due to the absence of OB-Rb on target cells (35). Even though our results are consistent with proliferative effect of leptin on stem and mature somatic cells shown in previous studies *in vitro*, controversial observations were reported in *in vivo* animal models with high leptin doses. Long term (2 to 6 weeks) systemic leptin administration in a dose range from 3 µg/kg to 3 mg/kg caused alteration in spermatogenesis by reduced sperm count, disruption of seminiferous tubules morphology and decreased germ cell apoptosis in adult male mice (236, 237) and rats (196, 238). Leptin at 0.1 and 0.5 mg/kg of dose led to no alteration in sperm parameters and number of apoptotic germ cells when applied daily for 2 weeks in mice (237). On the other hand, exogenous systemic leptins's effects were reported to be reversible on day 56 following 60 µg/kg treatment in rats (196). In our *in vitro* study we report the proliferative dose window for leptin on SSCs as 50-100 ng/ml in terms of colony number, colony diameter and proliferation rate by WST assay from day 5 to 7. Leptin was able to stimulate proliferation in SSC cultures as demonstrated by increase on colony formation (both colony number and diameter). Furthermore, we determined for the first time the accurate real time ED50 dose as 114 ng/ml for 7 days by xCELLigence RTCA. Notably, the ED50 is in the proliferative dose range of leptin determined by WST. Our results are limited to *in vitro* conditions On the other hand, *invivo* studies reveal some negative systemic effects of high doses of leptin. Leptin has not been investigated for it's dose dependent cellular effect on spermatogonial cells. Here we report for the first time the real time dose dependent effects of leptin at the cellular level by RTCA. xCELLigence real time analysis has been reported as a reliable method frequently used to investigate the effective and safe application dose window of several mediators including testosterone, on stem cells (272) or somatic cells (273) (274) so far.

In this thesis, western blotting results showed that the EC50 dose of leptin (114 ng/ml) significantly increased p-ERK 1/2 and p-STAT3 levels after 30 min of administration, when compared to those of the untreated control; while p-SHP2 protein level was lower with leptin treatment comparing to that of control. 30 minutes has been

reported to be adequate for the induction of p-ERK1/2 pathway in the literature (37, 38) and our results confirmed the induction at that time interval. 10 to 100 ng /ml leptin increased level of p-ERK1/2 in rat VSMC (37, 38). This dose range is almost similar to ours. Phosphorylation of Tyr^{985} via JAK2 provides a binding site for SHP2 (27, 197, 278) Leptin exerts its effect via SHP2- ERK pathway or ERK pathway can be activated independent of SHP2 activity (197). The SHP2 plays a role in neonatal SSCs (279). Thus, we hypothesized that leptin might show its proliferative effect on SSCs through SHP2/ERK signal pathway. We demonstrated that ERK1/2 phosphorylation increased and the p-SHP2 protein decreased significantly after leptin treatment in SSC cultures. Several findings reported that SHP2 might be important for the proliferation and survival of SSCs and to maintain BTB (279, 280). It also acts on bFGF and GDNF mediated activation of ERK signal pathway (280). Our findings suggest that SHP2 may not have any effective for the activation of ERK1/2 pathway to proliferate SSCs and. Additionally, we showed the STAT3 pathway activation in SSCs after leptin treatment. Previous studies showed that activated SHP2 can downregulate STAT3 (281). While STAT3 pathway promotes differentiation in mouse SSCs (192), this pathway is an effective pathway for stem cell renewal and the maintenance of pluripotency in human and mouse ESCs (282-284) and Drosophila male germline (285, 286). Leptin serves as a potent mitogen for somatic cells by phosphorylation of OB-Rb on Tyr^{1138}, which is the essential site for STAT-3 binding and activation (36). Leptin increased the renal cell carcinoma cell proliferation by enhancing the expression of both p-ERK and p- STAT3 (287). Our findings are in line with those previous studies that highlight the OB-Rb mediated effect of leptin via both SHP2 independent ERK and STAT3 pathway activation.

The results of the study in the first chapter of the thesis are limited to *in vitro* conditions and our leptin-induced enlarged SSC pool should further be tested *in vivo*. Leptin-proliferated SSCs need to be transplanted to nude mice in order to evaluate functional capability of these cells. This limitation however does not restrict future *in vivo* and clinical studies as statistical accuracy was validated in the present study. Furthermore, the xCELLigence RTCA has been reported as one of the most reliable *in vitro* techniques that provide assessment of the potential future personalized treatments before clinic. Although stem cell therapies are only option to regenerate

spermatogenesis in PCSs, techniques to remove malignant contamination from testicular tissue should be optimized. Ultimately leptin provides stepping-stone *in vitro* to proliferate SSCs and to maintain their stemness properties before human clinical applications.

Chapter 2. Correction of Genetic Defect Using CRISPR/Cas9 Gene Editing in *Mcm8*$^{-/-}$ Mouse Fibroblast-Derived iPSCs and Generation of PGCLCs from Gene Corrected Heterozygous iPSCs *In vitro*

Here we isolated fibroblasts from tail of *Mcm8*$^{-/-}$ mice and reprogrammed them to become iPSCs. Two novel *Mcm8*$^{-/-}$ mouse iPSC lines (591 and 574) were generated, cloned, and characterized. The two lines were positive for AP staining, expressed pluripotency markers Oct-4, Nanog Sox-2, and SSEA-1, and formed teratomas containing three germ layers. A validated *Mcm8*$^{-/-}$ iPSC clone was gene-edited using CRISPR/Cas9 and an oligonucleotide template containing the wildtype *Mcm8* sequence. We identified one clone with one *Mcm8* allele corrected back to the wild type (*Mcm8*$^{gc/-}$) by DNA sequencing. Gene-edited (*Mcm8*$^{gc/-}$) clone 14 was differentiated to PGCLCs that exhibited a SSEA1+/CD61+ phenotype.

Here we report for the first time fibroblasts from *Mcm8*$^{-/-}$ male mice tail can be isolated, maintained, and reprogrammed to iPSCs using reprogramming factors including Oct3/4, Sox2, Klf4, and c-Myc. Two novel *Mcm8*$^{-/-}$ mouse iPSC lines were generated, cloned, and characterized by morphological appearance, pluripotency markers and teratoma formation successfully. The *Mcm8*$^{-/-}$ iPSC lines were positive for alkaline phosphatase staining, pluripotency markers, and formed teratomas containing ectoderm, mesoderm, and endoderm. In our protocol, to deliver reprogramming vectors, integration-free method with Sendai virus was used to obtain iPSCs without genomic alterations. There have been several delivery methods to transfer exogenous genes into somatic cells for reprogramming. Retrovirus (288-292), lentivirus (293, 294), adenovirus (295, 296), adeno-associated virus (AAV) (297, 298) have been used to deliver exogenous transgene. While retrovirus-mediated delivery method requires an actively dividing somatic cell to integrate exogenous genes, lentivirus can be integrated into both dividing and non-dividing cells (293, 294). These vectors are usually silenced in iPSCs and ESCs, however; inefficient silencing is possible and silenced transgenes may be also reactivated. Random integration of these

vectors into the host genome increases the risk of insertional mutagenesis. Integration-free iPSCs from adult mouse hepatocytes (295) and human fibroblasts (296) were generated by adenovirus-mediated delivery method. The adenovirus and AAVs (Adeno-associated virus) are capable of transducing both dividing and non-dividing cells (299, 300) similar to lentivirus. However, AAV vector system has the limited packaging capacity of approximately ~5 kb. Since above mentioned delivery approaches have low reprogramming efficiency and/or chromosomal integration of exogenous reprogramming genes, integration-free method with SeV appears to be more convenient method to deliver reprogramming genes without chromosomal integration for clinical applications (301-307).

We corrected 11 base-pair deletion in *Mcm8* gene using CRISPR/Cas9 method gene editing system that consists of two key molecules gRNA and Cas9 nuclease and a 90 bp oligonucleotide repair template in *Mcm8*$^{-/-}$ iPSCs. For CRISPR/Cas9 gene editing approaches four sgRNAs sgRNA1, sgRNA2, sgRNA3 and sgRNA4 and to induce HDR pathway, ssODNs containing 60 bp or 90 bp homology arms flanking cutting side in either sense or antisense orientation relative to the gRNA sequence were designed. Moreover, to reduce activity of nucleases, ssODNs containing 60 bp homolog arms were chemically modified with phosphorotiate near both 5 prime and 3 prime ends. Since the incidence of HDR-mediated DNA repair is very low in mammalian cells and even in the presence of repair template, NHEJ is the more frequent repair mechanism. To overcome this challenge, some approaches have been developed to increase efficiency of HDR repair way and inhibit NHEJ (308). For this reason, in our study, Scr7 that inhibits NHEJ component DNA ligase IV was used at different concentrations in some trials to increase HDR efficiency. Even though different strategies have been tested, heterozygous gene corrected iPSC colony was obtained by electroporation-based delivery method of sgRNA1 and 90bp repair template. On the other hand, two heterozygous colonies transfected by lipofectamine-based delivery method of sgRNA1 and chemically modified 60 bp ssODN repair template and treated by 1μM SCR7 for 24 hours after transfection were confirmed by genotyping.

In this study, ribonucleoprotein (RNP) complex, consisting of Cas9 protein and guide RNA, was used because of its many advantages including reduced off-target

binding, less toxicity, higher efficiency and simpler design to deliver CRISPR/Cas9 components into the cells (242). The other methods are that gRNA can be delivered as DNA cloned into a plasmid (309, 310) or as in vitro transcript (311) on the other hand; Cas9 can be delivered as plasmid DNA (256, 260), *in vitro* transcribed mRNA (311) or as protein (258, 312) The later methods have some drawbacks: chosen of appropriate promoters for both Cas9 and gRNA expression, incorporation of designed plasmid DNA into the genome of targeted cells, off-target effects owing to prolonged expression of Cas9, transcription or translation of Cas9 and designed RNA.

Electroporation based transfection method and lipid based transfection methods were used to deliver this RNP complex into *Mcm8*$^{-/-}$ iPSCs in this study. There are many ways to introduce these CRISPR/Cas9 components into cells. In general, the delivery system can be divided into two main categories as the viral and non-viral delivery systems (313). Viral vectors include adenovirus, adeno-associated virus (AAVs) (314) and lentivirus (315), nonviral group can be subcategorized into two groups physical methods and chemical methods (313). Physical methods mainly include electroporation and microinjection (316). Chemical methods such as lipid, polymer gold nanoparticles, DNA nanostructures, cell-penetrating peptides can be used to deliver component of CRISPR/Cas9 (313, 316-319). We repaired mutation on *Mcm8*$^{-/-}$ iPSCs via delivering RNP complex and 90 bp oligonucleotide via electroporation based transfection method. Recently, mutation in Kit^{w}/Kit^{wv} mouse SSC has been corrected using electroporation based transfection approach. The gene edited SSCs were propagated, transplanted into testis, and completed spermatogenesis (154). Even though transfection efficiency was extremely low in *Mcm8*$^{-/-}$ iPSC in our study, using more cells, picking, and expanding mCherry(+) single colonies instead of FACS sorting helped to overcome this obstacle and gene repaired iPSCs were differentiated into PGCLC successfully. For PGCLCs induction we followed Hayashi's protocol published in 2011. Up to now, several reports have been published to obtain PGCLCs from iPSCs in several species including human (2, 136, 137, 139-149, 151-153, 240). Even though many attempts have been performed to obtain healthy offspring, Hayashi et al. (143) reported that PGCLCs were able to complete spermatogenesis and produced functional spermatozoa. Moreover, the researchers obtained healthy offspring when the eggs were fertilized by functional spermatozoa

recovered after transplantation of iPSC-derived PGCLCs. This successful protocol was composed of 2-step induction to mimic in vivo development of male germ cells. Our differentiation results from iPSCs to EpiLCs and from EpiLCs to PGCLCs were similar to Hayashi's protocol. EpiLCs were flat and simple epithelium like and PGCLCs formed aggregates with presence of BMP4, BMP8a, SCF, LIF and EGF. After PGCLCs induction, FCM results confirmed that 65.32% cells of induced PGCLCs both CD61(+) and SSEA1(+).

The second chapter of the thesis study was limited to mouse NOA model with single gene disorder. Although, CRISPR/Cas9 gene editing method has been used to correct single gene defect causing DMD, CFTR, Hemophilia A and B, SCD and β-thalassemia in human iPSCs and these gene corrected cells were differentiated into functional cells (254-260), we should take into consideration the long term effect of CRISPR/Cas9 gene editing method before clinical trials.

Collectively, *ex vivo* gene-editing of iPSC can restore gene function, gene repaired iPSCs can differentiate into PGCLCs and *in vivo* transplantation of gene-corrected PGCLCs can regenerate spermatogenesis in NOA males with single gene disorder and SSCs can be propagated by 100 ng/ml leptin and transplanted back into PCSs when they would like to have own their biological children. These approaches would help to provide effective treatment of male infertility in clinical trials.

6. CONCLUSION & FUTURE PERSPECTIVE

Several potential approaches have been emerged to solve infertility problem in PCSs and azoospermic men with germ cell genetic defect. Spermatogonial stem cells arise from PGCs during development are critical cells to maintain production of sperm and can be depleted by gonadotoxic treatment in PCPs. Therefore, a large and functional SSC pool is only available option to restore spermatogenesis in PCSs. Moreover, generation of germ cells from iPSCs after gene repair in NOA men with germ cell genetic defect is a promising approach to treat infertility. In this collaborative thesis study between Hacettepe and Pittsburgh Universities, propagation of SSCs by leptin supplementation and correction of an infertility-associated mutation by CRISPR/Cas9 gene editing method in *Mcm8*$^{-/-}$ iPSCs to generate PGCLCs were performed. The study results are limited to *in vitro* conditions and leptin-induced enlarged SSC pool and *Mcm8* gene corrected PGCLCs should further be tested *in vivo*. Leptin-proliferated SSCs and *Mcm8*$^{gc/-}$ PGCLCs need to be transplanted into infertile mouse recipients to evaluate functional capability to regenerate spermatogenesis.

In this study, we mimicked *in vivo* testicular environment in culture system to maintain and enrich cultured neonatal SSCs. In addition to most known growth factors secreted from somatic cells of testis niche, leptin, secreted by EWAT, promoted enrichment of SSCs without losing their stemness properties via activating ERK1/2 and JAK/STAT3 pathway *in vitro* (Figure 6.1). This approach allows the expansion of SSC pool such that they can be used for auto-transplantation to restore fertility in sterile PCSs. Even though leptin treated SSCs retained stemness characteristics in current study, leptin-proliferated SSCs need to be transplanted to nude mice in order to evaluate functional capability to regenerate spermatogenesis.

The majority of unknown causes in male infertility can have genetic origin. Genetic mutations causing infertility can be corrected by gene editing methods. Some single gene disorders including *MCM8* have been associated with male infertility. In theory, *Mcm8*$^{-/-}$ SSCs could be isolated, maintained in culture, gene corrected using CRISPR/Cas9 and transplanted to regenerate spermatogenesis. However, we found that it was difficult to maintain *Mcm8*$^{-/-}$ mouse SSCs in culture and, to date, there is not method to maintain human SSCs in culture. Therefore, in this study iPSCs derived from fibroblasts were modified to correct mutation via CRISPR/Cas9 to produce male

gametes. Because heterozygous *Mcm8* males are fertile and they are able to produce sperm, we used heterozygous *Mcm8*$^{gc/-}$ iPSCs to produce PGCLCs (Figure 6.1). We predict that gene corrected PGCLCs can restore spermatogenesis in neonatal *Mcm8*$^{-/-}$ infertile mice after transplantation. Furthermore, sperm cells should have corrected allele or mutant allele. If they are used to fertilize egg from WT female, two types of embryos will be produced: *Mcm8*$^{gc/-}$ and *Mcm8*$^{+/-}$ (Figure 6.1). In the clinic, *MCM8*$^{+/-}$ embryos could be selected by pre-implantation genetic diagnosis to avoid transmission of gene corrected allele to next generations. However; some concerns should be solved regarding CRISPR/Cas9 technique before clinical applications. A major concern is that scientists still do not know long-term side effects of genome editing techniques. Therefore, before clinical applications the long-term effects of CRISPR/Cas9 on cells should be evaluated.

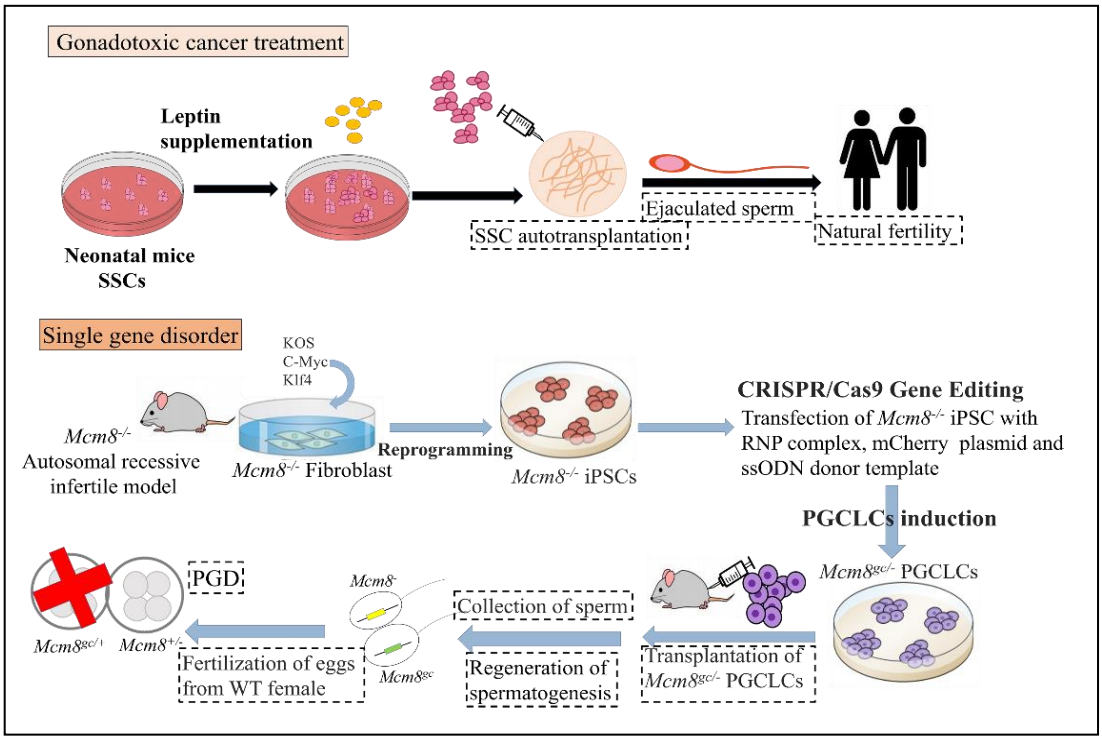

Figure 6.1. Schematic presentation of obtained results and future experiments. Leptin supplementation propagated SSCs *in vitro*. To test functionality of the leptin proliferated SSCs, these cells need to be transplanted back into testes so fertilization can be achieved naturally. 11 bp deletion in *Mcm8* exon4 was corrected by CRISPR/Cas9 and gene edited PGCLCs were generated from iPSCs. Gene corrected PGCLCs will be transplanted into testes of sterile mice. If gene edited $Mcm8^{gc/-}$ PGCLCs restore spermatogenesis in sterile mice after transplantation, sperm will be collected and used to fertilize egg from WT female. $Mcm8^{+/-}$ embryos can be selected by pre-implantation genetic diagnosis to avoid transmission of gene corrected allele to next generations. Potential future *in vivo* studies were indicated by dashed boxes.

Collectively, these approaches would help to provide effective treatment for male infertility by gene editing tool CRISPR/Cas9 to produce gametes and propagation of SSC pool for infertile male in the future clinical applications.

7. REFERENCES

1. Hamada AJ, Esteves SC, Agarwal A. A comprehensive review of genetics and genetic testing in azoospermia. Clinics (Sao Paulo). 2013;68 Suppl 1:39-60.
2. Zhao Y, Ye S, Liang D, Wang P, Fu J, Ma Q, et al. In Vitro Modeling of Human Germ Cell Development Using Pluripotent Stem Cells. Stem Cell Reports. 2018;10(2):509-23.
3. Hou J, Yang S, Yang H, Liu Y, Liu Y, Hai Y, et al. Generation of male differentiated germ cells from various types of stem cells. Reproduction. 2014;147(6):R179-88.
4. Krausz C, Escamilla AR, Chianese C. Genetics of male infertility: from research to clinic. Reproduction. 2015;150(5):R159-74.
5. Kenney LB, Laufer MR, Grant FD, Grier H, Diller L. High risk of infertility and long term gonadal damage in males treated with high dose cyclophosphamide for sarcoma during childhood. Cancer. 2001;91(3):613-21.
6. van Casteren NJ, van der Linden GH, Hakvoort-Cammel FG, Hahlen K, Dohle GR, van den Heuvel-Eibrink MM. Effect of childhood cancer treatment on fertility markers in adult male long-term survivors. Pediatr Blood Cancer. 2009;52(1):108-12.
7. Kanatsu-Shinohara M, Ogonuki N, Inoue K, Miki H, Ogura A, Toyokuni S, et al. Long-term proliferation in culture and germline transmission of mouse male germline stem cells. Biol Reprod. 2003;69(2):612-6.
8. Hamra FK, Chapman KM, Nguyen DM, Williams-Stephens AA, Hammer RE, Garbers DL. Self renewal, expansion, and transfection of rat spermatogonial stem cells in culture. Proc Natl Acad Sci U S A. 2005;102(48):17430-5.
9. Kubota H, Avarbock MR, Brinster RL. Growth factors essential for self-renewal and expansion of mouse spermatogonial stem cells. Proc Natl Acad Sci U S A. 2004;101(47):16489-94.
10. Kubota H, Avarbock MR, Brinster RL. Culture conditions and single growth factors affect fate determination of mouse spermatogonial stem cells. Biol Reprod. 2004;71(3):722-31.
11. Kubota H, Brinster RL. Culture of rodent spermatogonial stem cells, male germline stem cells of the postnatal animal. Methods Cell Biol. 2008;86:59-84.
12. Ryu BY, Kubota H, Avarbock MR, Brinster RL. Conservation of spermatogonial stem cell self-renewal signaling between mouse and rat. Proc Natl Acad Sci U S A. 2005;102(40):14302-7.
13. Smith JF, Yango P, Altman E, Choudhry S, Poelzl A, Zamah AM, et al. Testicular niche required for human spermatogonial stem cell expansion. Stem cells translational medicine. 2014;3(9):1043-54.
14. Chen B, Wang YB, Zhang ZL, Xia WL, Wang HX, Xiang ZQ, et al. Xeno-free culture of human spermatogonial stem cells supported by human embryonic stem cell-derived fibroblast-like cells. Asian J Androl. 2009;11(5):557-65.

15. Nowroozi MR, Ahmadi H, Rafiian S, Mirzapour T, Movahedin M. In vitro colonization of human spermatogonia stem cells: effect of patient's clinical characteristics and testicular histologic findings. Urology. 2011;78(5):1075-81.

16. Sadri-Ardekani H, Akhondi MA, van der Veen F, Repping S, van Pelt AM. In vitro propagation of human prepubertal spermatogonial stem cells. JAMA. 2011;305(23):2416-8.

17. Mirzapour T, Movahedin M, Tengku Ibrahim TA, Koruji M, Haron AW, Nowroozi MR, et al. Effects of basic fibroblast growth factor and leukaemia inhibitory factor on proliferation and short-term culture of human spermatogonial stem cells. Andrologia. 2012;44 Suppl 1:41-55.

18. Yang F, Silber S, Leu NA, Oates RD, Marszalek JD, Skaletsky H, et al. TEX11 is mutated in infertile men with azoospermia and regulates genome-wide recombination rates in mouse. EMBO Mol Med. 2015;7(9):1198-210.

19. Kose S, Yersal N, Onen S, Korkusuz P. Comparison of Hematopoietic and Spermatogonial Stem Cell Niches from the Regenerative Medicine Aspect. Adv Exp Med Biol. 2018;1107:15-40.

20. Hai Y, Hou J, Liu Y, Liu Y, Yang H, Li Z, et al. The roles and regulation of Sertoli cells in fate determinations of spermatogonial stem cells and spermatogenesis. Semin Cell Dev Biol. 2014;29:66-75.

21. Mayerhofer A. Human testicular peritubular cells: more than meets the eye. Reproduction. 2013;145(5):R107-16.

22. Oatley JM, Brinster RL. The germline stem cell niche unit in mammalian testes. Physiol Rev. 2012;92(2):577-95.

23. Malik IA, Durairajanayagam D, Singh HJ. Leptin and its actions on reproduction in males. Asian J Androl. 2019;21(3):296-9.

24. Ramos CF, Zamoner A. Thyroid hormone and leptin in the testis. Front Endocrinol (Lausanne). 2014;5:198.

25. Zhang J, Gong M. Review of the role of leptin in the regulation of male reproductive function. Andrologia. 2018;50(4):e12965.

26. Chu Y, Huddleston GG, Clancy AN, Harris RB, Bartness TJ. Epididymal fat is necessary for spermatogenesis, but not testosterone production or copulatory behavior. Endocrinology. 2010;151(12):5669-79.

27. Landry D, Cloutier F, Martin LJ. Implications of leptin in neuroendocrine regulation of male reproduction. Reprod Biol. 2013;13(1):1-14.

28. Herrid M, O'Shea T, McFarlane JR. Ontogeny of leptin and its receptor expression in mouse testis during the postnatal period. Mol Reprod Dev. 2008;75(5):874-80.

29. El-Hefnawy T, Ioffe S, Dym M. Expression of the leptin receptor during germ cell development in the mouse testis. Endocrinology. 2000;141(7):2624-30.

30. Takahashi Y, Okimura Y, Mizuno I, Iida K, Takahashi T, Kaji H, et al. Leptin induces mitogen-activated protein kinase-dependent proliferation of C3H10T1/2 cells. J Biol Chem. 1997;272(20):12897-900.

31. Wagoner B, Hausman DB, Harris RB. Direct and indirect effects of leptin on preadipocyte proliferation and differentiation. Am J Physiol Regul Integr Comp Physiol. 2006;290(6):R1557-64.

32. Yu T, Luo G, Zhang L, Wu J, Zhang H, Yang G. Leptin promotes proliferation and inhibits differentiation in porcine skeletal myoblasts. Biosci Biotechnol Biochem. 2008;72(1):13-21.

33. Esper RM, Dame M, McClintock S, Holt PR, Dannenberg AJ, Wicha MS, et al. Leptin and Adiponectin Modulate the Self-renewal of Normal Human Breast Epithelial Stem Cells. Cancer Prev Res (Phila). 2015;8(12):1174-83.

34. Taskin AC, Kocabay A, Ebrahimi A, Karahuseyinoglu S, Sahin GN, Ozcimen B, et al. Leptin treatment of in vitro cultured embryos increases outgrowth rate of inner cell mass during embryonic stem cell derivation. In Vitro Cell Dev Biol Anim. 2019;55(7):473-81.

35. Artwohl M, Roden M, Holzenbein T, Freudenthaler A, Waldhausl W, Baumgartner-Parzer SM. Modulation by leptin of proliferation and apoptosis in vascular endothelial cells. Int J Obes Relat Metab Disord. 2002;26(4):577-80.

36. Goren I, Pfeilschifter J, Frank S. Determination of leptin signaling pathways in human and murine keratinocytes. Biochem Biophys Res Commun. 2003;303(4):1080-5.

37. Huang F, Xiong X, Wang H, You S, Zeng H. Leptin-induced vascular smooth muscle cell proliferation via regulating cell cycle, activating ERK1/2 and NF-kappaB. Acta Biochim Biophys Sin (Shanghai). 2010;42(5):325-31.

38. Tsai YC, Lee YM, Hsu CH, Leu SY, Chiang HY, Yen MH, et al. The effect of ferulic acid ethyl ester on leptin-induced proliferation and migration of aortic smooth muscle cells. Exp Mol Med. 2015;47:e180.

39. Mitchell MJ, Metzler-Guillemain C, Toure A, Coutton C, Arnoult C, Ray PF. Single gene defects leading to sperm quantitative anomalies. Clin Genet. 2017;91(2):208-16.

40. Tenenbaum-Rakover Y, Weinberg-Shukron A, Renbaum P, Lobel O, Eideh H, Gulsuner S, et al. Minichromosome maintenance complex component 8 (MCM8) gene mutations result in primary gonadal failure. J Med Genet. 2015;52(6):391-9.

41. Yatsenko SA, Rajkovic A. Reproductive aging and MCM8/9. Oncotarget. 2015;6(18):15750-1.

42. Lutzmann M, Grey C, Traver S, Ganier O, Maya-Mendoza A, Ranisavljevic N, et al. MCM8- and MCM9-deficient mice reveal gametogenesis defects and genome instability due to impaired homologous recombination. Mol Cell. 2012;47(4):523-34.

43. Choy JT, Eisenberg ML. Male infertility as a window to health. Fertil Steril. 2018;110(5):810-4.

44. Fainberg J, Kashanian JA. Recent advances in understanding and managing male infertility. F1000Res. 2019;8.

45. Esteves SC, Roque M, Bedoschi G, Haahr T, Humaidan P. Intracytoplasmic sperm injection for male infertility and consequences for offspring. Nat Rev Urol. 2018;15(9):535-62.

46. Kolesnikova LI, Kolesnikov SI, Kurashova NA, Bairova TA. [Causes and Factors of Male Infertility]. Vestn Ross Akad Med Nauk. 2015(5):579-84.

47. Krausz C, Riera-Escamilla A. Genetics of male infertility. Nat Rev Urol. 2018;15(6):369-84.

48. Siegel RL, Miller KD, Jemal A. Cancer statistics, 2018. CA Cancer J Clin. 2018;68(1):7-30.

49. Benedict C, Shuk E, Ford JS. Fertility Issues in Adolescent and Young Adult Cancer Survivors. J Adolesc Young Adult Oncol. 2016;5(1):48-57.

50. Okada K, Fujisawa M. Recovery of Spermatogenesis Following Cancer Treatment with Cytotoxic Chemotherapy and Radiotherapy. World J Mens Health. 2019;37(2):166-74.

51. Anderson RA, Mitchell RT, Kelsey TW, Spears N, Telfer EE, Wallace WH. Cancer treatment and gonadal function: experimental and established strategies for fertility preservation in children and young adults. Lancet Diabetes Endocrinol. 2015;3(7):556-67.

52. Zavras N, Siristatidis C, Siatelis A, Koumarianou A. Fertility Risk Assessment and Preservation in Male and Female Prepubertal and Adolescent Cancer Patients. Clin Med Insights Oncol. 2016;10:49-57.

53. Smart E, Lopes F, Rice S, Nagy B, Anderson RA, Mitchell RT, et al. Chemotherapy drugs cyclophosphamide, cisplatin and doxorubicin induce germ cell loss in an in vitro model of the prepubertal testis. Sci Rep. 2018;8(1):1773.

54. Stumpp T, Freymuller E, Miraglia SM. Sertoli cell function in albino rats treated with etoposide during prepubertal phase. Histochem Cell Biol. 2006;126(3):353-61.

55. Nurmio M, Toppari J, Kallio J, Hou M, Soder O, Jahnukainen K. Functional in vitro model to examine cancer therapy cytotoxicity in maturing rat testis. Reprod Toxicol. 2009;27(1):28-34.

56. Lopes F, Smith R, Nash S, Mitchell RT, Spears N. Irinotecan metabolite SN38 results in germ cell loss in the testis but not in the ovary of prepubertal mice. Mol Hum Reprod. 2016;22(11):745-55.

57. Nurmio M, Toppari J, Zaman F, Andersson AM, Paranko J, Soder O, et al. Inhibition of tyrosine kinases PDGFR and C-Kit by imatinib mesylate interferes with postnatal testicular development in the rat. Int J Androl. 2007;30(4):366-76; discussion 76.

58. Liu M, Hales BF, Robaire B. Effects of four chemotherapeutic agents, bleomycin, etoposide, cisplatin, and cyclophosphamide, on DNA damage and telomeres in a mouse spermatogonial cell line. Biol Reprod. 2014;90(4):72.

59. Poganitsch-Korhonen M, Masliukaite I, Nurmio M, Lahteenmaki P, van Wely M, van Pelt AMM, et al. Decreased spermatogonial quantity in prepubertal boys with leukaemia treated with alkylating agents. Leukemia. 2017;31(6):1460-3.

60. Biedka M, Kuzba-Kryszak T, Nowikiewicz T, Zyromska A. Fertility impairment in radiotherapy. Contemp Oncol (Pozn). 2016;20(3):199-204.

61. Howell SJ, Shalet SM. Spermatogenesis after cancer treatment: damage and recovery. J Natl Cancer Inst Monogr. 2005(34):12-7.

62. Jarow JP, Sharlip ID, Belker AM, Lipshultz LI, Sigman M, Thomas AJ, et al. Best practice policies for male infertility. J Urol. 2002;167(5):2138-44.

63. Ferlin A, Raicu F, Gatta V, Zuccarello D, Palka G, Foresta C. Male infertility: role of genetic background. Reprod Biomed Online. 2007;14(6):734-45.

64. Choi Y, Jeon S, Choi M, Lee MH, Park M, Lee DR, et al. Mutations in SOHLH1 gene associate with nonobstructive azoospermia. Hum Mutat. 2010;31(7):788-93.

65. Song B, Zhang Y, He XJ, Du WD, Ruan J, Zhou FS, et al. Association of genetic variants in SOHLH1 and SOHLH2 with non-obstructive azoospermia risk in the Chinese population. Eur J Obstet Gynecol Reprod Biol. 2015;184:48-52.

66. Yatsenko AN, Georgiadis AP, Ropke A, Berman AJ, Jaffe T, Olszewska M, et al. X-linked TEX11 mutations, meiotic arrest, and azoospermia in infertile men. N Engl J Med. 2015;372(22):2097-107.

67. Okutman O, Muller J, Baert Y, Serdarogullari M, Gultomruk M, Piton A, et al. Exome sequencing reveals a nonsense mutation in TEX15 causing spermatogenic failure in a Turkish family. Hum Mol Genet. 2015;24(19):5581-8.

68. Miyamoto T, Hasuike S, Yogev L, Maduro MR, Ishikawa M, Westphal H, et al. Azoospermia in patients heterozygous for a mutation in SYCP3. Lancet. 2003;362(9397):1714-9.

69. Maor-Sagie E, Cinnamon Y, Yaacov B, Shaag A, Goldsmidt H, Zenvirt S, et al. Deleterious mutation in SYCE1 is associated with non-obstructive azoospermia. J Assist Reprod Genet. 2015;32(6):887-91.

70. Colaco S, Modi D. Genetics of the human Y chromosome and its association with male infertility. Reprod Biol Endocrinol. 2018;16(1):14.

71. Vogt PH. Azoospermia factor (AZF) in Yq11: towards a molecular understanding of its function for human male fertility and spermatogenesis. Reprod Biomed Online. 2005;10(1):81-93.

72. Nuti F, Krausz C. Gene polymorphisms/mutations relevant to abnormal spermatogenesis. Reprod Biomed Online. 2008;16(4):504-13.

73. Signore F, Gulia C, Votino R, De Leo V, Zaami S, Putignani L, et al. The Role of Number of Copies, Structure, Behavior and Copy Number Variations (CNV) of the Y Chromosome in Male Infertility. Genes (Basel). 2019;11(1).

74. Repping S, Skaletsky H, Lange J, Silber S, Van Der Veen F, Oates RD, et al. Recombination between palindromes P5 and P1 on the human Y chromosome

causes massive deletions and spermatogenic failure. Am J Hum Genet. 2002;71(4):906-22.

75. Jedidi I, Ouchari M, Yin Q. Sex chromosomes-linked single-gene disorders involved in human infertility. Eur J Med Genet. 2019;62(9):103560.

76. Page DC. 2003 Curt Stern Award address. On low expectation exceeded; or, the genomic salvation of the Y chromosome. Am J Hum Genet. 2004;74(3):399-402.

77. Hawksworth DJ, Szafran AA, Jordan PW, Dobs AS, Herati AS. Infertility in Patients With Klinefelter Syndrome: Optimal Timing for Sperm and Testicular Tissue Cryopreservation. Rev Urol. 2018;20(2):56-62.

78. Los E, Ford GA. Klinefelter Syndrome. StatPearls. Treasure Island (FL)2020.

79. Adelman CA, Petrini JH. ZIP4H (TEX11) deficiency in the mouse impairs meiotic double strand break repair and the regulation of crossing over. PLoS Genet. 2008;4(3):e1000042.

80. Yang F, Gell K, van der Heijden GW, Eckardt S, Leu NA, Page DC, et al. Meiotic failure in male mice lacking an X-linked factor. Genes Dev. 2008;22(5):682-91.

81. Greenbaum MP, Yan W, Wu MH, Lin YN, Agno JE, Sharma M, et al. TEX14 is essential for intercellular bridges and fertility in male mice. Proc Natl Acad Sci U S A. 2006;103(13):4982-7.

82. Yang F, Eckardt S, Leu NA, McLaughlin KJ, Wang PJ. Mouse TEX15 is essential for DNA double-strand break repair and chromosomal synapsis during male meiosis. J Cell Biol. 2008;180(4):673-9.

83. Ballow D, Meistrich ML, Matzuk M, Rajkovic A. Sohlh1 is essential for spermatogonial differentiation. Dev Biol. 2006;294(1):161-7.

84. Suzuki H, Ahn HW, Chu T, Bowden W, Gassei K, Orwig K, et al. SOHLH1 and SOHLH2 coordinate spermatogonial differentiation. Dev Biol. 2012;361(2):301-12.

85. Hao J, Yamamoto M, Richardson TE, Chapman KM, Denard BS, Hammer RE, et al. Sohlh2 knockout mice are male-sterile because of degeneration of differentiating type A spermatogonia. Stem Cells. 2008;26(6):1587-97.

86. Page SL, Hawley RS. The genetics and molecular biology of the synaptonemal complex. Annu Rev Cell Dev Biol. 2004;20:525-58.

87. Syrjanen JL, Pellegrini L, Davies OR. A molecular model for the role of SYCP3 in meiotic chromosome organisation. Elife. 2014;3.

88. Yuan L, Liu JG, Zhao J, Brundell E, Daneholt B, Hoog C. The murine SCP3 gene is required for synaptonemal complex assembly, chromosome synapsis, and male fertility. Mol Cell. 2000;5(1):73-83.

89. Bolcun-Filas E, Hall E, Speed R, Taggart M, Grey C, de Massy B, et al. Mutation of the mouse Syce1 gene disrupts synapsis and suggests a link between synaptonemal complex structural components and DNA repair. PLoS Genet. 2009;5(2):e1000393.

90. Johnson EM, Kinoshita Y, Daniel DC. A new member of the MCM protein family encoded by the human MCM8 gene, located contrapodal to GCD10 at chromosome band 20p12.3-13. Nucleic Acids Res. 2003;31(11):2915-25.

91. Handel MA, Schimenti JC. Genetics of mammalian meiosis: regulation, dynamics and impact on fertility. Nat Rev Genet. 2010;11(2):124-36.

92. Borde V. The multiple roles of the Mre11 complex for meiotic recombination. Chromosome Res. 2007;15(5):551-63.

93. Shibata A, Jeggo P, Lobrich M. The pendulum of the Ku-Ku clock. DNA Repair (Amst). 2018;71:164-71.

94. Lee KY, Im JS, Shibata E, Park J, Handa N, Kowalczykowski SC, et al. MCM8-9 complex promotes resection of double-strand break ends by MRE11-RAD50-NBS1 complex. Nat Commun. 2015;6:7744.

95. Park J, Long DT, Lee KY, Abbas T, Shibata E, Negishi M, et al. The MCM8-MCM9 complex promotes RAD51 recruitment at DNA damage sites to facilitate homologous recombination. Mol Cell Biol. 2013;33(8):1632-44.

96. Iyama T, Wilson DM, 3rd. DNA repair mechanisms in dividing and non-dividing cells. DNA Repair (Amst). 2013;12(8):620-36.

97. Sung P, Klein H. Mechanism of homologous recombination: mediators and helicases take on regulatory functions. Nat Rev Mol Cell Biol. 2006;7(10):739-50.

98. Dabaja AA, Schlegel PN. Microdissection testicular sperm extraction: an update. Asian J Androl. 2013;15(1):35-9.

99. Chan PT, Schlegel PN. Nonobstructive azoospermia. Curr Opin Urol. 2000;10(6):617-24.

100. Corona G, Minhas S, Giwercman A, Bettocchi C, Dinkelman-Smit M, Dohle G, et al. Sperm recovery and ICSI outcomes in men with non-obstructive azoospermia: a systematic review and meta-analysis. Hum Reprod Update. 2019;25(6):733-57.

101. van Casteren NJ, van Santbrink EJ, van Inzen W, Romijn JC, Dohle GR. Use rate and assisted reproduction technologies outcome of cryopreserved semen from 629 cancer patients. Fertil Steril. 2008;90(6):2245-50.

102. Agarwal A, Ranganathan P, Kattal N, Pasqualotto F, Hallak J, Khayal S, et al. Fertility after cancer: a prospective review of assisted reproductive outcome with banked semen specimens. Fertil Steril. 2004;81(2):342-8.

103. Kawai K, Nishiyama H. Preservation of fertility of adult male cancer patients treated with chemotherapy. Int J Clin Oncol. 2019;24(1):34-40.

104. Horne G, Atkinson AD, Pease EH, Logue JP, Brison DR, Lieberman BA. Live birth with sperm cryopreserved for 21 years prior to cancer treatment: case report. Hum Reprod. 2004;19(6):1448-9.

105. Feldschuh J, Brassel J, Durso N, Levine A. Successful sperm storage for 28 years. Fertil Steril. 2005;84(4):1017.

106. Szell AZ, Bierbaum RC, Hazelrigg WB, Chetkowski RJ. Live births from frozen human semen stored for 40 years. J Assist Reprod Genet. 2013;30(6):743-4.

107. Gassei K, Orwig KE. Experimental methods to preserve male fertility and treat male factor infertility. Fertil Steril. 2016;105(2):256-66.

108. Ogawa T, Dobrinski I, Avarbock MR, Brinster RL. Transplantation of male germ line stem cells restores fertility in infertile mice. Nat Med. 2000;6(1):29-34.

109. Honaramooz A, Behboodi E, Megee SO, Overton SA, Galantino-Homer H, Echelard Y, et al. Fertility and germline transmission of donor haplotype following germ cell transplantation in immunocompetent goats. Biol Reprod. 2003;69(4):1260-4.

110. Izadyar F, Den Ouden K, Stout TA, Stout J, Coret J, Lankveld DP, et al. Autologous and homologous transplantation of bovine spermatogonial stem cells. Reproduction. 2003;126(6):765-74.

111. Mikkola M, Sironen A, Kopp C, Taponen J, Sukura A, Vilkki J, et al. Transplantation of normal boar testicular cells resulted in complete focal spermatogenesis in a boar affected by the immotile short-tail sperm defect. Reprod Domest Anim. 2006;41(2):124-8.

112. Kim Y, Turner D, Nelson J, Dobrinski I, McEntee M, Travis AJ. Production of donor-derived sperm after spermatogonial stem cell transplantation in the dog. Reproduction. 2008;136(6):823-31.

113. Jahnukainen K, Ehmcke J, Quader MA, Saiful Huq M, Epperly MW, Hergenrother S, et al. Testicular recovery after irradiation differs in prepubertal and pubertal non-human primates, and can be enhanced by autologous germ cell transplantation. Hum Reprod. 2011;26(8):1945-54.

114. Hermann BP, Sukhwani M, Winkler F, Pascarella JN, Peters KA, Sheng Y, et al. Spermatogonial stem cell transplantation into rhesus testes regenerates spermatogenesis producing functional sperm. Cell Stem Cell. 2012;11(5):715-26.

115. Gassei K, Schlatt S, Ehmcke J. De novo morphogenesis of seminiferous tubules from dissociated immature rat testicular cells in xenografts. J Androl. 2006;27(4):611-8.

116. Honaramooz A, Megee SO, Rathi R, Dobrinski I. Building a testis: formation of functional testis tissue after transplantation of isolated porcine (Sus scrofa) testis cells. Biol Reprod. 2007;76(1):43-7.

117. Arregui L, Rathi R, Megee SO, Honaramooz A, Gomendio M, Roldan ER, et al. Xenografting of sheep testis tissue and isolated cells as a model for preservation of genetic material from endangered ungulates. Reproduction. 2008;136(1):85-93.

118. Kita K, Watanabe T, Ohsaka K, Hayashi H, Kubota Y, Nagashima Y, et al. Production of functional spermatids from mouse germline stem cells in ectopically reconstituted seminiferous tubules. Biol Reprod. 2007;76(2):211-7.